Membrane-Anchoring Interactions of Bacteriophage Major Coat Proteins

A.B. Meijer

promotor:

prof. dr. T.J. Schaafsma,
hoogleraar in de moleculaire fysica
Wageningen Universiteit

co-promotor:

dr. M.A. Hemminga, universitair hoofddocent
Laboratorium voor Biofysica
Wageningen Universiteit

Promotiecommissie:

prof. dr. R.W. Goldbach, Laboratorium voor Virologie, Wageningen Universiteit
prof. dr. A.J.W.G. Visser, Faculteit Biologie, Vrije Universiteit Amsterdam
prof. dr. A. Kuhn, Microbiologie, Universiteit van Hohenheim, Stuttgart
dr. D. Stopar, Laboratorium voor Microbiologie, Universiteit van Ljubljana

NN08201, 2975

Membrane-Anchoring Interactions of Bacteriophage Major Coat Proteins

A.B. Meijer

Proefschrift

ter verkrijging van de graad van doctor
op gezag van de rector magnificus
van Wageningen Universiteit,
prof. dr. ir. L. Speelman
in het openbaar te verdedigen
op woensdag 23 mei 2001
des namiddags te half twee in de aula.

1615 719

Meijer, A.B.
Membrane-Anchoring Interactions of Bacteriophage Major Coat Proteins
Thesis, Wageningen University
ISBN: 90-5808-407-8

NN08201,2982

Stellingen

De verankeringsinteracties van eiwitten met het membraan worden bepaald door de voorkeur van aminozuren voor een bepaalde positie in dit membraan.

Natriumdodecylsulfaat (SDS) heeft de eigenschap een membraaneiwit volledig in te pakken. Om deze reden is een eiwit-SDS complex geen goed modelsysteem voor membraaneiwitten.
(Helenius et al., (1975) Biochim. Biophys. Acta 415, 29-79)

De altijd aanwezige nadelen van een bepaalde techniek dienen gecompenseerd te worden door de altijd aanwezige voordelen van een andere techniek.

Er is grote onzekerheid over de invloed van de zon op het klimaat. De huidige klimaatmodellen over het effect van broeikasgassen moeten hierdoor in de toekomst bijgesteld worden.
(Beer et al., (2000) Quat. Sci. Rev. 19, 403-415, Svensmark et al., (1997) J. Atmos. Solar-Ter. Phys. 59, 1225-1232)

Reizen met openbaar vervoer blijkt alleen een goed alternatief voor de auto zolang men niet in het bezit is van een rijbewijs.

De verklaring waarom de oerknal ongeveer 15 miljard jaar geleden plaatsvond berust op het feit dat de ontwikkeling tot intelligente wezens zó lang duurt.
(Naar het heelal, S. Hawking)

Aangezien de evolutietheorie voor een groot deel bestaat uit aannames, kan gerust worden aangenomen dat er volgens vergelijkbare principes buitenaards leven is ontstaan op miljoenen planeten.

A.B. Meijer
Membrane-Anchoring Interactions of Bacteriophage Major Coat Proteins
Wageningen, 23 mei 2001

Voorwoord

In dit proefschrift worden de resultaten besproken van onderzoek dat is uitgevoerd bij het Laboratorium voor Biofysica aan de Wageningen Universiteit. Ik wil iedereen bedanken die een nuttige bijdrage heeft geleverd aan het tot stand komen van dit boekje, waaronder: de promotor Tjeerd Schaafsma en copromotor Marcus Hemminga; de analisten Cor Wolfs en met name Ruud Spruijt zonder wiens hulp ik nooit aan het schrijven van dit voorwoord zou zijn toegekomen; verder Ulrich, Tom, Carel en Frank voor de waardevolle discussies na 17.30; de rest van de vakgroep en een ieder die ik vergeten ben te noemen. Yolanda is de laatste en natuurlijk de belangrijkste persoon die ik wil bedanken voor alles wat was en alles wat komen gaat.

Sander Meijer
April 2001

Contents

Abbreviations

Chapter 1: Introduction 1

Chapter 2: Localization and rearrangement modulation of the N-terminal arm of the membrane-bound major coat protein of bacteriophage M13 13
(Biochim. Biophys. Acta, 2000, 1509, 311-323)

Chapter 3: Configurations of the N-terminal amphipathic domain of the membrane-bound M13 major coat protein 37
(Biochemistry in press)

Chapter 4: Membrane assembly of the bacteriophage Pf3 major coat protein 53
(Biochemistry, 2000, 39, 6157-6163)

Chapter 5: Membrane-anchoring interactions of M13 major coat protein 75
(Submitted to Biochemistry)

Chapter 6: Summarizing discussion 91

Summary 99

Samenvatting 101

Curriculum vitae 102

Abbreviations

τ_c	rotational correlation time
λ_{max}	wavelength of maximum emission
5-SASL	5-(4,4,-dimethyloxazolidine-N-oxyl)stearic acid
CD	circular dichroism
CL	cardiolipin
DEiPC	di20C:1Δ11c PC (dieicosenoyl-PC)
DEuPC	di22C:1 Δ13c PC (dierucoy-PC)
DMoPC	di14C:1Δ9c PC (dimirystoleoyl-PC)
DOPC	di18C:1Δ9c PC (dioleoyl-PC)
DTT	dithiothreitol
EDTA	ethylene-diamine-tetraacetic acid
ESR	electron spin resonance
F	fluorescence intensity in the presence of quencher
F_0	fluorescence intensity in the absence of quencher
HPSEC	high performance size exclusion chromatography
IAEDANS	N-(iodoacetylaminoethyl)-5-naphtylamine-1-sulfonic acid
IPTG	isopropylthio-β-D-galactoside
K_{SV}	Stern-Volmer constant
L/P	lipid to protein molar ratio
NMR	nuclear magnetic resonance
PAGE	polyacrylamide gel electrophoresis
PC	phosphatidylcholine
PE	phosphatidylethanolamine
RPC	reverse phase chromatography
SDS	sodium dodecyl sulfate
TEA	triethylamine
TFE	trifluoroethanol
WT coat protein	wild type major coat protein

Key words in the PhD Thesis:

M13 and Pf3 bacteriophage, major coat protein, ESR spectroscopy, fluorescence spectroscopy, *site-directed mutagenesis*, cysteine scanning approach, membrane anchoring interactions, membrane model systems, fluorescence quenching

Chapter 1

Introduction

A biological membrane performs one of the most important functions in cell life. It is not only a barrier for unwanted materials, but it also retains the important substances of the cell itself. The membrane is further responsible for communication with the outside world. For this reason, the cell membrane is involved in a large number of processes. Another important function of specific cell membranes is to divide a cell into compartments where separate biochemical pathways can be operational without interference. These multifunctional biological membranes are two-dimensional fluids, which are composed of a large variety of macromolecules. The fluid mosaic model of Singer and Nicolson describes the membrane as a fluid phospholipid bilayer, wherein proteins and phospholipids can freely diffuse within the plane of the membrane (*1*).

Phospholipids

The main building blocks of biological membranes are phospholipids. A striking feature of phospholipids is their enormous diversity in chemical and physical properties, but also the lipid composition of different membranes can vary considerably (*2*). The most common membrane lipids are the glycerophospholipids, which consists of a glycerol backbone, two fatty acid chains, and a phosphorylated alcohol. The length of the fatty acid chains is typically between 14 and 24 carbon atoms, of which 16 and 18 carbon fatty acids are the most common. The length and degree of unsaturation of the chain strongly affect membrane fluidity. The common alcohol moieties of the phospholipids in cells are choline, glycerol and ethanolamine. A combination of the apolar fatty chains and polar head-group creates amphiphilic molecules, which adopt a bilayer, or non-bilayer structure in an aqueous environment (*3, 4*). The ability of a phospholipid to form a bilayer roughly depends on the ratio of the cross sectional areas between the head-group and fatty acids chains. A cylindrical shape of a phospholipid will result in the formation of a bilayer, as is the case with lipids, which have a phosphatidylcholine head-group. On the other hand, a cone-shaped molecule, with a small head-group like phosphatidyl-ethanolamine, will produce a non-bilayer structure and form a hexagonal phase. The overall organization of the membrane components in a biological membrane leads to a bilayer structure (*5*).

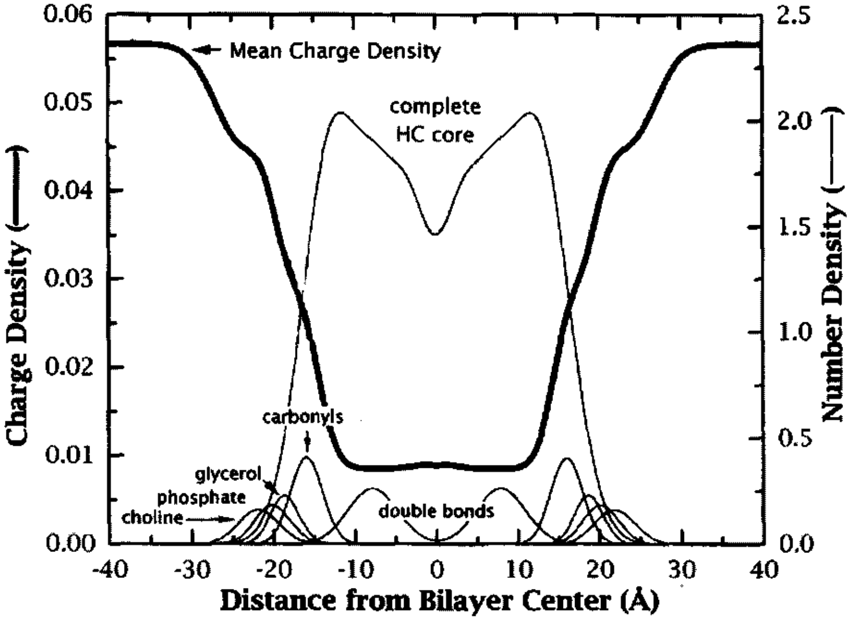

Figure 1: Group distribution of 1,2 dioleoyl-*sn*-glycero-3-phosphocholine (DOPC) assembled in a fluid bilayer. The thick line indicates the polarity profile from the outside to the inside of the membrane (after White and Whimley (*47*)).

The bilayer can be divided into a hydrophobic and an interface region, or head-group region. There are no sharp boundaries between these regions. Wiener and White proposed a model of the structure of fluid phase dioleoylphosphatidylcholine bilayers by interpreting X-ray and neutron diffraction data (Figure 1) (*6*). Their model shows a gaussian distribution of the different membrane components, giving rise to a chemically highly heterogeneous interface. This leads to a polarity gradient from the outside to the inside of the membrane, which is the steepest around the carbonyl groups. The combined interfacial region is about 50% of the total thickness of the membrane.

Membrane proteins

Membrane proteins can be associated with or buried inside the membrane. Those proteins are called peripheral or integral membrane proteins, respectively. Two common basic structures of polypeptide chains can be found in integral membrane proteins. The polypeptide chains can be arranged as α-helices, or as β-strands. The β-strands are the result of hydrogen bonding between adjacent polypeptide chains, and can lead to cylindrical β-barrels as is the case for bacterial porins (*7*). A α-helix is formed by hydrogen bonding within the polypeptide chain. A single helix, containing about 21 amino acid residues, can accommodate the membrane (*8*). Many membrane proteins are found to span the membrane with several α-helices.

The formation of the correct structure of a transmembrane protein, or its vertical position parallel to the membrane normal, requires specific properties of the involved amino acid side chains. The interactions of a protein with the hydrophobic core of the membrane are accomplished via a domain of amino acids containing preferentially hydrophobic side chains. The degree of hydrophobicity and length of this domain will determine the strength of these interactions. A specific set of amino acids is usually found in the polar head-group region of the bilayer. For example, statistical analysis of multiple and single membrane-spanning helical proteins shows a recurrence of tryptophan and tyrosine amino acid residues in the membrane interface region. Furthermore, in this polar region, a statistical preference is found for charged amino acid residues (*8, 9*). It is thought that these amino acids contribute to anchoring interactions of a protein with the membrane interface region (*10, 11*).

From an energetics point of view, it can be expected that the length of the hydrophobic transmembrane helix matches with the hydrophobic thickness of the bilayer. However, there are examples of proteins that differ in hydrophobic length within one membrane. For example, the predicted length of one of the two transmembrane helices of leader peptidase from *E.coli* is 15 amino acids, whereas, the mean length the helices of lactose permease, which resides in the same membrane, is estimated to be 24 amino acids. There are several possible mechanisms by which a protein or a membrane can react to hydrophobic mismatch, for example: protein segregation in domains, tilting of protein segments, protein backbone adaptation, and preferential surrounding of proteins by lipids with matching acyl chain lengths (*10, 11*).

M13 and Pf3 bacteriophages

The subject of this thesis is about the membrane-bound M13 and Pf3 major coat protein, which are the main building blocks of their respective filamentous bacteriophages. The major coat proteins form a rod-like tubular protein coat around a circular single stranded DNA molecule. The M13 and Pf3 bacteriophages belong to the large family of *Inoviridae*, which infect a variety of gram-negative bacteria. M13 and Pf3 bacteriophages are male-specific and infect *Escherichia coli* and *Pseudomonas aeruginosa*, respectively (*12, 13*). The infected bacteria continuously produce new phages, without the destruction of the cell (*14*). Considering the differences in the helical symmetry of the protein coat, bacteriophage M13 and Pf3 belong to different classes (*15*). In spite of this distinction, both phages are similar in their life-cycle processes (*16*).

The sequence homology of the Pf3 and M13 major coat protein is low. However, both primary structures can be divided into several domains. The proteins contain a basic C-terminus, a hydrophobic domain, an amphipathic domain and an acidic N-terminus. Figure 2 shows the primary sequence of both the M13 and Pf3 major coat protein (*17-19*). The proteins are largely α-helical when part of the phage, and the axis of the α-helix makes a small angle with the long axis of the virion. The basic residues in the C-terminus interact with the DNA core in the phage. The hydrophobic amino acids mainly interact with each other, and the acidic N-terminus renders the solubility of the phage. For further details about the structure and reproductive cycle of Pf3 and M13 bacteriophages, see Welsh et al. and Marvin et al. (*20, 21*).

M13 major coat protein				Pf3 major coat protein			
1	Ala		**Trp**	1	Met		Ile
	Glu		Ala		Gln		Ile
	Gly		Met		Ser		Val
	Asp		Val		Val		Leu
5	*Asp*	30	Val	5	Ile	30	Ala
	Pro		Val		Thr		Ala
	Ala		Ile		*Asp*		Val
	Lys		Val		Val		Val
	Ala		Gly		Thr		Leu
10	Ala	35	Ala	10	Gly	35	Gly
	Phe		Thr		Gln		Ile
	Asn		Ile		Leu		*Arg*
	Ser		Gly		Thr		**Trp**
	Leu		Ile		Ala		Ile
15	Gln	40	*Lys*	15	Val	40	*Lys*
	Ala		Leu		Gln		Ala
	Ser		**Phe**		Ala		Gln
	Ala		*Lys*		*Asp*		**Phe**
	Thr		*Lys*		Ile		**Phe**
20	*Glu*	45	**Phe**	20	Thr		
	Tyr		Thr		Thr		
	Ile		Ser		Ile		
	Gly		*Lys*		Gly		
	Tyr		Ala		Gly		
25	Ala	50	Ser	25	Ala		

Figure 2: Primary structure of the M13 major coat protein (*17*) and Pf3 major coat protein (*18, 19*). The aromatic amino acids are printed in bold and the charged amino acids are printed in italic.

Membrane-bound structure of major coat protein

After infection, newly synthesized proteins insert into the membrane. M13 major coat protein is produced with a leader sequence, which is clipped off after insertion by leader peptidase (*22, 23*). On the other hand, the Pf3 protein is synthesized in its mature form (*18*). After insertion, the C-terminus of the M13 and Pf3 protein remains in the cytoplasm and the N-terminal part is translocated into the periplasm (*24, 25*). Not much is known about the structure of the membrane-bound Pf3 major coat protein. However, the M13 major coat protein has been extensively studied in detergents and phospholipid model systems.

The secondary structures of the M13, and strongly related fd major coat protein have been characterized in SDS by NMR spectroscopy (*26-29*). The only difference between both proteins is that fd major coat protein contains an aspartic acid at position 12, whereas the M13 major coat protein contains an asparagine at this position. It is shown that the protein contains two α-helical segments in SDS. The residues 7 to 16 and 25 to 45 construct the helices. The amino acids between both helices, called the hinge, show a high residue flexibility. In spite of the valuable information obtained from these model systems, it is suggested that detergents do not produce a good membrane-mimicking system. SDS covers the entire major coat protein, without a well-defined boundary as found in a bilayer (*30, 31*). This is not surprising since SDS is a strong amphiphilic molecule, which binds to the protein on a gram to gram basis (*32*).

Much less detailed information is known about the secondary structure of the M13 major coat protein in phospholipid bilayers. A number of spectroscopic approaches has been used to study the α-helical content, yielding a diversity of results. Up to 95% α-helical content has been found with CD spectroscopy of M13 major coat protein reconstituted into phospholipid bilayers (*33*). More detailed studies with FTIR spectroscopy showed α-helical contents up to 60%, which was surprisingly stable up to 70°C (*34*). An FTIR study of the reconstituted M13 protein in D_2O revealed not only a 42% α-helical content but also 56% of turn, coil and disordered α-helix (*35*).

NMR studies on oriented bilayers incorporated with the related fd, and Pf1 major coat proteins have revealed information about the tertiary structure of the M13 protein in the membrane. Hereto, ^{15}N labeled amino acids are introduced into the primary structure of the protein. The results suggest that the N-terminal section of the protein is parallel to the surface of the membrane, leading to an "L-shaped" tertiary structure of membrane-bound major coat protein (*26, 36, 37*). Apart from the structure determination of major coat protein in bilayers, the depth and local dynamics of specific positions of the protein in the membrane are measured by ESR and fluorescence spectroscopy methods (*30, 31, 38, 39*). It is shown that the section of the M13 major coat protein around Thr36 is in the middle of the membrane. The amino acid residues 25 and 46 are suggested to reside in the polar head-group region of the membrane. Furthermore, these studies surprisingly revealed a deep burial of the Lys40 in the membrane. The ε-amino group of the lysine side chain can probably just reach the polar head-group region, via the so-called snorkeling effect (*40, 41*).

Site-directed fluorescence and ESR spectroscopy

The single tryptophan amino acid residue in both the M13 and Pf3 major coat protein provides information about the local environment of their specific position in the membrane by using fluorescence spectroscopy. The wavelength of maximum emission (λ_{max}) of the tryptophan residue is sensitive to the polarity of the environment. Typically, red shifts are observed in a more hydrophilic environment, while blue shifts are indicative for a more apolar or hydrophobic environment. Therefore, information about the relative depth in the membrane is obtained via λ_{max}. Further insight in the depth of the tryptophan residue can be obtained by the use of fluorescence quenchers that specifically act on the in or outside of the membrane (*42, 43*).

Specific information about the other positions in the protein is not readily available since a natural reporter group is lacking. Site-directed fluorescence and ESR spectroscopy, however, are excellent techniques to obtain information about the local environment and dynamics of specific positions. The M13 and Pf3 major coat protein do not contain a site for site-specific labeling. The replacement of an amino acid for a cysteine residue provides a reactive group to which a fluorescence or ESR spin probe can be attached for the purpose of fluorescence or ESR spectroscopy. In this respect, the entire protein can be systematically scanned, which is referred to as the cysteine-scanning approach (*30, 31, 38, 44, 45*). The attachment of a fluorescence probe, which is sensitive to the polarity of the environment, provides comparable information as is described for the tryptophan residue.

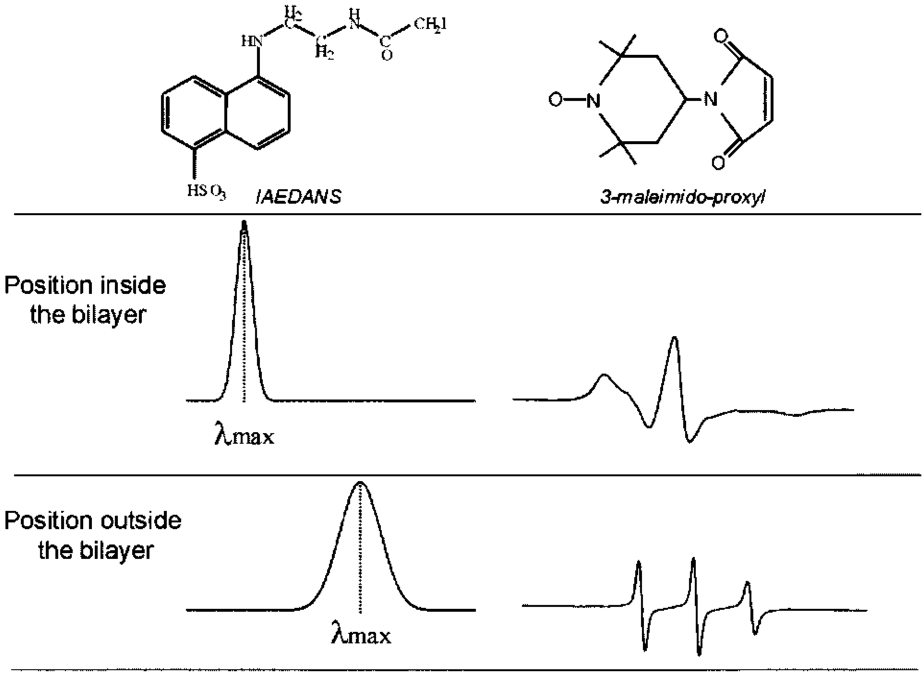

Figure 3: Schematic representation of the spectroscopic labels IAEDANS and 3-maleimido-proxyl used in site-directed spectroscopy. The emission maximum (λ_{max}) of IAEDANS is sensitive to the polarity of the environment (*48*). AEDANS-labeled positions in a protein inside the membrane have a blue shifted λ_{max} as compared to the λ_{max} of labeled positions at the outside of the membrane. Proxyl-labeled positions inside the membrane show broad spectra representing immobile probes, and positions at the outside of the membrane show sharp spectra representing probes with a high mobility (*31*).

The local dynamics of specific sites in the protein can be studied via ESR spin labeling spectroscopy. Nitroxide spin-labeled proteins are sensitive to molecular motions on the time scale determined by the ^{14}N hyperfine splitting anisotropy, typically in the nanosecond domain. The hyperfine splitting of the nitroxide spin labels are partially averaged by the anisotropic motion of the protein backbone. The line widths in the spectra are differentially broadened by an extent, which depends on the rate of molecular motion. The local structure and environment of the site, to which the probe is attached, can affect the motion of the spin probe (*46*). Fluorescence and ESR spectroscopy are particularly useful for studying relative depths and dynamics of specific sites in the membrane. Figure 3 schematically shows the probes that are used in this study for site-specific labeling, and the type of information that can be obtained using these probes.

Scope of this dissertation

The main question of this thesis is to elucidate how specific amino acid residues determine the position of the M13 and Pf3 major coat proteins in the membrane. The problem is approached by studying protein-phospholipid interactions in reconstituted model systems using fluorescence and ESR spectroscopy. For this purpose, single cysteine mutants of the protein are specifically labeled with a fluorescence or ESR probe. Furthermore, the natural single tryptophan residue is studied via fluorescence spectroscopy.

The location and possible anchoring interactions of the N-terminal arm of the M13 coat protein are addressed in chapter 2 and 3. The focus in chapter 2 will be on the localization of specific sites of the protein in the membrane. For this purpose, a number of single-cysteine mutants are labeled with a fluorescence probe to determine the relative depth of these sites in the membrane. Additional mutants, containing a single cysteine residue, are prepared to measure the influence of specific amino acids on the location of the N-terminus on the surface of the membrane. In chapter 3, these cysteine mutants are labeled with an ESR spin probe. This provides information about the local dynamics of the probed position in the membrane-bound protein.

In chapter 4, the relatively unknown Pf3 major coat protein is studied using a comparable approach. By comparing the relative depth measurements of this protein with the results obtained from the M13 major coat protein, valuable information is obtained about the membrane-bound position of the Pf3 protein. The possible membrane anchoring interactions of the hinge region and the transmembrane α-helical domain from the M13 coat protein are studied in chapter 5. Mutants, with a cysteine residue at key positions in the protein, are labeled with a fluorescence probe. The location of these sites is monitored in response to hydrophobic mismatch using reconstitution of mutant and wild type protein into phosphatidylcholine bilayers of varying thickness. In addition, mutants are studied in which possible membrane-anchoring residues are removed. Finally, the result of these studies is summarized and discussed in chapter 6.

References

1. Singer, S. J., and Nicolson, G. L. (1972) *Science 175*, 720-31.
2. Gennis, R. B. (1989) *Cantor C.R., Ed. Springer-Verlag New York Inc, USA*, 1-36.
3. Cullis, P. R., and de Kruijff, B. (1979) *Biochim. Biophys. Acta. 559*, 399-420.
4. Seddon, J. M. (1990) *Biochim. Biophys. Acta 1031*, 1-69.
5. De Kruijff, B. (1987) *Nature 329*, 587-8.
6. Wiener, M. C., and White, S. H. (1992) *Biophys. J. 61*, 428-33.
7. Schulz, G. E. (1993) *Curr. Opin. Cell Biol. 5*, 701-7.
8. Arkin, I. T., and Brunger, A. T. (1998) *Biochim. Biophys. Acta*, 113-128.
9. Landolt Marticorena, C., Williams, K. A., Deber, C. M., and Reithmeier, R. A. (1993) *J. Mol. Biol. 229*, 602-8.
10. Killian, J. A., and von Heijne, G. (2000) *Trends Biochem. Sci. 25*, 429-434.
11. Killian, J. A. (1998) *Biochim. Biophys. Acta.*, 401-416.
12. Hofschneider, P. H. (1963) *Z. Natur. Forsch. B 18*, 203-210.
13. Stanisich, V. A. (1974) *J. Gen. Microbiol. 84*, 332-342.
14. Marvin, D. A., and Hohn, B. (1969) *Bacteriol. Rev. 33*, 172-209.
15. Marvin, D. A. (1998) *Curr. Opin. Struct. Biol. 8*, 150-158.
16. Russel, M. (1991) *Mol. Microbiol. 5*, 1607-13.
17. Van Wezenbeek, P. M. G. F., Hulsebos, T. J. M., and Schoenmakers, J. G. G. (1980) *Gene 11*, 129-48.
18. Luiten, R. G. M., Schoenmakers, J. G. G., and Konings, R. N. H. (1983) *Nucleic. Acids. Res. 11*, 8073-85.

19. Putterman, D. G., Casadevall, A., Boyle, P. D., Yang, H. L., Frangione, B., and Day, L. A. (1984) *Proc. Natl. Acad. Sci. USA 81*, 699-703.
20. Welsh, L. C., Symmons, M. F., Sturtevant, J. M., Marvin, D. A., and Perham, R. N. (1998) *J. Mol. Biol. 283*, 155-177.
21. Marvin, D. A., Hale, R. D., Nave, C., and Citterich, M. H. (1994) *J. Mol. Biol. 235*, 260-286.
22. Chang, C. N., Blobel, G., and Model, P. (1978) *Proc. Natl. Acad. Sci. U. S. A. 75*, 361-5.
23. Mandel, G., and Wickner, W. (1979) *Proc. Natl. Acad. Sci. U. S. A. 76*, 236-40.
24. Kuhn, A., Rohrer, J., and Gallusser, A. (1990) *J. Struct. Biol. 104*, 38-43.
25. Kiefer, D., Hu, X., Dalbey, R., and Kuhn, A. (1997) *EMBO J. 16*, 2197-2204.
26. McDonnell, P. A., Shon, K., Kim, Y., and Opella, S. J. (1993) *J. Mol. Biol. 233*, 447-463.
27. Van de Ven, F. J. M., Van Os, J. W. M., Aelen, J. M. A., Wymenga, S. S., Remerowski, M. L., Konings, R. N. H., and Hilbers, C. W. (1993) *Biochemistry 32*, 8322-8328.
28. Almeida, F. C. L., and Opella, S. J. (1997) *J. Mol. Biol. 270*, 481-495.
29. Papavoine, C. H. M., Christiaans, B. E. C., Folmer, R. H. A., Konings, R. N. H., and Hilbers, C. W. (1998) *J. Mol. Biol. 282*, 401-419.
30. Spruijt, R. B., Wolfs, C. J. A. M., Verver, J. W. G., and Hemminga, M. A. (1996) *Biochemistry 35*, 10383-10391.
31. Stopar, D., Spruijt, R. B., Wolfs, C. J. A. M., and Hemminga, M. A. (1996) *Biochemistry 35*, 15467-15473.
32. Helenius, A., and Simons, K. (1975) *Biochim. Biophys. Acta 415*, 29-79.
33. Sanders, J. C., Haris, P. I., Chapman, D., Otto, C., and Hemminga, M. A. (1993) *Biochemistry 32*, 12446-12454.
34. Thiaudiere, E., Soekarjo, M., Kuchinka, E., Kuhn, A., and Vogel, H. (1993) *Biochemistry 32*, 12186-12196.
35. Wolkers, W. F., Haris, P. I., Pistorius, A. M. A., Chapman, D., and Hemminga, M. A. (1995) *Biochemistry 34*, 7825-7833.
36. Shon, K. J., Kim, Y. G., Colnago, L. A., and Opella, S. J. (1991) *Science 252*, 1303-1304.
37. Marassi, F. M., Ramamoorthy, A., and Opella, S. J. (1997) *Proc. Natl. Acad. Sci. USA 94*, 8551-8556.
38. Stopar, D., Jansen, K. A. J., Pali, T., Marsh, D., and Hemminga, M. A. (1997) *Biochemistry 36*, 8261-8268.
39. Wolkers, W. F., Spruijt, R. B., Kaan, A., Konings, R. N. H., and Hemminga, M. A. (1997) *Biochem. Biophys. Acta 1327*, 5-16.
40. Mishra, V. K., Palgunachari, M. N., Segrest, J. P., and Anantharamaiah, G. M. (1994) *J. Biol. Chem. 269*, 7185-91.
41. Tanford, C., and Reynolds, J. A. (1976) *Biochim. Biophys. Acta 457*, 133-70.
42. Lehrer, S. S., and Leavis, P. C. (1978) *Methods Enzymol. 49*, 222-236.
43. Lakowicz, J. R. (1983) *Principles of Fluorescence Spectroscopy*, Plenum Press, New York.
44. Stopar, D., Spruijt, R. B., Wolfs, C. J. A. M., and Hemminga, M. A. (1997) *Biochemistry 36*, 12268-12275.

45. Stopar, D., Spruijt, R. B., Wolfs, C. J. A. M., and Hemminga, M. A. (1998) *Biochemistry 37*, 10181-10187.
46. Marsh, D., and Horvath, L. I. (1998) *Biochem. Biophys. Acta 1376*, 267-296.
47. White, S. H., Wimley, W. C., Ladokhin, A. S., and Hristova, K. (1998) *Ener. Biol. Macromol. B 295*, 62-87.
48. Hudson, E. N., and Weber, G. (1973) *Biochemistry 12*, 4154-61.

Chapter 2

Localization and rearrangement modulation of the N-terminal arm of the membrane-bound major coat protein of bacteriophage M13

Ruud B. Spruijt, Alexander B. Meijer, Cor J.A.M. Wolfs,
and Marcus A. Hemminga

Abstract

During infection, the major coat protein of the filamentous bacteriophage M13 is in the cytoplasmic membrane of the host *Escherichia coli.* This study focuses on the configurational properties of the N-terminal part of the coat protein in the membrane-bound state. For this purpose, X-Cys substitutions are generated at coat protein positions 3, 7, 9, 10, 11, 12, 13, 14, 15, 17, 19, 21, 22, 23 and 24, covering the N-terminal protein part. All coat protein mutants are successfully produced in mg quantities by overexpression in *E.coli.* Mutant coat proteins are labeled and reconstituted into mixed bilayers of phospholipids. Information about the polarity of the local environment around the labeled sites is deduced from the wavelength of maximum emission using AEDANS attached to the SH groups of the cysteines as a fluorescent probe. Additional information is obtained by determining the accessibility of the fluorescence quenchers' acrylamide and 5-doxyl stearic acid. By employing uniform coat protein surroundings provided by TFE and SDS, local effects of the backbone of the coat proteins or polarity of the residues could be excluded. Our data suggest that at a lipid to protein ratio of about 100, the N-terminal arm of the protein gradually enters the membrane from residue 3 towards residue 19. The hinge region (residues 17 to 24), connecting the helical parts of the coat protein, is found to be more embedded in the membrane. Substitution of one or more of the membrane-anchoring amino acid residues lysine 8, phenylalanine 11 and leucine 14, results in a rearrangement of the N-terminal protein part into a more extended conformation. The N-terminal arm can also be forced in this conformation by allowing

less space per coat protein at the membrane surface by decreasing the lipid to protein ratio. The influence of the phospholipid head-group composition on the rearrangement of the N-terminal part of the protein is found to be negligible within the range thought to be relevant in vivo. From our experiments, we conclude that membrane-anchoring and space-limiting effects are key factors for the structural rearrangement of the N-terminal protein part of the coat protein in the membrane.

Introduction

In the filamentous bacteriophage M13 a large number of copies of the major coat protein forms a cylindrical coat around the circular, single-stranded DNA genome. During infection, the major coat protein (the product of gene VIII) is involved in various environmental and structural rearrangements. First there are the processes of phage disassembly and subsequent deposition of the coat protein into the *Escherichia coli* inner membrane. These processes are followed by the biosynthesis of the procoat, the membrane insertion and subsequent removal of the signal sequence by the host cell leader peptidase. Finally, the protein takes part in the complex process of cooperative assembly and phage-extrusion (*1-4*). To accomplish all these different functions of the coat protein, the primary sequence must be such to enable sufficient functioning in all processes, which of course not necessarily imply optimal functioning with respect to one specific aspect. In this sense, a proper functioning of the coat protein will be generally achieved by adapting its secondary and tertiary structure.

Much is known about the aggregational behavior and overall secondary structure of the coat protein embedded in phospholipid bilayers (*5-8*). The primary and secondary structures of the coat protein are depicted in Figure 1. New insights about the conformation mainly originate from experiments performed on the coat protein solubilized in detergents as membrane-mimicking systems. Detailed secondary structure determination as performed on the coat protein solubilized in sodium dodecyl sulfate (SDS) or dodecyl phosphatidylcholine micelles clearly shows an α-helix ranging from residues 25 up to 45 (*9, 10*). This finding is in agreement with the result of a cysteine-scanning study on the putative transmembrane domain performed on the coat protein reconstituted in phospholipid bilayers (*11, 12*), and appeared to be shifted from the predicted transmembrane domain (*13, 14*). In the N-terminal part of the coat protein a short amphipathic α-helical structure (residues 7 to 16) has been established, with residues demonstrating considerable motion on the nanosecond and picosecond time scales. Furthermore, a motion of the amphipathic helical arm with respect to the transmembrane helix has been proposed (*15*). The hinge region, connecting the two helices, exhibits α-helical, turn-like features as well as additional flexibility of its residues (*9, 10*).

5 10
H_2N-Ala-Glu-Gly-Asp-Asp-Pro-Ala-Lys-Ala-Ala-Phe-Asn-

15 20 25
Ser-Leu-Gln-Ala-Ser-Ala-Thr-Glu-Tyr-Ile-Gly-Tyr-Ala-

30 35
Trp-Ala-Met-Val-Val-Val-Ile-Val-Gly-Ala-Thr-Ile-Gly-

40 45 50
Ile-Lys-Leu-Phe-Lys-Lys-Phe-Thr-Ser-Lys-Ala-Ser-COOH

Figure 1: The primary and secondary structure of the mature part of the major coat protein of bacteriophage M13. The amphipathic α-helix and the transmembrane α-helix are underlined. The part of the protein connecting the two helical domains is called the hinge region.

Between the amphipathic N-terminal helix and the transmembrane helix of the membrane-bound coat protein, an angle is found of about 90° (*16-18*). This L-shape implies that the N-terminal helix lies in the plane of the membrane. However, when the coat protein is part of the M13 phage particle, it is arranged in one continuous, slightly bend helix (*19, 20*). No information is available about what factors direct the rearrangement of the two helices in the viral and membrane-bound states of the coat protein, which will take place during the phage assembly process. However, an extended N-terminal protein part could well be a structural and functional intermediate of the membrane-bound coat protein in various stages of the viral replication process.

In the present study, we follow a site-specific probing approach for the N-terminal part, similar as has been carried out for the C-terminal part of the M13 major coat protein (*11*), and recently for the Pf3 major coat protein (see, chapter 4 of this thesis, *21*). The cysteine-scanning method is a suitable technique to obtain information about the local polarity of the probe, which can be related to the membrane-embedment of the protein. The method has been described for various membrane proteins (*12, 22-24*). We prepared a number of coat protein mutants containing unique cysteine residues at specific positions along the N-terminal amino acid sequence. The cysteine residues were specifically labeled with the fluorescent environmental probe N-(iodoacetylaminoethyl)-5-naphtylamine-1-sulfonic acid (AEDANS). The fluorescence properties and accessibilities towards various quencher molecules are reported to be dependent on polarity as well as steric effects (*25, 26*). By employing uniform coat protein surroundings provided by an organic solvent (TFE) or a micellar system (SDS), local effects of the backbone of the coat proteins or polarity of the residues could be excluded. Based on a fixed labeling position, additional substitutions of various N-terminal amino acid residues in double protein mutants elucidate the importance of these residues in affecting the association of the N-terminal protein arm to the membrane. Phospholipid composition and lipid to protein ratio are further tested for their possible involvement in the membrane-binding behavior of this protein domain.

Materials and Methods

Cloning procedures

Both the mature coat protein part of bacteriophage M13 gene VIII (without the leader sequence), and the complete bacteriophage M13 gene VIII (including the leader sequence) were obtained by the polymerase chain reaction (PCR) using M13 mp18 RF

DNA as template and primers based on the sequence as determined by Van Wezenbeek (*27*). Oligonucleotide primers (Amersham Pharmacia Biotech) were designed to add a *NdeI* restriction site upstream of the start codon (5'GGGCATATGGCTGAGGGTGACGAT for the mature coat protein part of the gene, and 5'GGGCATATGAAAAAGTCTTTAGTCCT for the complete gene VIII) and a *BamHI* restriction site downstream of the stop codon (5'CCCGGATCCTCAGCTTGCTTTCGAGG for both reactions). The PCR amplified fragments were purified by polyacrylamide gel electrophoresis. After digestion with *NdeI* and *BamHI,* they were cloned into the respective sites of a pT7-7 expression vector (*28*). *E.coli* strain DH5αF' was used for the cloning vector.

Preparation of cysteine-containing major coat protein mutants

The QuikChange site directed mutagenesis procedure (Stratagene) was used to introduce unique cysteine residues at various positions along the primary structure of the major coat protein. The procedure was also used for other modifications of the coat protein. For each modification two complementary synthetic oligonucleotide primers (Amersham Pharmacia Biotech) were designed, and used together with the double stranded pT7-7 expression vector (containing the cloned M13 gene VIII) as a template. Following temperature cycling and the selection for mutated DNA by DpnI digestion, the expression vectors were transformed into supercompetent cells of *E.coli* XL1-Blue. Plasmid DNA was isolated using the Wizard DNA purification system (Promega) and used for transformation into competent cells of *E.coli* BL21 (DE3) (*29*). Transformed cells were incubated in LB medium (1% (w/v) select pepton, 0.5% (w/v) yeast extract, 1% (w/v) NaCl) to allow expression of ampicillin resistance, and grown overnight on LB-agar in the presence of 0.01% (w/v) ampicillin (Boehringer). Plasmid DNA, isolated from a liquid culture as mentioned before, was used for automated DNA sequencing. Ready-to-use inoculates were prepared in the presence of glycerol (22% w/w, final concentration) and stored at -70°C.

Expression of modified M13 gene VIII and identification of the gene product

Cells of *E.coli* BL21 (DE3) containing pT7-7 (gene VIII mutant) were grown at 37°C in LB medium supplemented with 0.2% (w/v) glucose and 0.01% (w/v) ampicillin. The optical density at 600 nm of the culture was monitored. At an OD_{600nm} of about 0.6, the expression of the target gene was induced by adding IPTG up to 0.15-mM final concentration. Aliquots (25 µl) were taken before induction and after different times of incubation after induction, and checked for the presence of the gene product using Tricine SDS polyacrylamide gel electrophoresis, as described in Schägger et al. (*30*). Western blotting (*31*) and immunodetection were performed using anti-rabbit IgG conjugated with alkaline phosphatase (Boehringer). Primary antibodies against the major coat protein of bacteriophage M13 were raised in female New Zealand White rabbits using highly purified biosynthetic major coat protein as obtained from the phenol extraction procedure described previously (*32*). The serum exclusively reacted with the major coat protein applied to the gel and not with proteins of host *E.coli* BL21 (DE3).

Expression, labeling and purification of modified M13 major coat proteins

E.coli BL21 (DE3), containing the respective pT7-7 plasmids, were grown in 8 L cultures as described before. Cells were harvested by centrifugation (10 minutes at 7000g) within 45 to 90 minutes after induction. The cells were resuspended in TBS/DTT (Tris buffered saline/dithiothreitol) buffer (25 mM Tris-HCl pH 7.5, 137 mM NaCl, 2.7 mM KCl, 1 mM DTT) and stored at -20°C. The total membrane fraction was isolated after cell lysis by sonication (Branson B15 sonifier, 5 minutes, 90 W output, 50% pulse, on ice) and subsequent centrifugation (30 min 45000g at 4°C). The pelleted membrane fraction was resuspended in TBS/DTT buffer by brief sonication. Amounts of cellular material out of 2 L cell culture were used for further treatment. Prior to Reverse Phase Chromatography (RPC) the major coat protein was extracted from the total membrane fraction. Equal volumes of resuspended total membrane fraction and trifluoroethanol (TFE) were thoroughly mixed for 1 min and non-extractable material was removed by centrifugation (5 min 10000g). The clear membrane extract in the supernatant was immediately applied on a Source 15RPC HR10/10 column (Amersham Pharmacia Biotech), and eluted with water (flow 1.0 ml/min) using a Pharmacia-LKB Ultrochrom GTi Bioseparation system. After elution of all non-binding material (as monitored at 280 nm) the major coat protein was eluted using a steep linear gradient of mixtures of solvent A: pure water and solvent B: isopropanol/0.2% (v/v) triethylamine (TEA). Starting at 0% (v/v), solvent B increased with a rate of 5%/min up to 100%, and decreased with a rate of 10%/min back to 0% of solvent B. Fractions were collected and analyzed by Tricine SDS PAGE. For the purpose of labeling with IAEDANS (purchased from Molecular Probes), the fractions containing the major coat protein were pooled and mixed with TFE to achieve optimal accessibility conditions. After the pH was adjusted to approx. 8 by addition of a small amount of TEA, an estimated small molar excess of IAEDANS was added, and the mixture was stirred in the dark at room temperature for 3 h. The reaction was stopped by addition of an excess of β-mercaptoethanol. Solid sodium cholate (Sigma) was added up to 500 mM and dissolved completely before the reaction mixture was applied on a preparative HiLoad Superdex 75 prepgrade column (2.6 x 60.0 cm) (Amersham Pharmacia Biotech). This column was eluted with 50 mM sodium cholate, 10 mM Tris-HCl pH 8.0, 0.2 mM EDTA, 150 mM NaCl at a flow of 2 ml/min to separate the labeled coat protein from accompanying proteins and excess unbound AEDANS. Fractions containing the AEDANS-labeled coat protein, as monitored by a linear fluorescence detector (excitation wavelength set at 340 nm, emission wavelength set at 480 nm) were pooled and concentrated using ultrafiltration over an Amicon YM3 membrane. The AEDANS-labeled coat protein fractions were checked for purity and protein content by Tricine SDS PAGE. Wild-type major coat protein as well as mutant coat proteins with a cysteine at position 25 and 46 were obtained, and labeled with IAEDANS and purified as described before (*11*).

Reconstitution of the AEDANS-labeled coat protein into phospholipid bilayers

Unless stated otherwise, reconstitution of the labeled coat protein mutants into dioleoyl phosphatidylcholine (DOPC) and dioleoyl phosphatidylglycerol (DOPG) vesicles (both lipids obtained from Sigma) in a 80%/20% (mol/mol) ratio was performed in the dark using the cholate-dialysis procedure as described earlier (*32*). The final molar lipid to protein ratio was 100. The resulting proteoliposomes in 10 mM Tris-HCl pH 8.0, 0.2 mM EDTA, 150 mM NaCl were directly used for fluorescence and circular dichroism measurements.

Circular dichroism measurements

Circular dichroism spectra were recorded from 200 to 260 nm on a JASCO 715 spectrometer at room temperature, using a 1 mm path length cell, 1 nm bandwidth, 0.1 nm resolution and 1 s response time. Spectra were corrected for the background and protein content.

Steady-state fluorescence measurements

The fluorescence properties of the AEDANS-labeled major coat protein, reconstituted into DOPC/DOPG bilayers, were recorded at room temperature on a Perkin-Elmer LS-5 luminescence spectrophotometer. The excitation wavelength was 340 nm and emission scans were recorded from 470 to 530 nm. Excitation and emission slits were set at 5 nm. The concentration of labeled coat protein was kept constant at 2.5 or 5 μM, which is mentioned in the tables and figure legends. The optical density at the excitation wavelength never exceeded 0.1. Fluorescence intensities were corrected for background by subtracting the spectrum of unlabeled wild-type major coat protein, reconstituted into the same phospholipid bilayers, and recorded under the same conditions. Due to a different instrumental set-up of the luminescence spectrophotometer, the wavelength of maximum emission intensity showed an 8 nm red shift as compared to the results reported earlier (*11*). To enable comparison, two major coat protein mutants, labeled to a unique cysteine at positions 25 and 46, were included in all experiments. The variations of the measured wavelengths of maximum emission are always found to be within 1 nm. Steady-state quenching studies were performed by addition of various amounts of a 2.67 M acrylamide solution (Merck, electrophoresis quality) to a final concentration of 242 mM. Alternatively 5-doxyl stearic acid (Aldrich Chemical Co.) was added from a 12.5 mM solution to a fixed final overall concentration of 0.2 mM. Emission spectra were recorded 1 min after each addition and the stable fluorescence intensities were corrected for background and dilution. Variations of the calculated K_{SV} and F_0/F-values are usually within 5%.

Results

Expression of the target gene and identification of the gene product

Since no coat protein mutants containing a cysteine residue in the N-terminal protein part could be generated resulting in the appearance of viable bacteriophages (as has been employed earlier (*11*)), we have cloned the coat protein gene into the pT7-7 expression vector. As a consequence, the control for proper functioning of the coat protein by phage viability is lacking. Moreover, the target protein now needs to be purified from the host cell, requiring excessive and complicated purification protocols. The expression of the target gene results in a reduced cell growth and even a decrease in optical density of the cell culture after prolonged times. As the synthesis of the gene product is accompanied by membrane insertion, high amounts of the coat protein appear to be toxic and will finally result in cell lysis. Attempts were made to direct the synthesized coat protein into the cell cytoplasm by removal of the leader sequence of the coat protein (the first 23 amino acids coded by gene VIII). However, no mature coat protein could be detected, even not by employing immunodetection. Therefore, it is essential to apply the complete gene VIII (including the leader sequence) for coat protein synthesis. Also fusion to a water-soluble protein appeared not to be an alternative as was demonstrated for the closely related M13 minor coat proteins, which were still found preferentially present in the *E.coli* inner membrane (*33*).

Neither decreasing the growth temperature nor lowering the level of expression (by lowering the final IPTG concentration) did result in a higher yield. To obtain appropriate amounts of coat protein, large volumes of growing culture were required. Moreover, cell growth is only allowed for quite a short time (within 45 to 90 min) after the induction of coat protein synthesis. In case of prolonged growing times after induction of the target gene expression, an additional small band of a larger protein is detected by the Tricine SDS PAGE and subsequent immunodetection. This band is identified to contain M13 procoat based on recognition by the antiserum, which is raised against the mature part of the gene VIII product. The protein also migrated identically on gel as compared to the procoat mutant (gene VIII S-3F), which was characterized by a strongly decreased processing rate by leader peptidase (*34*). The appearance of the procoat after prolonged incubation times is indicative for defects in the processing by leader peptidase, because the cell integrity or functioning is distorted. To localize the coat protein after expression, cells were fractionated according to Russel & Kazmierczak (*35*) and subjected to gel electrophoresis. The coat protein is predominantly found in the fraction containing the inner or cytoplasmic membranes (data not shown). X-Cys substitutions are generated at coat protein positions 3, 7, 9, 10, 11, 12, 13, 14, 15, 17, 19, 21, 22, 23, and 24, covering the entire N-terminal part of the M13 major coat protein (see Figure 1). All coat protein mutants, in which an amino acid residue has been substituted for a cysteine residue, are obtained in amounts comparable to that of wild-type coat protein, i.e. mg quantities. However, severe additional modifications (Table 1) occasionally resulted in lower amounts of coat protein.

Table 1: Quencher efficiencies and environmental polarity of various AEDANS-labeled M13 major coat protein A7C-derived double mutants in DOPC/DOPG membranes. Wavelengths of maximum emission and accessibilities to the hydrophilic quencher acrylamide and hydrophobic quencher 5-doxyl stearic acid are determined on AEDANS, attached to various M13 coat protein mutants at cysteine position 7. The coat protein at a final concentration of 2.5 μM is reconstituted into DOPC/DOPG at L/P 100. The concentrations of the quencher molecules are given in the materials and methods section. "Emission maxima and quenching efficiencies of these double mutants were equal and constant at 498 nm and F/F_0=1.25 when brought in a homogeneous environment provided by TFE.

M13 coat protein mutant	Emission maximum (nm)"	Quenching by acrylamide K_{SV} (M^{-1}) "	Quenching by 5-doxyl stearic acid F/F_0
A7C	495	2.99	0.54
A7C/K8A	499	3.85	0.63
A7C/A10I	492	2.62	0.48
A7C/F11A	502	5.18	0.71
A7C/L14A	502	5.37	0.81
A7C/F11A/L14A	505	5.98	0.83
A7C/L14D	502	5.07	0.70

Purification and labeling of the coat protein mutants

A combined protein labeling and purification protocol was developed. Organic solvents are applied to enable RPC and to serve optimal labeling conditions. After achieving a major purification effect by RPC, care has to be taken in proper solubilizing the coat protein by detergents. After harvesting the cells by centrifugation and the preparation of the membrane fraction, almost all mature coat protein (but not the unprocessed procoat; data not shown) is successfully extracted using the organic solvent TFE and subsequently purified on a Source 15RPC HR10/10 column. The pooled major coat protein containing fractions are diluted with TFE to prevent protein-protein interactions, and to achieve an optimal accessibility of the cysteines thiol group for the fluorescent probe AEDANS to be attached. The AEDANS-labeled coat protein is further purified from other cellular impurities and excess free label, using high performance size exclusion chromatography (HPSEC). For this purpose, it is essential to add a huge excess of the detergent sodium cholate to get an appropriate solubilization of the coat protein. The final isolates of labeled coat protein are applied to Tricine SDS PAGE to check the purity and the yield of coat protein. Typically, 0.5 to 1 mg of labeled mutant coat protein is obtained per liter cell culture. The purity is found to exceed at least 95%, as is judged from stained protein bands on gel. Circular dichroism spectra of mutant protein, containing the mutation L14A or A10I, reconstituted into phospholipid, were found to be identical to that of reconstituted wild-type coat protein (data not shown).

Environmental polarity probing approach in a uniform protein surrounding

The spectral properties of AEDANS provide local environmental information concerning the extent of membrane penetration (*11, 22, 36*). To check whether also the protein itself affects the fluorescence results, the coat protein was brought into a homogeneous environment. For these experiments we used 85% (v/v) TFE in water, and the strong cationic detergent SDS. The wavelengths of maximum emission of the attached AEDANS probes at the different N-terminal positions and the transmembrane boundary positions (25 and 46) are given in Figure 2A. The wavelengths of maximum emission of the coat protein mutants, dissolved in 85% (v/v) TFE/water, are almost constant at a value of 498 nm, with only small variations (within 3 nm) at position 3 and position 25: 501

and 495 nm, respectively. It should be noted that the wavelength of maximum emission of unbound AEDANS (represented as amino acid residue number 0) is also 498 nm. Similar results are obtained in SDS, showing a higher average wavelength of maximum emission at 508 nm, and again small variations within 4 nm. The wavelength of maximum emission of the unbound AEDANS solubilized by SDS is slightly higher at 513 nm (see Figure 2A; unbound AEDANS is represented again on position 0).

Since it is known that the accessibility of a fluorophore to a quencher depends upon the polarity and steric effects (*25, 37, 38*), the quenching efficiency can also provide information about the local surrounding. The reduced fluorescence intensities, due to the presence of the quencher molecule acrylamide (125 mM, final concentration), as a function of the different AEDANS attachment sites on the coat protein, are given in Figure 2B. Although the quenching efficiency in SDS is twice as much of that found in TFE, only small differences in quenching efficiency between the various coat protein mutants are found in TFE and SDS. Moreover, the wavelengths of maximum emission of the AEDANS probes attached to the different positions along the coat proteins primary structure do hardly shift upon addition of the hydrophilic quencher acrylamide (data not shown), indicating again a homogeneous environment. These experiments underline the uniformity of the local environment of the N-terminal part of the coat protein provided by these two media, and greatly reduces the local environmental influence of the coat protein itself. Therefore, the local amino acid effect on the optical properties of the probe can be neglected in the following experiments, where the environment is imposed by a phospholipid bilayer.

Localization of the N-terminal part of membrane-bound coat protein

Figure 3A shows the wavelengths of maximum emission of the AEDANS probes, attached to different positions in the N-terminal part of membrane-bound coat proteins (residues 3 to 24), as well as to the previously established transmembrane and C-terminal positions 25 to 50 (*11*). The coat protein is reconstituted into DOPC/DOPG 80%/20% (mol/mol) bilayers at L/P 100. Apart from positions 3, 11, 13 and 14, the probes attached to the N-terminal arm show wavelengths of maximum emission varying between 494 and

496 nm, which is higher as compared to the wavelength of maximum emission of AEDANS attached to the transmembrane boundary positions 25 and 46.

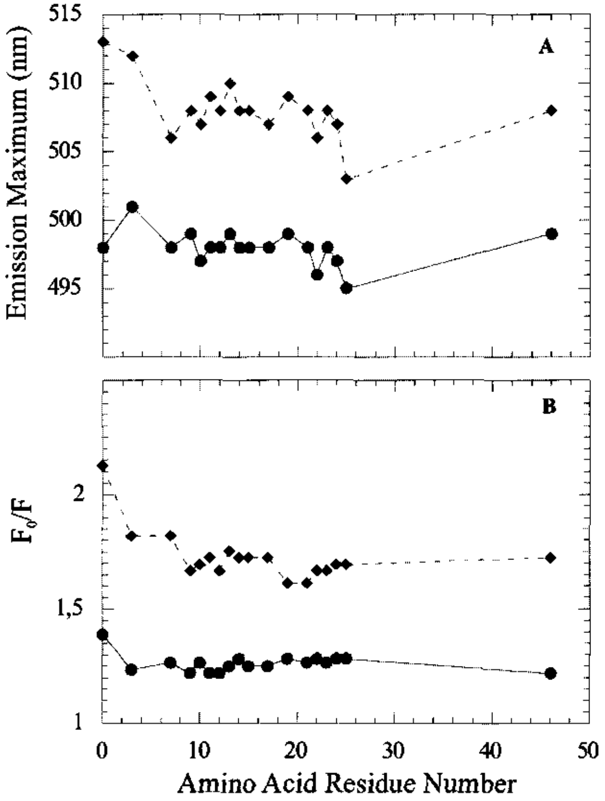

Figure 2: Wavelengths of maximum emission (A) and acrylamide quenching efficiency profiles (B) of AEDANS attached at different positions along the primary structure the N-terminal part of the M13 coat protein when solubilized in 85% (v/v) TFE in water (solid lines) and when solubilized in SDS at 50 mM final concentration (dashed line). The coat protein concentration was kept constant at 5 μM. The values at position 0 represent unbound AEDANS. The quenching efficiency is expressed as F_0/F after addition of acrylamide at a concentration of 125 mM.

In case of position 3 (the outermost N-terminal position measured and not part of the amphipathic helix), a much higher wavelength (507 nm) is found, which is quite close to the value found for unbound AEDANS in aqueous buffer (512 nm). Also the AEDANS attached to the cysteine at positions 11 (phenylalanine replacement) and 14 (leucine replacement), show remarkable high wavelengths of maximum emission of 502 and 499 nm, respectively. These latter wavelengths are about 6 nm higher than the average wavelength of maximum emission of the neighboring amino acid residues. Going from position 17 to 25 (representing the hinge region, connecting the N-terminal and transmembrane helices), a gradual decrease of wavelength of maximum emission from 494 to 485 nm is observed. In case of positions 23 and 24 slightly higher wavelengths are observed. Overall, these wavelengths are well below the average wavelengths of maximum emission of the N-terminal arm of the major coat protein.

For the quenching experiments, both a polar but uncharged quencher molecule (acrylamide) and a hydrophobic quencher molecule (5-doxyl stearic acid) are used. The quenching results are shown in Figure 3B as a function of different AEDANS attachment sites on the N-terminal part of the coat protein. The quenching efficiency is expressed differently for the two quenchers. In the case of acrylamide, the Stern-Volmer constant K_{SV} is given, as calculated from a series of concentration-dependent experiments. However, in the case of the hydrophobic and, thus, membrane-associated quencher 5-doxyl stearic acid the actual concentrations are unknown due to accumulation of the fatty acid in the small partial volume occupied by the bilayers interior. Therefore, F/F_O at a constant overall quencher concentration is used instead. As observed before (*11*), the wavelengths of maximum emission showed again a small blue and red shift upon addition of acrylamide and 5-doxyl stearic acid, respectively.

The quenching efficiencies of acrylamide that are found for the N-terminal part of the protein, are higher as compared to those found for the transmembrane boundary positions 25 and 46. Another striking feature is the gradual decrease in quenching efficiency going from the N-terminus towards the transmembrane boundary position 25. Clearly, the more N-terminal positions are better accessible to acrylamide than those closer to position 25.

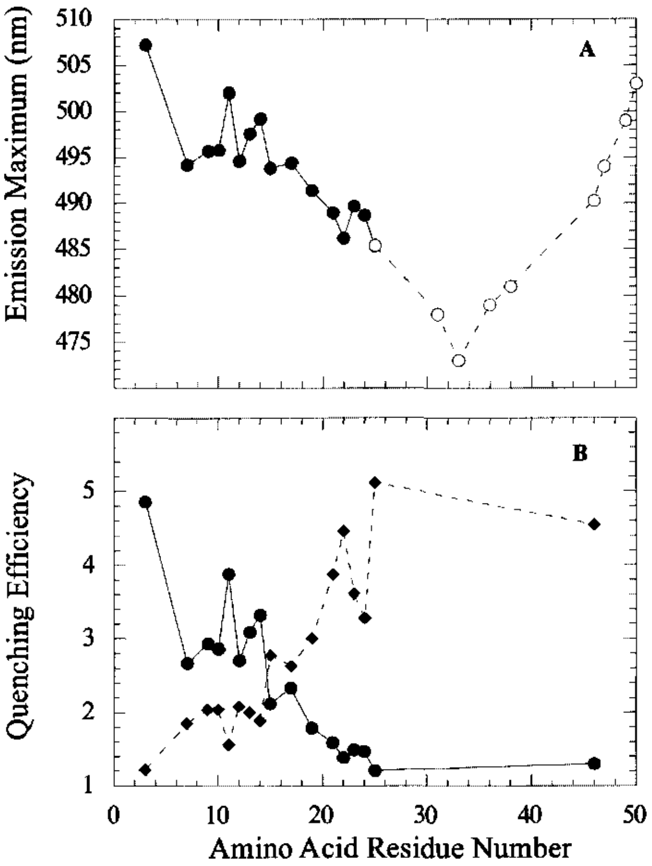

Figure 3: Wavelengths of maximum emission of AEDANS attached to different positions along the primary structure the N-terminal part of the M13 coat protein (solid line, closed symbols) after reconstitution into DOPC/DOPG at L/P 100 (A). The values for the positions 25 to 50 (dashed line, open symbols) were adapted from a previous study (*11*). Quenching efficiency profiles after addition of acrylamide (solid line, values expressed as K_{SV} (M^{-1})) and 5-doxyl stearic acid (dashed line, values expressed as F_0/F) are shown in Figure 3B. The coat protein concentration was kept constant at 5 μM.

Similar, as observed for the exceptional high wavelengths of maximum emission (Figure 3A), the quenching efficiency of acrylamide on AEDANS attached to positions 3, 11, and 14 is also remarkably high. The quenching results of the hydrophobic membrane-embedded 5-doxyl stearic acid are opposite to that of acrylamide, and a remarkable mirror resemblance is found (Figure 3B). In this case, the lowest quenching efficiencies are obtained for the outermost N-terminal positions, and again a gradual but now increasing quenching efficiency is observed towards the transmembrane boundary position 25.

Influence of membrane-anchoring residues

Based on the typical results obtained for the coat protein labeled at position 11 (phenylalanine replacement) and position 14 (leucine replacement), these two amino acids are subject for a further study. In addition the influence of lysine at position 8 is also examined, as lysine residues are reported to be involved in membrane anchoring as well (*11, 12, 39*). To monitor the configuration of the N-terminal arm, the A7C coat protein mutant is selected. This labeling position is quite far away from the putative hinge between the two helical parts of the coat protein, and therefore highly sensitive for monitoring any change in protein configuration. Table 1 shows the fluorescence properties of the AEDANS labeled A7C-derived double mutants, after reconstitution into DOPC/DOPG 80%/20% (mol/mol) at L/P 100. Compared to the single A7C coat protein mutant, the additional substitutions K8A, F11A, and L14A result in higher wavelengths of maximum emission, indicative for an increased polar environment. An enhanced quenching efficiency of the polar quencher acrylamide, and a lower quenching efficiency of the hydrophobic quencher 5-doxyl stearic acid support this observation. Removal of both two hydrophobic residues phenylalanine 11 and leucine 14 results in a high emission maximum (505 nm) and a K_{SV} value for the hydrophilic quencher acrylamide of almost 6 M^{-1}. No enhanced effect was observed when the hydrophobic leucine at position 14 was replaced for the negatively charged aspartic acid (i.e. A7C/L14D). In contrast, the addition of an extra hydrophobic amino acid (A7C/A10I) results in a somewhat lower wavelength of maximum emission and concomitant quenching features.

Influence of lipid to protein ratio

The fluorescence properties of the AEDANS labeled A7C mutant, reconstituted into DOPC/DOPG 80%/20% (mol/mol) at different L/P ratios, are shown in Figure 4. Both the wavelength of maximum emission and accessibility to the hydrophilic quencher acrylamide show maximal values around L/P 30. At L/P ratios below 30 a blue shift of the wavelength of maximum emission is observed. This blue shift is apparently a result of probe-probe interaction, since it appeared to be absent when the concentration of labeled coat protein was diluted tenfold with unlabeled wild-type coat protein (Figure 4A).

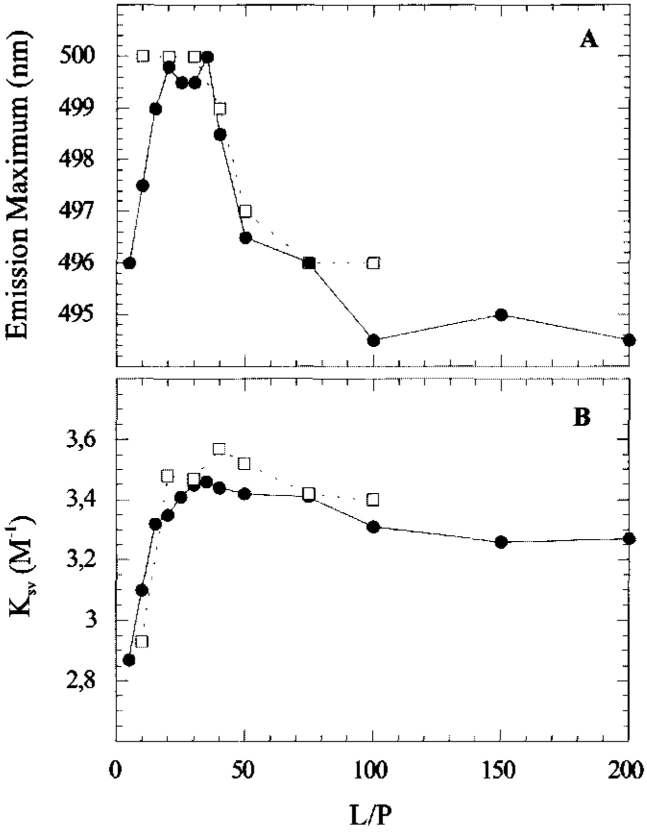

Figure 4: Wavelengths of maximum emission (A) and acrylamide quenching profile (B) of AEDANS attached to the cysteine of M13 coat protein mutant A7C (closed circles; solid line) and of AEDANS-labeled M13 coat protein mutant A7C, which is tenfold diluted with unlabeled wild-type coat protein (open squares; dotted line), reconstituted into DOPC/DOPG at different L/P ratios. The coat protein concentration was kept constant at 2.5 μM

At L/P ratios below 20 lower quenching efficiencies are observed (Figure 4B). These lower quencher accessibilities are probably due to steric hindrance at reduced protein-protein distances. The major coat protein was found to be predominantly monomeric as judged from SDS-PAGE, and no higher order oligomers could be detected. At L/P ratios around L/P 20 to 35, the red shifted wavelength of maximum emission and an increased accessibility for acrylamide both indicate a more polar environment around the N-terminal protein part.

Table 2: Quencher efficiencies and environmental polarity of the AEDANS-labeled A7C coat protein mutant in different phospholipid systems. Wavelengths of maximum emission and accessibilities to the hydrophilic quencher acrylamide and hydrophobic quencher 5-doxyl stearic acid are determined on AEDANS attached to the cysteine of M13 coat protein mutant A7C. The coat protein is reconstituted at a final concentration of 2.5 μM into DOPC/DOPG at a fixed L/P ratio of 40. The concentrations of the quencher molecules are mentioned in the materials and methods section.

Phospholipid composition	Emission maximum (nm)	Quenching by acrylamide K_{SV} (M^{-1})	Quenching by 5-SASL F/F_0
DOPC (100%)	498	3.17	0.63
DOPC/DOPG (80%/20%)	499	3.60	0.67
DOPG (100%)	504	5.03	0.81
DOPE/DOPC (70%/30%)	500	3.61	0.66
DOPE/DOPG (70%/30%)	500	3.83	0.68
DOPE/DOPG/CL (70%/20%/10%)	500	3.83	0.67

Influence of phospholipid head-group

The fluorescence properties of AEDANS-labeled A7C coat protein mutant in different phospholipid systems are listed in Table 2. In case of the pure zwitterionic DOPC an emission maximum of about 498 nm is observed. Addition of negatively charged DOPG up to 20% results in a small red shift, whereas in pure negatively charged DOPG a wavelength of maximum emission of 504 nm is obtained. In analogy to previous observations, the accessibilities observed for the hydrophilic acrylamide are lower in case of a lower wavelength of maximum emission and higher in case of a higher wavelength of maximum emission. Again, this effect is reversed using the hydrophobic quencher 5-doxyl stearic acid. In case of PE-containing mixtures, however, both the wavelength of maximum emission and quenching efficiencies are slightly affected.

Discussion

Coat protein mutant approach

In this paper, we describe a new method to produce mutants of the major coat protein of bacteriophage M13. All overexpressed coat protein mutants are successfully inserted into the cytoplasmic membrane as they are subsequently processed by *E.coli* leader peptidase. This justifies a study of the membrane-bound state of these coat protein mutants. This approach opens unlimited possibilities to study the properties of the membrane-bound protein by site-specific labeling. It is now possible to study the role of individual amino acids residues throughout the whole primary sequence of the protein. In the present work, we focus on the N-terminal part of the protein. By employing fluorescence spectroscopy of AEDANS-labeled single and double mutants, detailed information can be obtained about the N-terminal protein part. The double mutant approach (Table 1) comprises the monitoring of the N-terminal arm at a fixed position as a function of various supplemental X-Ala substitutions. This approach reduces a possible disturbing effect of site-specific labeling on our results. With the current state-of-the-art of mutagenesis and purification of small membrane-proteins, a wealth of additional biophysical results may be expected in the coming years.

Fluorescence analysis

From the fluorescence experiments, a clear tendency is observed: A higher value of the wavelength of maximum emission is always concomitant with an enhanced quenching efficiency of the hydrophilic acrylamide, and a lower quenching efficiency of the hydrophobic quencher 5-doxyl stearic acid. This observation indicates that environmental polarity as observed by the wavelength of maximum emission is related to accessibility as monitored predominantly by quenching. In addition, from Figure 2 it follows that there is hardly any effect of the neighboring amino acid residues. Therefore we interpret this tendency as moving the labeled site away from the membrane surface. Because the fluorescent label as well as the N-terminal protein part may exhibit local motions, the fluorescence results will always show the average of an ensemble of conformations.

Membrane assembly of M13 coat protein

Compared to the previously established locations of the transmembrane helix boundary positions 25 and 46 (*11*), the amphipathic N-terminal arm is located in a more polar environment. Based on the fluorescence results in Figure 3, the N-terminal arm is embedded along the membrane surface. This L-shaped configuration is in agreement with other studies on the M13 coat protein (*16-18*). In detail, the data show a gradual decrease in wavelength and concomitant quenching efficiency going from residue 3 towards residue 19. These data can be interpreted in a structural way as a gradual entry into the membrane. Apart from the results obtained for the labeled mutant coat proteins F11C and L14C, which will be explained in the next section, it is clear that the most N-terminal labeled position 3 within the acidic amino acid block (Glu2, Asp4, Asp5) is most far outside the net negatively-charged DOPC/DOPG membrane. This is related to the high polarity and membrane-repelling electrostatic properties of this domain, as well as to the observed high mobility features (*40*). In contrast, the amino acid residues at positions 19 to 24, flanking the other side of the N-terminal arm and comprising the hinge region, are more buried into the membrane. The combination of these two effects results in a slight apparent tilt of the N-terminal arm with respect to the membrane surface. In agreement with this view, a more dynamic interpretation can be used to explain the gradual changes in wavelength of maximum emission and quenching efficiencies. As the N-terminal arm of the coat protein is only loosely associated to the membrane surface (see the sections below) the N-terminal arm will be movable, and the most N-terminal positions will apparently show the lowest probability to assume a location close to the membrane surface.

Rearrangement of the N-terminal arm of the coat protein

The fluorescence results obtained for the labeled mutant coat proteins F11C and L14C indicate a location of the AEDANS probe relatively far from the membrane surface (see Figure 3). This effect may be related to the substitution of the hydrophobic amino acids phenylalanine and leucine, respectively, by a labeled cysteine. This substitution probably affects the membrane-anchoring properties of the N-terminal protein arm. To investigate this effect more closely, double-mutants were prepared based on the A7C mutant. An additional hydrophobic residue on position 10 (A7C/A10I) results in a somewhat decreased polarity surrounding the AEDANS at position 7 (see Table 1). This suggests that the N-terminal arm becomes closer to the membrane surface when it contains more hydrophobic amino acid residues. In contrast, substitution of the hydrophobic amino acid residues phenylalanine and leucine by alanine results in a substantially increased polarity (see Table 1). Similar effects are observed in case of substitution of lysine by alanine, and by replacement of the hydrophobic leucine by the negatively charged aspartic acid. This means that, on the average, the N-terminal arm (probed at position 7) is located more outside the membrane. This indicates a loss of membrane-anchoring capacity and a rearrangement of the N-terminal protein part with respect to the membrane surface. From these experiments, it follows that by slight modifications in the polar-hydrophobic balance of the amphipathic N-terminal protein part the L-shaped configuration can easily change into a more extended one, perpendicular to the membrane surface.

Phospholipid composition

Other factors that could affect the configuration of the N-terminal part of the protein may be related to the phospholipid composition of the membranes as well as the lipid to protein ratio. The phospholipid composition of the inner membrane of *E.coli* is about 70% phosphatidylethanolamine (PE), 25% phosphatidylglycerol (PG), and 5% cardiolipin (*41, 42*). During the normal development of the bacteriophage M13 infection process, the phospholipid composition of the inner membrane is little affected in favor of the charged phospholipids PG and especially CL (*43-45*). It has been shown that accumulation of high amounts of the major coat protein in the inner membrane result in significantly increased levels of CL and PG, and a compensating decline in PE (*41, 43, 45*). This strongly suggests a role of CL and PG in conserving the functional state of the membrane-bound coat protein. The effect of the composition of the model membranes used in our experiments is shown in Table 2. From this table it is clear that the influence of the phospholipid head-group composition on the fluorescence results is small. This result indicates that within the range thought to be relevant in vivo, the membrane composition can be excluded as a direct factor in the structural rearrangement of the N-terminal arm.

Space-limiting effects

Local accumulation of major coat proteins possibly may create a lack of space at the membrane surface. It can easily be imagined that the N-terminal part of the protein partially embedded in the phospholipid head-group region will occupy more space in the membrane as compared to an extended configuration. Experimentally, the position of the N-terminal protein part can be forced to adapt just by varying the lipid to protein ratio. As shown in Figure 4, a more polar environment and increased quenching efficiency of acrylamide can be seen around L/P 20-35. This effect can be explained by assuming that the N-terminal arm moves away from the membrane surface. From these results we conclude that effects related to membrane-anchoring and space-limiting effects are key factors for the structural rearrangement of the N-terminal arm of the membrane-bound major coat protein.

Conclusions

In previous structural views of the membrane-bound state of the M13 coat protein, the protein is in an L-shape in which the N-terminal arm is embedded along the membrane surface (*16-18*). In the present work, it is demonstrated that the N-terminal arm can exist in an L-shape as well as in a more extended I-shape. The N-terminal arm of the membrane-associated coat protein is not just firmly fixed to the membrane and can move off the membrane surface and into solution. Apparently, there is no tight association of the N-terminal arm to the membrane surface. This structural modulation may have consequences for the protein in its role in the assembly process of the phage. During assembly the proteins must come together in the membrane. This requires a close approach of the transmembrane domains of the coat protein, which may be hindered by steric effects of the protein in the L-shape. However, as the N-terminal arm of the membrane-bound protein is loosely associated to the membrane, it can easily adapt to a more extended I-shape. In this state, the protein also has the proper configuration to form the viral coat, enabling fast and efficient phage assembly.

References

1. Model, P., and Russel, M. (1988) *Filamentous Bacteriophage*, Plenum Press, New York.
2. Russel, M. (1995) *Trends Microbiol. 3*, 223-8.
3. Webster, R. E. (1996) *Biology of the filamentous bacteriophage*, Academic Press Inc, 525 B Street/Suite 1900/San Diego/CA 92101-4495.
4. Marvin, D. A. (1998) *Curr. Opin. Struct. Biol. 8*, 150-158.
5. Spruijt, R. B., and Hemminga, M. A. (1991) *Biochemistry 30*, 11147-11154.
6. Li, Z. M., Glibowicka, M., Joensson, C., and Deber, C. M. (1993) *J. Biol. Chem. 268*, 4584-4587.
7. Stopar, D., Jansen, K. A. J., Pali, T., Marsh, D., and Hemminga, M. A. (1997) *Biochemistry 36*, 8261-8268.
8. Haigh, N. G., and Webster, R. E. (1998) *J. Mol. Biol. 279*, 19-29.
9. Almeida, F. C. L., and Opella, S. J. (1997) *J. Mol. Biol. 270*, 481-495.
10. Papavoine, C. H. M., Christiaans, B. E. C., Folmer, R. H. A., Konings, R. N. H., and Hilbers, C. W. (1998) *J. Mol. Biol. 282*, 401-419.
11. Spruijt, R. B., Wolfs, C. J. A. M., Verver, J. W. G., and Hemminga, M. A. (1996) *Biochemistry 35*, 10383-10391.
12. Stopar, D., Spruijt, R. B., Wolfs, C. J. A. M., and Hemminga, M. A. (1996) *Biochemistry 35*, 15467-15473.
13. Kyte, J., and Doolittle, R. F. (1982) *J. Mol. Biol. 157*, 105-32.
14. Turner, R. J., and Weiner, J. H. (1993) *Biochim. Biophys. Acta 1202*, 161-168.
15. Papavoine, C. H. M., Remerowski, M. L., Horstink, L. M., Konings, R. N. H., Hilbers, C. W., and van de Ven, F. J. M. (1997) *Biochemistry 36*, 4015-4026.
16. McDonnell, P. A., Shon, K., Kim, Y., and Opella, S. J. (1993) *J. Mol. Biol. 233*, 447-463.
17. Marassi, F. M., Ramamoorthy, A., and Opella, S. J. (1997) *Proc. Natl Acad. Sci. USA 94*, 8551-8556.
18. Wolkers, W. F., Spruijt, R. B., Kaan, A., Konings, R. N. H., and Hemminga, M. A. (1997) *Biochem. Biophys. Acta 1327*, 5-16.
19. Marvin, D. A., Hale, R. D., Nave, C., and Citterich, M. H. (1994) *J. Mol. Biol. 235*, 260-286.
20. Tan, W. M., Jelinek, R., Opella, S. J., Malik, P., Terry, T. D., and Perham, R. N. (1999) *J. Mol. Biol. 286*, 787-796.
21. Meijer, A. B., Spruijt, R. B., Wolfs, C., and Hemminga, M. A. (2000) *Biochemistry 39*, 6157-6163.
22. Flitsch, S. L., and Khorana, H. G. (1989) *Biochemistry 28*, 7800-7805.

23. Lakey, J. H., Baty, D., and Pattus, F. (1991) *J. Mol. Biol. 218*, 639-53.
24. Jones, P. C., Sivaprasadarao, A., Wray, D., and Findlay, J. B. C. (1996) *Mol. Membr. Biol. 13*, 53-60.
25. Eftink, M. R., and A., G. C. (1981) *Anal. Chemistry 114*, 199-227.
26. Hudson, E. N., and Weber, G. (1973) *Biochemistry 12*, 4154-61.
27. Van Wezenbeek, P. M. G. F., Hulsebos, T. J. M., and Schoenmakers, J. G. G. (1980) *Gene 11*, 129-48.
28. Tabor, S. (1990) in *Curr. Prot. Mol. Biol.* (Ausubel, F. A., Brent, R., Kingston, R.E., Moore, D.D., Seidman, J.G., Smith, J.A. and Struhl, K., Ed.) pp 16.2.1-16.2.11, Green Publishing and Wiley-Interscience, New York.
29. Studier, F. W., Rosenberg, A. H., Dunn, J. J., and Dubendorf, J. W. (1990) *Methods Enzymol. 185*, 60-89.
30. Schägger, H., and Von Jagow, G. (1987) *Anal. Biochem. 166*, 368-79.
31. Sambrook, J., Fritsch, E. F., and Maniatis, T. (1989) *Molecular Cloning: A laboratory manual*, Cold Spring Harbor Laboratory, New York.
32. Spruijt, R. B., Wolfs, C. J. A. M., and Hemminga, M. A. (1989) *Biochemistry 28*, 9158-65.
33. Endemann, H., and Model, P. (1995) *J. Mol. Biol. 250*, 496-506.
34. Kuhn, A., and Wickner, W. (1985) *J. Biol. Chem. 260*, 15907-13.
35. Russel, M., and Kazmierczak, B. (1993) *J. Bacteriol. 175*, 3998-4007.
36. LaPorte, D. C., Keller, C. H., Olwin, B. B., and Storm, D. R. (1981) *Biochemistry 20*, 3965-3972.
37. Lehrer, S. S., and Leavis, P. C. (1978) *Methods Enzymol. 49*, 222-236.
38. Mandal, K., and Chakrabarti, B. (1988) *Biochemistry 27*, 4564-4571.
39. Ren, J., Lew, S., Wang, Z., and London, E. (1997) *Biochemistry 36*, 10213-20.
40. Bogusky, M. J., Leo, G. C., and Opella, S. J. (1988) *Proteins: Struct. Funct. Genet. 4*, 123-30.
41. Woolford, J. L., Jr., Cashman, J. S., and Webster, R. E. (1974) *Virology 58*, 544-60.
42. Burnell, E., Van Alphen, L., Verkleij, A., and De Kruijff, B. (1980) *Biochim. Biophys. Acta 597*, 492-501.
43. Ohnishi, Y. (1971) *J. Bacteriol. 107*, 918-25.
44. Chamberlain, B. K., and Webster, R. E. (1976) *J. Biol. Chem. 251*, 7739-45.
45. Pluschke, G., Hirota, Y., and Overath, P. (1978) *J. Biol. Chem. 253*, 5048-55.

Chapter 3

Configurations of the N-terminal amphipathic domain of the membrane-bound M13 major coat protein

Alexander B. Meijer, Ruud B. Spruijt, Cor J. A. M. Wolfs,
and Marcus A. Hemminga

Abstract

The M13 major coat protein has been extensively studied in detergent-based and phospholipid model systems to elucidate its structure. This resulted in an L-shaped model structure of the protein in membranes. An amphipathic α-helical N-terminal arm, which is parallel to the surface of the membrane, is connected via a flexible linker to an α-helical transmembrane domain. In the present study, a fluorescence polarity probe or ESR spin probe is attached to the SH group of a series of N-terminal single cysteine mutants, which were reconstituted into DOPC model membranes. With ESR spectroscopy, we measured the local mobility of N-terminal positions of the protein in the membrane. This is supplemented with relative depth measurements at these positions by fluorescence spectroscopy via the wavelength of maximum emission and fluorescence quenching. Results show the existence of at least two possible configurations of the M13 amphipathic N-terminal arm on the ESR time scale. The arm is either bound to the membrane surface, or in the water phase. The removal or addition of a hydrophobic membrane-anchor by site-specific mutagenisis changes the ratio between the membrane-bound and the water phase fraction.

Introduction

The M13 major coat protein of the filamentous bacteriophage M13 is studied to elucidate fundamental questions involving protein-DNA, protein-lipid, and protein-protein interactions. With about 2800 copies, the M13 major coat protein is most abundant protein in the phage, where it protects the single stranded viral DNA (for a review see, Marvin et al. (1998) (*1*)). During the infection of the *E. coli* cell, newly synthesized protein is stored into the inner membrane before it is used in the production of new bacteriophages (*2*). For understanding the mechanisms involved in the viral reproduction cycle, knowledge is essential about the membrane-bound assembly, and dynamics of the M13 coat protein.

The primary structure of the coat protein consists of 50 amino acids (Figure 1) in which three domains can be distinguished: an acidic amphipathic N-terminal arm, a hydrophobic segment, and a basic C-terminus (*3, 4*). The protein has been extensively studied in membrane-model systems by biophysical techniques. These studies resulted in an L-shaped structure of the protein in a membrane (*5-7*). In this model, an amphipathic N-terminal helix is oriented parallel to the surface of the membrane, and is connected with a flexible linker to a transmembrane α-helix. The assignments of amino acids in the helical domains are schematically depicted in Figure 1. The N-terminal segment of SDS-bound M13 coat protein showed dynamics on the picosecond and nanosecond time scale as was shown by NMR spectroscopy (*8, 9*).

Relative depth and local dynamics of specific sites in the protein, reconstituted in phospholipid model membranes, were measured by a single cysteine-scanning approach. In this approach, a fluorescence or ESR probe was attached to specific sites in the M13 major coat protein (*10-12*). Fluorescence quenching, magnetization quenching, mobility, and polarity probing showed a surprisingly deep burial of the C-terminal lysine residues in the membrane. In contrast the two phenylalanines are in a more shallow position. The organization of those amino acids are suggested to comprise an anchor of the C-terminal end to the membrane (*10, 11*). Furthermore, a fluorescence study showed the importance of leucine 14 and phenylalanine 11 for the anchoring interactions of the amphipathic N-terminal arm to the membrane. Replacement of those amino acids residues by alanines resulted in a more extended configuration of the N-terminal arm (see, chapter 2 of this thesis, (*12*)).

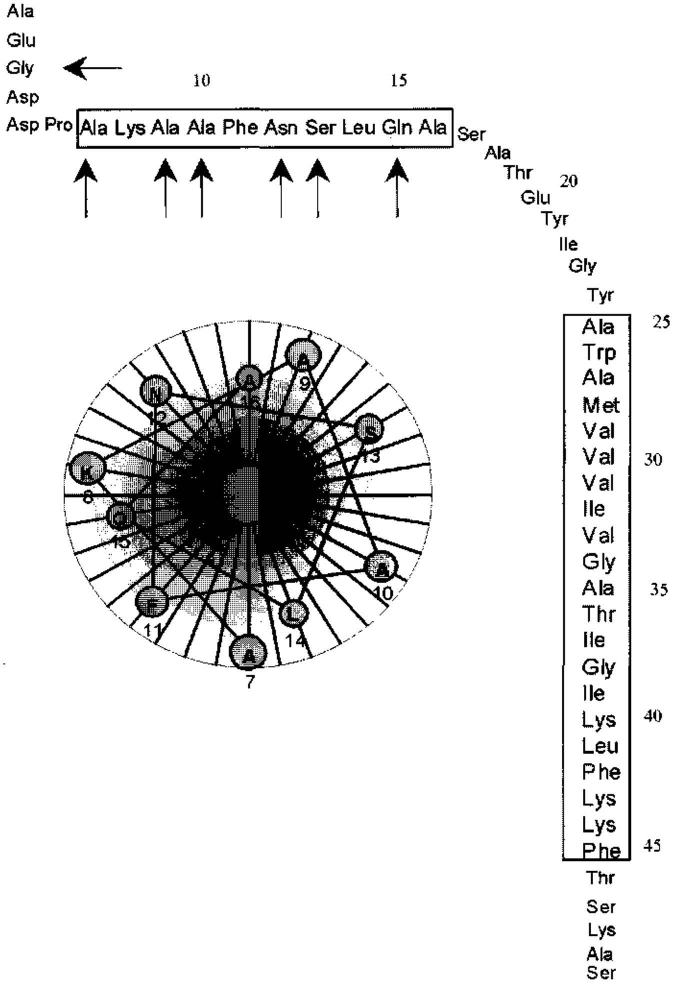
Ala
Glu
Gly
Asp
Asp Pro
10
15
Ala Lys Ala Ala Phe Asn Ser Leu Gln Ala
Ser
Ala
Thr
20
Glu
Tyr
Ile
Gly
Tyr
Ala
25
Trp
Ala
Met
Val
Val
30
Val
Ile
Val
Gly
Ala
35
Thr
Ile
Gly
Ile
Lys
40
Leu
Phe
Lys
Lys
Phe
45
Thr
Ser
Lys
Ala
Ser
A 9
A 16
N 12
S 13
K 8
Q 15
A 10
F 11
L 14
A 7

Figure 1: Arbitrary representation of the primary structure of the M13 major coat protein (*3*). The arrows point to the positions that are mutated into cysteine residues. The boxed regions represent the amphipathic and transmembrane helix (*9, 26*). The inset shows amino acids 7 to 16 in a α-helix.

Site-specific spin labeling has been employed for a number of membrane and soluble proteins to obtain structural information (*13, 14*). The dynamics of nitroxide spin labels are significantly affected by the local structure and environment of the position to which they are attached to the M13 protein (*11*). In the present study, additional information is obtained about the N-terminal section of the protein, reconstituted in DOPC, by using ESR and fluorescence spectroscopy. Our results indicate the presence of a membrane-bound and a more extended configuration of the N-terminal section of the protein.

Materials and methods

Preparation and purification of labeled single cysteine mutants

Site-specific cysteine mutants were prepared with the QuikChange™ Site-Directed Mutagenisis Kit from Stratagene. The vector pT7-7, with the major coat protein geneVIII as insert was used as the template for this procedure. The oligo-nucleotides were purchased from Amersham Pharmacia Biotech. The sequence of the mutant DNA was verified using automated DNA sequencing. Correctly mutated plasmid DNA was transformed into competent *E. coli* BL21(DE3) cells (*15*).

Mutant M13 coat protein was purified, and labeled with IAEDANS as is described by Spruijt et al. (see, chapter 2 of this thesis (*12*)). First was mutant protein overexpressed in *E. coli,* and the membrane fraction was collected. Secondly, the membrane proteins were extracted from the membrane, and separated on hydrophobicity using reversed phase chromatography. After this step, the about 85% pure mutant coat protein was in a mixture of 35% isopropanol/water (v/v) and 0.1% triethylamine (v/v). The mutant coat protein was subsequently labeled with IAEDANS (Molecular Probes) or maleimido-proxyl (Sigma). Slight modifications were introduced in the procedure for the attachment of 3-maleimido-proxyl spin label to the single cysteine mutants. An excess of spin-label was added to the protein fraction after reversed phase chromatography. The label was allowed to react with the SH-groups of the mutants for 30 min at 20°C. The labeling reaction was stopped by an addition of an excess of β-mercaptoethanol. In the final step, free label and remaining impurities were removed from the labeled mutant coat proteins using size exclusion chromatography. The about 95% pure protein, labeled with IAEDANS or maleimido-proxyl, was now in a buffer containing 50 mM cholate, 10 mM Tris-HCl, 1 mM EDTA, 150 mM NaCl at pH 8.

Reconstitution of labeled M13 coat protein

Labeled M13 major coat protein was reconstituted into DOPC (Avanti polar lipids) using the cholate-dialysis method (*16*). The amount of protein was chosen such that the lipid-to-protein molar ratio (L/P) was about 100. Samples contained about 4 mg of phospholipids for ESR spectroscopy and about 1 mg for fluorescence spectroscopy. Chloroform was evaporated from the desired amount of phospholipid solution and the residual traces of chloroform were removed by drying under vacuum for at least two hours. The lipids were subsequently solubilized in 50 mM cholate, 1 mM EDTA, 150 mM NaCl, 10 mM Tris-HCl, pH 8, and mixed with labeled protein. In the following step, the lipid-protein mixture was dialyzed for 60 hours against a 100-fold excess buffer containing 1 mM EDTA, 150 mM NaCl, 10 mM Tris-HCl at pH 8. The buffer was replaced every 12 hours.

Steady-state fluorescence spectroscopy

Fluorescence spectra of the labeled mutants were collected at 22±0.5°C using an excitation wavelength of 340 nm on a SPEX Fluorolog 3-22 fluorometer equipped with a 450 W Xenon lamp as an excitation source. Excitation and emission bandwidths were set to 1 and 3 nm, and spectra were recorded between 400 and 600 nm. 1 ml samples were in 1 cm light-path fused silica cuvettes (Hellma model 114F-QS), and the optical density at 340 nm never exceeded 0.1. The spectra were corrected for background signal (empty vesicles) and sensitivity of the photomultiplier. The wavelength of maximum emission (λ_{max}) was obtained from the fluorescence data

Fluorescence quenching data were obtained and analyzed as described by Meijer et al., 2000 (*17*). Aliquots of an acrylamide stock solution (3 M acrylamide, 150 mM NaCl, 10 mM Tris-HCl, 1 mM EDTA, pH 8) were added to samples of labeled protein that was reconstituted into in DOPC. After every addition of acrylamide, the decrease in fluorescence intensity was measured. Appropriate corrections for dilution were made for these quenching experiment. The Stern-Volmer constant (K_{sv}) was obtained from the fluorescence data (*18, 19*) according to the Stern-Volmer equation for colisional quenching:

$$\frac{F_o}{F} = 1 + K_{sv}[Q]$$

where F_0 and F are the fluorescence intensities in the absence and the presence of the quencher Q. K_{sv} is the Stern-Volmer quenching constant.

ESR spectroscopy

A comparable experimental set up was used as is described in Stopar et al. 1996 (*20*). 1 ml samples of reconstituted mutant coat protein were freeze-dried overnight, and dissolved in 10 mM Tris-HCl, 1 mM EDTA, 150 mM NaCl, pH 8, yielding multilamellar vesicles. The vesicles were concentrated by centrifugation at 20,000 rpm in a Beckman Ti75 rotor at 20°C. 50 µl glass capillaries were filled up to 5 mm with vesicles containing labeled mutant coat protein. These capillaries were inserted into standard 4 mm diameter quartz tubes. ESR spectra were recorded on a Bruker ESP 300E ESR spectrometer equipped with a 108TMH/9103-microwave cavity. The temperature was regulated with a nitrogen gas-flow temperature system. The ESR settings for all recorded spectra were: 6.38 mW microwave power, 0.1 mT modulation amplitude, 40 ms time constant, 160 s scan time, 10 mT scan width, and a 342.0 mT center field. Up to 20 recorded spectra were accumulated.

Stopar et al. 1996 (*20*) calculated the rotational correlation time τ_c for the labeled A49C and S30C mutants according to Marsh et al. (*21*). The same approach was used to calculate the rotational correlation time of mobile single component spectra (10^{-11} s $\leq \tau_c \leq$ $3\text{x}10^{-9}$ s). It is not possible to characterize the rotational mobility of the mobile component in spectra, which display two spectral components. Especially, the center linewidth is distorted because of the overlap of the spectral components. However, τ_c was estimated using the line width of the high field line. For this purpose, the single component spectrum of the A7C/L14A mutant was recorded at various temperatures, and τ_c was subsequently calculated according to Marsh et al. (*21*). By plotting the line width vs. τ_c, a reference is acquired for the corresponding τ_c in the mixed spectra.

To determine the amount of non-specific labeling of mutant coat protein with 3-maleimido-proxyl, the purification and labeling procedure was repeated for the wild-type coat protein. Labeled wild-type protein was reconstituted into DOPC and the ESR spectrum was recorded. The result showed the presence of a small amount (about 5%) of non-specific labeling for all mutant coat proteins.

Results

The ESR spectra of the A7C, A7C/A10I, Q15C, Q15C/L14A, and Q15C/A10I mutants (in DOPC) displayed a superposition of two components at 20°C. The resolution between both components was enhanced at lower temperatures, therefore, the spectra were acquired at 5°C.

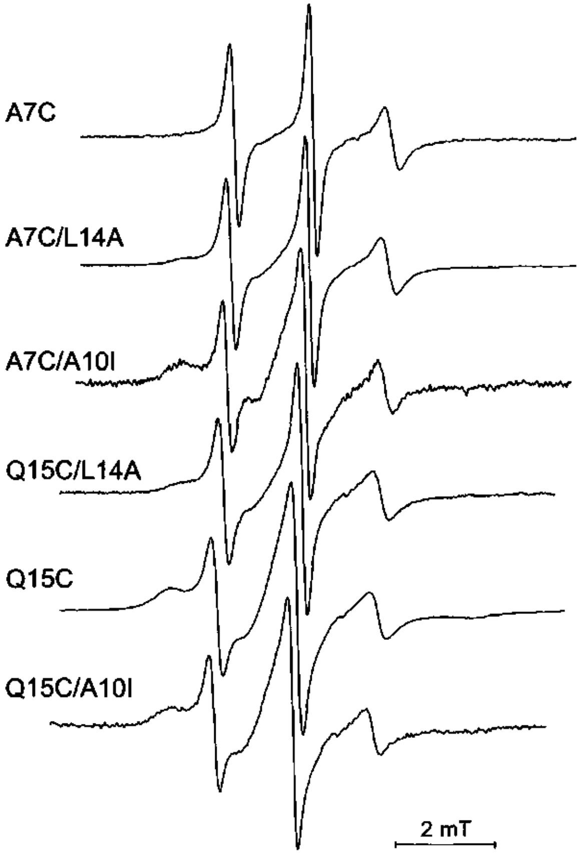

Figure 2: ESR spectra of the 3-maleimido proxyl site-specific labeled A7C/L14A, A7C, A7C/A10I, Q15C/L14A, Q15C and Q15C/A10I mutants, which were reconstituted into DOPC multilamellar vesicles at L/P 100 in 150 mM NaCl, 10 mM Tris-HCl,1 mM EDTA, pH 8 at 5°C. The central spectral line-heights are normalized to each other.

The spectra consisted of a sharp three-line spectrum representing mobile probes on the ESR time-scale (10^{-11} s $\leq \tau_c \leq 3 \times 10^{-9}$ s), and a broad spectral component indicative for motion in the slow regime ($\tau_c \geq 2 \times 10^{-9}$ s) *(21)*. On the other hand, the spectrum of the A7C/L14A mutant only consisted of a mobile component. Figure 2 shows the spectra of the A7C, A7C/L14A, A7C/A10I, Q15C/L14A, Q15C, and Q15C/A10I mutants. An estimate of the immobile fraction was acquired in a subtraction procedure by using the spectrum of the A7C/L14A mutants as a reference. Table 1 shows the estimated fractions of immobile component per mutant.

Table 1: The environmental polarity and Stern-Volmer quenching constant of A7C-derived mutants in DOPC/DOPG (4/1 molar ratio) and Q15C- derived mutants in DOPC, and the fraction immobile ESR spectral component of the A7C and Q15C-derived mutants in DOPC. * Wavelengths of maximum emission (λ_{max}) and Stern-Volmer constant (K_{sv}) were measured by Spruijt et al., 2000 (see, chapter 2 of this thesis *(12)*) on AEDANS labeled A7C-derived mutant coat proteins, which were reconstituted into DOPC/DOPG (4/1 molar ratio) at an L/P of 100. Acrylamide was used as a fluorescence quencher.

Mutant	λ_{max}	K_{sv} (M^{-1})	Estimated fraction Immobile component in the ESR spectrum (%)
A7C	495*	3.0*	33
A7C/L14A	502*	5.4*	-
A7C/A10I	492*	2.6*	75
Q15C	492	1.2	77
Q15C/L14A	497	1.9	53
Q15C/A10I	491	0.9	80

Spruijt et al. (2000) labeled the A7C, A7C/L14A, and A7C/A10I with IAEDANS, and the mutants were reconstituted into DOPC/DOPG (4:1 molar ratio) to obtain the relative depth of the probe in the membrane. In the present study, this approach was repeated for the Q15C, Q15C/L14A, and Q15C/A10I mutants, which were reconstituted into DOPC for optimal comparison with the ESR spectra. The fluorescence data of the Q15C, Q15C/L14A, and Q15C/A10I are shown in Table 1. This table also shows the results from the fluorescence study by Spruijt et al. (2000) (*12*).

ESR spectra of the seven labeled single-cysteine mutants (indicated in Figure 1) were recorded to study the properties of the N-terminus of the M13 major coat protein. Except from the G3C spectrum, the spectra clearly show two spectral components. Figure 3 shows the spectra of the G3C, A9C, A10C, N12C, and S13C mutants reconstituted into DOPC.

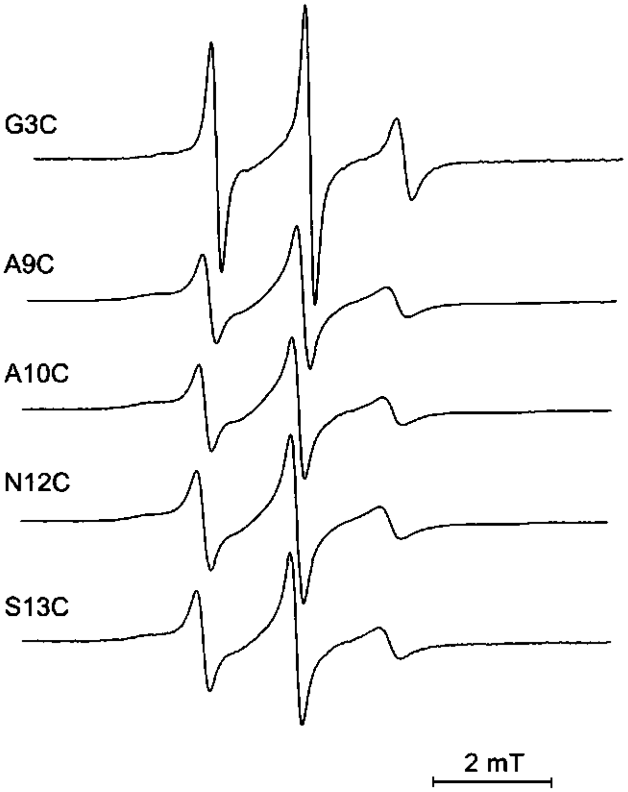

Figure 3: ESR spectra of the 3-maleimido proxyl site-specific labeled G3C, A9C, A10C, N12C, and S13C mutants, which were reconstituted into DOPC multilamellar vesicles at L/P 100 in 150 mM NaCl, 10 mM Tris-HCl, 1 mM EDTA, pH 8 at 5°C. The spectra are normalized to one in the double intregral.

The fraction of immobile component was again estimated from the spectra (Figure 4). Only a small fraction of the G3C mutant spectrum consisted of immobile component, therefore, the immobile fraction was set to zero percent. A rotational correlation time τ_c was calculated from the single component spectra of the A7C/L14A and G3C mutants. This resulted in a τ_c of about 1.1 ns. The estimated rotational correlation time of the mobile components in the mixed spectra was about 1.4 ns for the A7C mutant, and about 1.7 ns for the mutants with a cysteine at the positions 9, 10, 12, 13 and 15. The outer hyperfine splitting $2A_{zz}$ of the immobile component was between 5.9 and 6.0 mT in the mixed spectra of the mutant coat proteins.

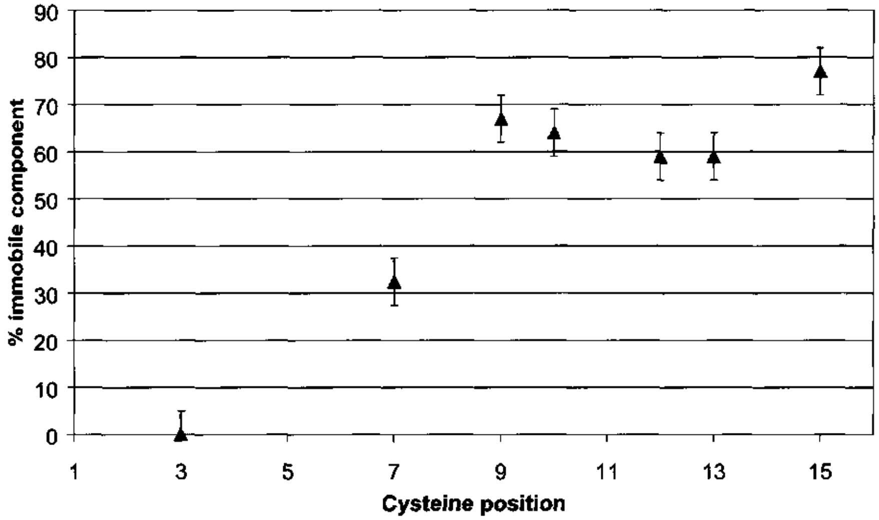

Figure 4: Estimated fraction of immobile component from the ESR spectra of 3-maleimido proxyl site-specific spin-labeled mutant coat proteins at various positions. The labeled proteins were reconstituted in DOPC multilamellar vesicles at L/P 100 in 150 mM NaCl, 10 mM Tris-HCl, 1 mM EDTA, pH 8 at 5°C. The A7C/L14A spectrum was used as a reference in the spectral subtraction procedure.

Discussion

With the cysteine scanning approach, information can be obtained at specific sites in the reconstituted M13 coat protein (*10-12, 20*). The relative depth of sites in the membrane was assessed by attaching the fluorescence polarity probe IAEDANS to mutant proteins. The depth was subsequently determined via the wavelength of maximum emission (λ_{max}), because probes have a more red-shifted λ_{max} outside than inside the membrane (*10, 12, 17, 22*). This was further substantiated by using fluorescence quenchers that predominantly affect probes inside (5-SASL) or outside (acrylamide) the membrane.

By using the above mentioned approach (see, chapter 2 of this thesis, *12*), the importance is shown of phenylalanine 11 and leucine 14 for the anchoring interactions of the amphipathic N-terminal arm to the surface of a DOPC/DOPG (4/1 molar ratio) model membrane. After replacement of leucine 14 by an alanine, the monitored position 7 moved towards the water phase. On the other hand, the replacement of alanine 10 for an isoleucine resulted in a deeper burial of position 7 into the membrane (see, table 1).

In the present study, the N-terminal arm is studied with spin label ESR spectroscopy. The spin probe 3-maleimido-proxyl, which is used in this study, is smaller in size than the IAEDANS probe, and mainly provides information about the local dynamics of the site to which the probes is attached. Surprisingly, the ESR data of the 3-maleimido-proxyl labeled position 7 shows the presence of two species of motion on the ESR time scale, represented by broad and a sharp spectral component. The sharp component exhibited an isotropic hyperfine splitting of about 1.6 mT. Earlier studies with 3-maleimido-proxyl, and related nitroxide probes have shown that this is an indication for a hydrophilic environment (*20, 23*).

The replacement of hydrophobic leucine 14 by alanine, which decreases the anchoring capacity of the N-terminus to the surface of the membrane, results in the disappearance of the broad component in the spectrum of the A7C/L14A mutant. As compared to the mobile component in the spectrum of A7C mutant, the rotational correlation time slightly decreases in the spectrum of the A7C/L14A mutant. This suggests a higher segmental motion at this position. This change in mobility can not be caused by a dramatic change in secondary structure, because no conformational change was detected with CD spectroscopy in the L14A and A10I mutant coat proteins (*12*). The mutation of an alanine 10 to an isoleucine, which increases the anchoring capacity of the N-terminal arm to the surface of the membrane, results in a higher fraction of immobile component. This components increases with about 42% upon comparing the spectra of the A7C and A7C/A10I mutant (see, Table 1). The combination of the fluorescence and ESR results strongly suggests that the mobile component represents a position in the water phase, and the immobile component a membrane-bound fraction of the protein.

The replacement of leucine 14 by alanine has an effect throughout the N-terminal section of the protein as is demonstrated with the Q15C and Q15C/L14A mutants. The λ_{max} of AEDANS is red-shifted by 5 nm as a result of the mutation, which suggests a more polar environment for position 15. This is in agreement with the finding that the probe is also more easily quenched by acrylamide, as is demonstrated by the higher Stern-Volmer constant (Table 1). Finally, the ESR data show a decrease of 24% in the fraction of immobile component in the Q15C/L14A mutant as compared to the ESR data of the Q15C mutant. These results show that the monitored position 15 shifts towards the water phase when the hydrophobic "membrane-anchor" leucine 14 is replaced by an alanine.

However, the immobile component does not completely disappear, as is the case in the spectrum of the A7C/L14A mutant. In other words, about 53% of the N-terminal arms remain bound to the surface of the membrane in the Q15C/L14A mutant on the ESR time-scale (Table 1). This shows that the N-terminus does not entirely shifts to the water phase as a result of the removal of leucine 14. Position 15 in the Q15C/A10I mutant is hardly sensitive to the addition of the hydrophobic amino acid isoleucine at position 10. The ESR spectrum of the Q15C/A10I mutant showed only a small increase of about 3% in the fraction of immobile component as compared to the Q15C mutant. Such a small effect is also seen in the fluorescence results (Table 1). This apparent insensitivity to the additional "anchoring" amino acid isoleucine (with position 7 being highly sensitive) shows that position 15 is close to a hinge point when the N-terminal arm is more tightly bound to the surface of the membrane.

The ESR data of the measured positions in the N-terminal section of the protein clearly show the presence of two fractions at every position (Figure 3). The positions 9 to 13 show an about equal membrane-bound fraction of about 65%. Position 7 displays a smaller membrane-bound fraction of 30%. This is not a surprise, since it is close to the unstructured (acidic) end of the protein, which is probably most of the time in the water phase. On the contrary, position 15 exhibits a higher percentage (77%) of membrane-bound fraction. Fluorescence quenching results by Spruijt et al. (2000) showed that position 15 is buried deeper into the membrane as compared to the other N-terminal positions. It should be noted that the amino acid residues 17 to 24 between the amphipathic N-terminal arm and the transmembrane helix are even deeper buried in the membrane (*12*). This can explain the higher membrane-bound fraction in the spectrum of position 15.

Information about local dynamics at the labeled positions can be obtained from the spectral components in the spectra. The motion of the spin probe attached to the protein will be determined by the local environment as well as the local conformation of the protein. The hyperfine splitting $2A_{zz}$ of 5.9-6.0 mT of the broad membrane-bound component in the ESR spectra is less than the rigid limit nitroxide spectrum (≈7.0 mT). Probably, the spin label 3-maleimido-proxyl exhibits a wobbling motion in a cone at the cysteine residue as was suggested in earlier studies with 3-maleimido-proxyl labeled protein (*20, 24, 25*). The membrane-bound components in the spectra do not reveal much details about the local mobility. However, it is conceivable that the probes in this membrane-bound fraction represent the N-terminal amphipathic helix in the L-shaped model of the protein. One would expect that probes at positions facing the water phase side of the helix exhibit a higher mobility than do probes facing the membrane side of the helix. Indeed, $2A_{zz}$ of the positions 9, 12 and 13 are smaller than $2A_{zz}$ of the positions 7, 10 and 15 (5.9 mT vs. 60 mT). However, these differences in $2A_{zz}$ are too small to draw reliable conclusions about changes in the probe mobility of the membrane-bound fractions. The mobility of the spin-probes is apparently mainly affected by the local structure of the N-terminal helix.

The linewidth of the mobile components from the single cysteine mutant spectra result in a rotational correlation time (τ_c) between 1.1 and 1.7 ns. Apparently, there is a higher backbone mobility in the water-phase fraction as compared to the membrane bound fraction of the N-terminal arm of the protein. Interestingly, the measured rotational correlation times of the water-phase fraction correspond to a motional freedom in the nanosecond time scale, similar as found for the N-terminal part of SDS-dissolved M13 coat protein with NMR spectroscopy (*8, 9*). The local conformation of the N-terminal arm probably unfolds when the N-terminal arm is relocated to the water phase, which subsequently produces the higher backbone mobility. The relocation of the N-terminal arm from the water phase to the surface of the membrane, and subsequent refolding into the amphipathic helix is sufficiently slow (on the ESR time scale) to detect two clearly resolved spectral components.

Conclusion

With a cysteine scanning approach, information about dynamics and penetration depth in a phospholipid model membrane can be acquired of specific sites in the protein. The amphipathic N-terminal section of the M13 major coat protein exists in at least two possible configurations. One fraction of the protein has its N-terminal arm in the water phase. In the other fraction, the N-terminus is bound to the surface of the membrane. The water phase component shows high segmental (backbone) mobility. On the contrary, the membrane-bound N-terminus is much slower in motion, and probably represents the "L-shaped" structure of the protein. The ratio between both fractions can be modified by the addition or removal of an hydrophobic "membrane-anchor".

References

1. Marvin, D. A. (1998) *Curr. Opin. Struct. Biol. 8*, 150-158.
2. Mandel, G., and Wickner, W. (1979) *Proc. Natl. Acad. Sci. USA 76*, 236-40.
3. Van Wezenbeek, P. M. G. F., Hulsebos, T. J. M., and Schoenmakers, J. G. G. (1980) *Gene 11*, 129-48.
4. Marvin, D. A., Hale, R. D., Nave, C., and Citterich, M. H. (1994) *J. Mol. Biol. 235*, 260-286.
5. McDonnell, P. A., Shon, K., Kim, Y., and Opella, S. J. (1993) *J. Mol. Biol. 233*, 447-463.
6. Wolkers, W. F., Spruijt, R. B., Kaan, A., Konings, R. N. H., and Hemminga, M. A. (1997) *Biochem. Biophys. Acta 1327*, 5-16.
7. Marassi, F. M., Ramamoorthy, A., and Opella, S. J. (1997) *Proc. Natl. Acad. Sci. USA 94*, 8551-8556.
8. Papavoine, C. H. M., Remerowski, M. L., Horstink, L. M., Konings, R. N. H., Hilbers, C. W., and van de Ven, F. J. M. (1997) *Biochemistry 36*, 4015-4026.
9. Almeida, F. C. L., and Opella, S. J. (1997) *J. Mol. Biol. 270*, 481-495.
10. Spruijt, R. B., Wolfs, C. J. A. M., Verver, J. W. G., and Hemminga, M. A. (1996) *Biochemistry 35*, 10383-10391.
11. Stopar, D., Jansen, K. A. J., Pali, T., Marsh, D., and Hemminga, M. A. (1997) *Biochemistry 36*, 8261-8268.
12. Spruijt, R. B., Meijer, A. B., Wolfs, C. J. A. M., and Hemminga, M. A. (2000) *Biochim. Biophys. Acta. 1509, 311-323*
13. Hubbell, W. L., and Altenbach, C. (1994) *Curr. Opin. Struct. Biol. 4*, 566-573.
14. Hubbell, W. L., Gross, A., Langen, R., and Lietzow, M. A. (1998) *Curr. Opin. Struc. Biol. 8*, 649-656.
15. Studier, F. W., Rosenberg, A. H., Dunn, J. J., and Dubendorf, J. W. (1990) *Methods Enzymol. 185*, 60-89.
16. Spruijt, R. B., Wolfs, C. J. A. M., and Hemminga, M. A. (1989) *Biochemistry 28*, 9158-65.
17. Meijer, A. B., Spruijt, R. B., Wolfs, C., and Hemminga, M. A. (2000) *Biochemistry 39*, 6157-6163.
18. Lehrer, S. S., and Leavis, P. C. (1978) *Methods Enzymol. 49*, 222-236.
19. Lehrer, S., S. (1971) *Biochemistry 10*, 3254-63.
20. Stopar, D., Spruijt, R. B., Wolfs, C. J. A. M., and Hemminga, M. A. (1996) *Biochemistry 35*, 15467-15473.
21. Marsh, D. (1981) in *Membrane Spectroscopy* (Grell, E., Ed.) pp 51-142, Springer-Verlag, Berlin Heidelberg New York.
22. Hudson, E. N., and Weber, G. (1973) *Biochemistry 12*, 4154-61.
23. Fretten, P., Morris, S. J., Watts, A., and Marsh, D. (1980) *Biochim. Biophys. Acta 598*, 247-259.
24. Vriend, G., Schilthuis, J. G., Verduin, B. J. M., and Hemminga, M. A. (1984) *J. Magn. Reson. 58*, 421-7.
25. Hemminga, M. A., and Faber, A. J. (1986) *J. Magn. Reson. 66*, 1-8.
26. Papavoine, C. H. M., Christiaans, B. E. C., Folmer, R. H. A., Konings, R. N. H., and Hilbers, C. W. (1998) *J. Mol. Biol. 282*, 401-419.

Chapter 4

Membrane assembly of the bacteriophage Pf3 major coat protein

Alexander B. Meijer, Ruud B. Spruijt, Cor J.A.M. Wolfs,
and Marcus A. Hemminga

Abstract

The Pf3 major coat protein of the Pf3 bacteriophage is stored into the inner membrane of the infected cell during the reproductive cycle. The protein consists of 44 amino acids, and contains an acidic amphipathic N-terminal domain, a hydrophobic domain, and a short basic C-terminal domain. The mainly α-helical membrane-bound protein traverses the membrane once, leaving the C-terminus in the cytoplasm, and the N-terminus in the periplasm. A cysteine-scanning approach was followed to measure which part of the membrane-bound Pf3 protein is in or outside the membrane. In this approach the fluorescence probe N- ((iodoacetyl)-amino)ethyl-1-sulfonaphthyl-amine (IAEDANS) was attached to single cysteine mutants of the Pf3 coat protein. The labeled mutant coat proteins were reconstituted into the phospholipid model membranes DOPC/DOPG (80/20 mol/mol) and DOPE/DOPG (80/20 mol/mol). We subsequently studied the fluorescence characteristics at the different positions in the protein. We measured the local polarity of the environment of the probe, as well as the accessibility of the probe to the fluorescence quencher acrylamide. The results of this study show a single membrane spanning protein with both the C- and N-terminus remaining close to the surface of the membrane. A nearly identical result was shown earlier for the membrane-bound M13 coat protein. Based on a comparison between the results from both studies, we suggest an "L-shaped" membrane-bound model for the Pf3 coat protein. DOPE containing model membranes

revealed a higher polarity, and quenching efficiency in the membrane-water interface. Furthermore, from the outside to the inside of the membrane, a steeper polarity gradient was measured in the PE/PG interface as compared to the PC/PG interface. These results suggest a smaller thickness of the interface of DOPE/DOPG than that of DOPC/DOPG.

Introduction

The subject of this paper is the membrane-bound Pf3 major coat protein of the filamentous bacteriophage Pf3, which specifically infects *Pseudomonas aeruginosa* (*1*). Pf3 bacteriophage belongs to the family of the *Inoviridae*, which all share structural and biological features. In spite of striking similarities in life-cycle processes and structural aspects, the sequence homology of the involved proteins can be low (*2*). Among the best studies filamentous phages are the M13, fd and Pf1 bacteriophages.

The flexible rod-like bacteriophages consist of single-stranded DNA encapsulated by a tubular protein coat. The most abundant protein in this coat is the gene VIII product, which is called the major coat protein. A few copies of minor coat proteins can be found at the tips (for a recent review, see Marvin et al. (*3*)). The coat of the Pf3 bacteriophage consists of about 2500 copies of Pf3 major coat protein (for specific construction details see, Welsh et al. (*4*)). During the reproductive cycle, the major coat protein is stripped from the viral DNA, and stored into the inner membrane of the cell. New major coat proteins are synthesized without a leader sequence, and insert Sec-independently into the membrane. The protein traverses the membrane once, leaving the C-terminus in the cytoplasm, and the N-terminus in the periplasm (*5, 6*).

The biological aspects of the filamentous bacteriophage life-cycle have been studied for several years as model systems for a wide range of complicated biological processes and interactions. A number of processes from the bacteriophage life-cycle serve as model for protein-membrane interactions, macromolecular assembly, and protein-DNA interactions.

In our group we are interested in two different aspects of the membrane-bound Pf3 major coat protein. Firstly, the structure-function relation of the membrane-bound Pf3 major coat protein with respect to the Pf3 bacteriophage life-cycle. To understand this relation, we require information about the topology and conformation of the membrane bound protein. Secondly, because of its relative simplicity, the protein is an excellent model to study fundamental aspects of protein-lipid interactions in detail. Topics of interest are e.g. protein insertion into the membrane, anchoring interactions of proteins with the membrane, and the preferred location of specific amino acids in a phospholipid bilayer.

When looking at the first mentioned aspect, it turns out that only limited structural information is available about the membrane-bound Pf3 major coat protein. The protein consists of 44 amino acids (*7, 8*), in which three domains can be distinguished: a basic C-terminal domain, a hydrophobic domain and an acidic amphipathic N-terminal domain (Figure 1). The membrane-bound protein mainly adopts a α-helical conformation. Results from infrared spectroscopy and circular dichroism showed a α-helical content of about 75% for the membrane-bound Pf3 major coat protein (*9*).

To obtain more knowledge of the structure of the Pf3 coat protein, a comparison can be made with the M13 and Pf1 major coat protein, because much more information is available about these proteins. M13 and Pf1 major coat proteins are extensively studied in detergent micellar and phospholipid model systems. Similar to the Pf3 major coat protein, the primary structures of the M13 (*10*) and Pf1 (*11*) major coat protein reveal a basic C-terminal domain, an acidic amphipathic N-terminal domain and a hydrophobic domain. Biophysical techniques (e.g. NMR) showed two α-helical segments, connected with a flexible linker, in detergent-bound M13 (*12*) and Pf1 (*13*) coat protein. These (and other) studies resulted in an "L-shaped" model structure of the M13 and Pf1 major coat proteins in the membrane. One helix spans the membrane, and the second N-terminal amphipathic helix is parallel to the membrane surface (*13-15*). Since the structural features between the Pf3, M13 and Pf1 bacteriophages are similar, it is interesting to ascertain whether this is also true for both membrane-bound major coat proteins, even though there is no primary sequence homology.

1 5 10
Met-Gln-*Ser*-Val-Ile-Thr-*Asp*-*Val*-*Thr*-Gly-
11 15 20
Gln-*Leu*-*Thr*-Ala-*Val*-Gln-*Ala*-Asp-Ile-*Thr*-
21 25 30
Thr-*Ile*-Gly-Gly-*Ala*-Ile-Ile-*Val*-Leu-Ala-
31 35 40
Ala-Val-Val-*Leu*-Gly-*Ile*-Arg-Trp-*Ile*-Lys
41 44
Ala-Gln-Phe-Phe

Figure 1: Primary structure of the Pf3 major coat protein (*7, 8*). The hydrophobic domain is underlined. The amino acid residues that were replaced for cysteines in the single cysteine mutants are printed in italic. In one of the mutants a cysteine was placed at the C-terminal end of the protein.

Furthermore, our aim is to study which part of the protein is in or outside the membrane to obtain membrane-anchoring information. These interactions can be important for many processes e.g. membrane assembly, topology, and protein insertion (*16*). Anchoring can be accomplished by several factors. Firstly, by hydrophobic interactions with the phospholipid tails that will be mainly determined by the length of the transmembrane helix. The α-helices generally contain 20 amino acids or more, and consists of highly non-polar residues. The Pf3 major coat protein has a stretch of 15 hydrophobic amino acids, which is rather short for a membrane spanning protein.

Secondly, an important factor for anchoring can be the electrostatic interactions between charged amino acid residues and e.g. charged head-groups of phospholipids. Positive charged residues frequently reside in the cytoplasmic space (positive inside rule) (*17*), and are thought to have anchoring interactions with the membrane. Lysine residues can be found well inside the membrane leaving the charged amino group in the membrane-water interface as was found for the M13 coat protein (*18, 19*), which is called the 'snorkeling effect' (*20*). There are two positively charged residues in the C-terminus of the Pf3 protein. Therefore, we are interested to determine whether this 'snorkeling effect' occurs in this protein. Thirdly, important for anchoring are also the aromatic amino-acid residues (*21*). Tryptophan residues are often found near the membrane-water interface (*22-25*), although the mechanism for this interaction is not fully understood. The Pf3 major coat protein contains a tryptophan residue in the C-terminus and two phenylalanines at the very end. Therefore, the protein is an excellent model to study the location of those residues.

To study the above mentioned aspects, membrane-bound Pf3 coat protein was studied with site-specific probing, as was described for the M13 coat protein, bacteriorhodopsin and colicin (*26-29*). For this purpose, we prepared mutants such that single cysteines were present regularly spaced along the primary structure of the protein. The fluorescence probe IAEDANS was specifically attached to the cysteine residue. The labeled mutant coat proteins are subsequently reconstituted into phospholipid model systems, and we studied the fluorescence characteristics of the probe at the specific positions. One of these characteristics was the sensitivity of the probe to the polarity of the environment (*30*). The quenching efficiency was also measured using the polar quencher acrylamide. In this way information is obtained about the depth of amino acids with respect to the membrane. This information supports an "L-shaped" membrane assembly of the Pf3 coat protein, as was found for the membrane-bound M13 and Pf1 coat proteins.

Materials and Methods

Chemicals

The phospholipids dioleoylphosphatidylcholine and dioleoylphosphatidylglycerol (DOPC and DOPG) were obtained from Sigma. Dioleoylphosphatidylethanolamine (DOPE) was purchased from Avanti. Other fine chemicals were from Merck.

Preparation of cysteine mutants

The pT7-7 plasmid with the Pf3 major coat protein gene as insert (pT7-7p44) was a generous gift from Prof. Dr. A. Kuhn (University of Hohenheim, Department of Microbiology at Stuttgart, Germany). For details of the construction of this plasmid, see Kiefer et al (*6*). Site-specific cysteine mutants were prepared with the QuikChange™ Site-Directed Mutagenesis Kit from Stratagene. The oligo-nucleotides used in this procedure were purchased from Amersham Pharmacia Biotech. The sequence of the mutant DNA was verified using automated DNA sequencing. Correctly mutated plasmid DNA was transformed into competent *E. coli* BL21(DE3) cells (*31*).

Overexpression of Pf3 major coat protein

E. coli BL21-DE3 with plasmid pT7-7p44 was grown at 37°C to an optical density at 600 nm of about 0.7, under continuous shaking and aeration in an 8 liter LB culture (containing 0.5% (w/v) yeast extract, 1% (w/v) tryptone, 1% (w/v) NaCl, 0.2% (w/v) glucose, 0.01% (w/v) ampicillin). The cells were induced with isopropyl-β-D-thiogalactopyranoside (final concentration of 0.15 mM). One hour after induction, the cells were harvested by centrifugation at 7,000 g for 10 minutes at 4°C. The cells were re-suspended in 150 ml lysis buffer (137 mM NaCl, 2.7 mM KCl, 25 mM Tris-HCl, 1 mM DTT, 1 mM PMSF, pH 7.5) and sonicated on ice with a Branson B15 cell disrupter (90 W, 6 min, 50% duty cycle). The membrane fraction was collected by centrifugation for 30 minutes at 29,500 rpm in a 60Ti rotor using a Beckman XL-90 ultracentrifuge. The membrane fraction was finally re-suspended in 8 ml lysis buffer and stored at -20°C. Samples of the overexpressed single cysteine mutants were analyzed with Tricine SDS polyacrylamide gel electrophoresis (*32*).

Purification and labeling of the Pf3 major coat protein

To extract the protein from the membrane, 5 ml of the re-suspended membrane fraction, from the above-described procedure, was thawed and mixed with 5 ml TFE. Membrane proteins were collected in the supernatant after the remaining membrane debris had been removed by centrifugation at 17,000 rpm in a MSE 8×50 rotor (20°C). The extract proved to be unstable in time. Therefore, it was immediately loaded (two times 5 ml protein extract) onto a Source 15 RPC reversed phase column (1×10 cm, Pharmacia Biotech) running in 20% (v/v) isopropanol and 0.1% (v/v) triethylamine with a flow-rate of 1 ml/min. Immediately after loading, an isopropanol/water gradient was started keeping the concentration of triethylamine at a constant level of 0.1% (v/v). Triethylamine proved to be crucial for releasing the coat proteins from the column. The following gradient was used: 0 to 5 minutes, 20 to 35% isopropanol; 5 to 50 minutes 35-70% isopropanol, 50 to 55 to 60 minutes 70-100-20% isopropanol.

After reversed phase chromatography, a fraction of about 80% pure Pf3 coat protein was collected and diluted (1:1 v/v) with TFE. In the following step, 2 mg IAEDANS (Molecular Probes) were added to the protein-fraction in the presence of 16‰ (v/v) tributylphosphine (Fluka Chemie). The reducing agent tributylphosphine was selected because it does not interfere with the reaction between IAEDANS and the thiol group of the cysteine residue (*33*). The fluorescence probe was allowed to react (in the dark) with the cysteine's thiol-group of the mutant coat protein for 3 hours under continuous stirring at room temperature. The labeling reaction was stopped with an excess of DTT. At the end of the reaction, the detergent cholate was added to the mixture (final concentration 50 mM).

In the next step, unbound label and remaining impurities were separated from the labeled major coat protein by HPSEC using a Superdex75 prep-grade column (HR 16/50) running in 50 mM sodium cholate, 1 mM EDTA, 150 mM NaCl, 10 mM Tris-HCl, pH 8) at a flow-rate of 1 ml/min. Volumes of 2 ml reaction mixture were loaded on the column. The presence of TFE in the reaction mixture was essential for the success of the purification procedure. The retention time of the Pf3 coat protein on the Superdex 75 column was prolonged by 5 minutes. This resulted in a higher efficiency in size-separation, and therefore a better removal of the remaining larger proteins. This observation suggests a decrease in the aggregational size of the coat proteins in the presence in TFE.

After size-exclusion chromatography, fractions of about 95% pure labeled Pf3 protein (assessed by Tricine SDS polyacrylamide gel electrophoreses) were pooled, and concentrated using ultra-filtration over an Amicon YM10 membrane. Pure labeled mutant protein was finally stored at -20°C. The final concentration of purified protein depended on which mutant was purified because the initial level of expression was an important factor in the final yield of the protein. The concentration of protein varied between 2 and 20 µg/ml. Because of the absence of a cysteine amino acid residue, we could not label the wild-type protein with this procedure. This result showed a high specificity in the labeling reaction between IAEDANS and the cysteine residues in the mutant coat proteins.

Reconstitution into phospholipid model membranes

Labeled Pf3 major coat protein was reconstituted into DOPC/DOPG (80/20 mol/mol) and DOPE/DOPG (80/20 mol/mol) using the cholate-dialysis method (*34*). The amount of phospholipids was chosen such that the lipid-to-protein molar ratio (L/P) was above 250. Chloroform was evaporated from the desired amount of phospholipid solution and the residual traces of chloroform were removed by drying under vacuum for at least two hours. The lipids were subsequently solubilized in 50 mM cholate, 1 mM EDTA, 150 mM NaCl, 10 mM Tris-HCl, pH 8, and mixed with labeled protein. In the following step, the lipid-protein mixture was dialyzed for 60 hours against a 1000-fold excess buffer containing 1 mM EDTA, 150 mM NaCl, 10 mM Tris-HCl, and pH 8. The buffer was replaced every 12 hours. Typically, samples for the steady-state fluorescence measurements contained about 0.9 mg of phospholipids.

Steady-state fluorescence

1 ml samples of every reconstituted mutant in DOPC/DOPG (80/20 mol/mol) and DOPE/DOPG (80/20 mol/mol) were prepared for the steady-state fluorescence experiment. The background samples contained DOPC/DOPG (80/20 mol/mol) and DOPE/DOPC (80/20 mol/mol) with and without wild-type protein. Fluorescence spectra of the labeled mutants were collected at 22±0.5°C using a excitation wavelength of 340 nm on a SPEX Fluorolog 3-22 fluorometer equipped with a 450 W Xenon lamp as an excitation source. Excitation and emission bandwidths were set to 1 and 3 nm, and

spectra were recorded between 400 and 600 nm with an integration time of 0.5 s. 1 ml samples were in 1 cm light-path fused silica cuvettes (Hellma model 114F-QS), and the optical density at 340 nm never exceeded 0.1. The spectra were corrected for background signal and sensitivity of the photomultiplier.

For steady-state fluorescence quenching experiments, aliquots of an acrylamide stock solution (3 M acrylamide, 150 mM NaCl, 10 mM Tris-HCl, 1 mM EDTA, pH 8) were added to samples of labeled protein reconstituted into in DOPC/DOPG (80/20 mol/mol) and DOPE/DOPG (80/20 mol/mol) after the steady-state fluorescence experiments. After every addition of acrylamide (steps of 5 or 10 µl to a final concentration of 176 mM), the decrease in fluorescence intensity was measured. Appropriate corrections for dilution were made for these quenching experiment.

The fluorescence data were analyzed according to the Stern-Volmer equation for collisional quenching *(35, 36)*:

$$\frac{F_o}{F} = 1 + K_{sv}[Q]$$

with

$$K_{sv} = k_q \tau$$

where F_0 and F are the fluorescence intensities in the absence and the presence of the quencher Q. K_{sv} is the Stern-Volmer quenching constant. It equals the fluorescence lifetime (τ) times the accessibility constant k_q. Before and after the fluorescence experiments the aggregational state of the protein was checked by HPSEC as described by Spruijt et al. *(37)*.

Results

Preparation of single-cysteine mutants

Seventeen single-cysteine mutants were prepared of the Pf3 major coat protein to obtain the presence of a cysteine residue well spread along the primary structure of the protein (see, Figure 1). One of these mutant coat proteins contained an additional cysteine residue at the C-terminal end of the protein.

The level of expression in *E. coli* was reduced by a factor of ten in most single-cysteine mutants, as compared to the level of expression of the wild-type protein. Replacement of the amino acids at positions 8 and 12 resulted in a dramatic decrease in the level of expression, and those mutants could not be purified in sufficient amounts for the fluorescence experiments. Interestingly, the three-threonine residues in the N-terminus at positions 9, 13 and 20 could be replaced without any decrease in the expression level. In contrast, all cell cultures producing mutant coat proteins showed a comparable growth pattern. First, the optical density at 600 nm of the cell culture increased to about 0.7. After induction of the target protein synthesis, the optical density decreased slightly, and reached a constant value of about 0.6.

After collection and fractionation of the cells, Pf3 major coat protein mutants were predominantly (about 95%) found in the membrane fraction. Incorrectly inserted protein is probably rapidly degraded by cell protease activity. It is difficult to assess the reason for the decrease in the level of expression of coat protein mutants, because a large number of cellular processes are involved in protein synthesis and membrane insertion. For instance, the production of the protein might be reduced on the DNA level resulting in a lower level of expression. On the other hand, perhaps the membrane insertion process is slowed down or even blocked because of the replacement of a specific amino acid residue by a cysteine residue.

Steady-state fluorescence spectroscopy

The polarity of the environment around the AEDANS probe was measured by steady-state fluorescence spectroscopy. This polarity is reflected in the wavelength of maximum emission, which is specified as λ_{max}. Figure 2 shows λ_{max} of the AEDANS probes attached to the different positions in the coat proteins, which were reconstituted into DOPC/DOPG (80/20 mol/mol) and DOPE/DOPG (80/20 mol/mol).

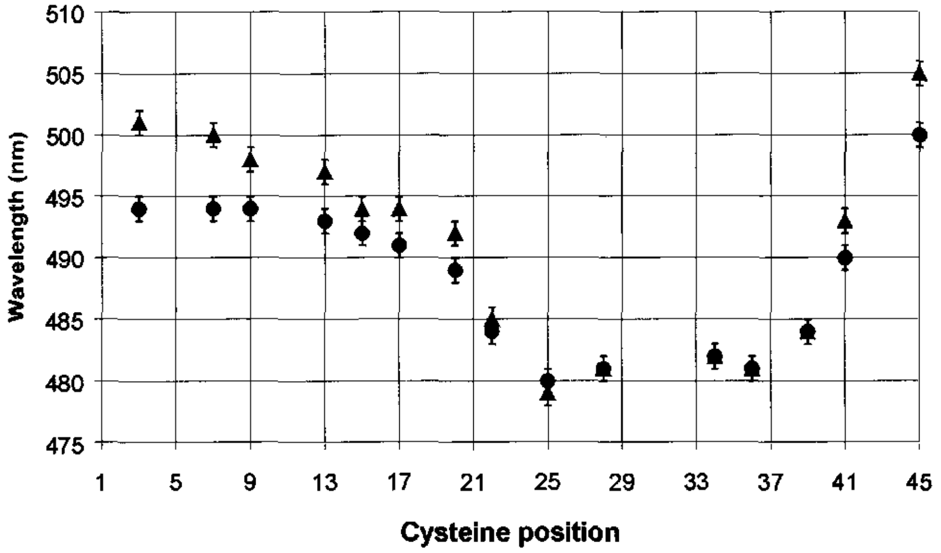

Figure 2: Polarity plot of the labeled Pf3 major coat protein. The wavelength of maximum emission, λ_{max}, of AEDANS is plotted as a function of the cysteine position to which the probe is attached with: in circles, labeled mutant coat proteins reconstituted in DOPC/DOPG (80/20 mol/mol); in triangles, labeled mutant coat proteins reconstituted in DOPE/DOPG (80/20 mol/mol).

The probe attached to amino acid position 45 has the highest value of λ_{max} (500 nm) in DOPC/DOPG indicating that this position is in the most polar environment. λ_{max} decreases to 481 nm at position 36, and is almost constant between position 36 and 25. From position 25 to 13, λ_{max} gradually increases to 493 nm. The positions 3, 7, and 9 have a constant emission maximum of 494 nm. A similar trend is observed In DOPE/DOPG. Upon comparing the obtained results of both DOPC/DOPG and

DOPE/DOPG, a difference can be seen in λ_{max} at N- and C-terminal positions of the protein. These positions exhibit a higher value of λ_{max} in DOPE/DOPG suggesting a higher polarity of the environment.

After the quenching experiment, Stern-Volmer plots were constructed. The plots showed a nearly linear relation between F_o/F and the acrylamide quencher concentration Q (data not shown). The Stern-Volmer constant K_{sv} was determined for all the labeled mutant coat proteins reconstituted in DOPC/DOPG and DOPE/DOPG. Figure 3 shows K_{sv} for both model systems as a function of the cysteine position to which the probe is attached.

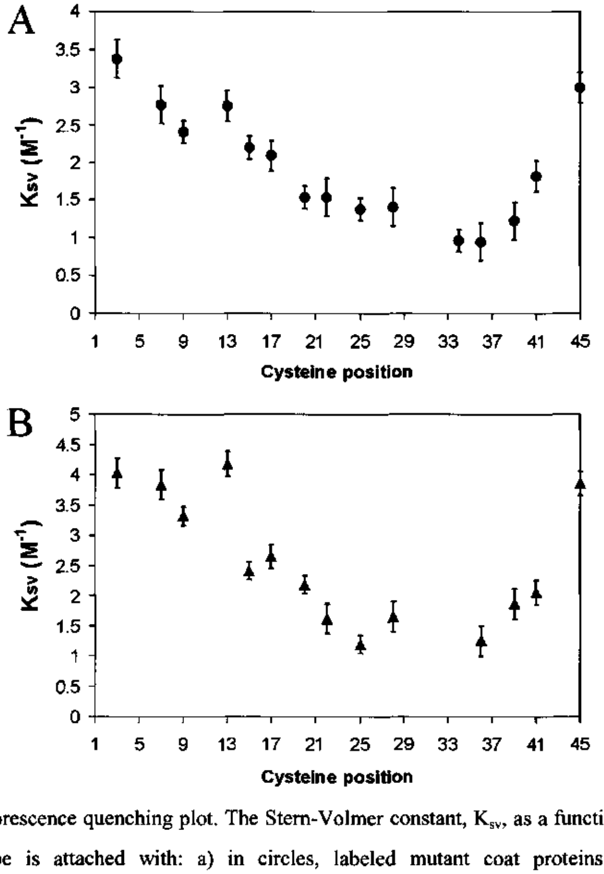

Figure 3: The fluorescence quenching plot. The Stern-Volmer constant, K_{sv}, as a function of the position to which the probe is attached with: a) in circles, labeled mutant coat proteins reconstituted in DOPC/DOPG (80/20 mol/mol); b) in triangles, labeled mutant coat proteins reconstituted in DOPE/DOPG (80/20 mol/mol).

In DOPC/DOPG it can be seen that K_{sv} rapidly decreases from 3 M^{-1} at position 45 to 0.95 M^{-1} at position 36. Going form position 36 to position 13, a gradual increase in K_{sv} is observed from 0.95 to 2.75 M^{-1}. K_{sv} decreases slightly at position 9 to 2.41 M^{-1} and increases again to 3.38 M^{-1} at position 3. Again, in DOPE/DOPG we observed a similar trend in K_{sv} as a function of the positions in the protein. In comparing the two model systems in figure 3, the N-terminal and C-terminal positions clearly have higher K_{sv} in DOPE/DOPG. Furthermore, the fluctuations in K_{sv} between (especially) N-terminal positions are stronger in DOPE/DOPG compared to those in DOPC/DOPG.

Discussion

An "L-shaped" assembly of the membrane-bound Pf3 coat protein

We measured the location of amino acid residues in the membrane of reconstituted Pf3 major coat protein using site-specific probing. The cysteine residues of the coat protein mutants were regularly spaced along the primary structure of the protein. The mutants are assumed to be similar to wild-type protein, as we selected and purified mutant proteins from the membrane fraction of *E. coli* cells, thereby minimizing the possibility of isolating misfolded and not inserted protein. Moreover, the chemical and physical behavior of all mutants is equal to that of the wild-type Pf3 coat protein during the purification procedure.

With the fluorescence probe IAEDANS attached to the cysteine residues of the reconstituted mutants, we monitored the polarity of the environment at specific positions of the protein in the membrane. This polarity is reflected in the wavelength of maximum emission (λ_{max}) of the IAEDANS probe (*30*). Probes will have a smaller λ_{max} in the membrane than do probes at the outside. The location of amino acids is also measured with fluorescence quenching. The uncharged polar quencher acrylamide quenches the fluorescence of IAEDANS more efficiently when the probe is in the aqueous phase (*26, 38*). This will result in a large Stern-Volmer constant (K_{sv}). In contrast, probes in the membrane exhibit a small value. K_{sv} is correlated to the accessibility of the probe to the fluorescence quencher.

Roughly three environments can be distinguished in the membrane. Firstly, a hydrophobic environment between the phospholipid carbon tails. Secondly, a more polar region in the phospholipid head-group region (interface), and finally the most polar region in the water phase. There are no sharp boundaries between these three regions. Wiener and White proposed a model of the structure of L_α -phase DOPC bilayers by interpreting X-ray and neutron diffraction data (*39*). Their model shows a gaussian distribution of the different membrane components, giving rise to a chemically highly heterogeneous interface. The combined interfacial region is about 50% of the total thickness of the membrane. This leads to a polarity gradient from the outside to the inside of the membrane (*40*).

IAEDANS would ideally reflect this polarity gradient as a symmetrical "cup-like" shape when λ_{max} is measured as a function of membrane depth. A similar symmetrical pattern is expected for the K_{sv} as a function of membrane depth. In contrast, the measured polarity and fluorescence-quenching plot (Figure 2 and 3a,b) show asymmetrical patterns in DOPC/DOPG and DOPE/DOPG. A close examination of these figures reveals a more gradual increase in K_{sv} and λ_{max} at the N-terminal side (positions 25 to 13) of the protein than the C-terminal side (position 34 to 45). These results suggest that the "simple" model of a Pf3 protein spanning the entire membrane, with the C- and N-terminus in the aqueous phase, is not valid.

Upon comparing both phospholipid systems, a difference in λ_{max} and K_{sv} can be seen at the C- and N-terminus. At these positions the wavelengths of maximal emission are red-shifted, and more efficiently quenched in DOPE/DOPG. We can explain this result by closer examining the PE head-group region. The clearly more polar PE head-group brings a higher polarity in the interface than does the PC head-group, which subsequently leads to a more red-shifted λ_{max} in DOPE/DOPG. Furthermore, Molecular dynamic studies (reviewed in Tieleman et al. (*41*)) showed that the thickness of the interface is smaller in PE containing membranes as compared to PC membranes. Therefore, probes are more accessible to aqueous quencher (acrylamide) in the PE containing membrane resulting in a larger K_{sv}. One would expect that the interfacial differences between both phospholipid systems are no longer observed for positions, which are completely in the water-phase. However, those positions were not found in this study. Consequently, the C- and N-terminus remain in (or are close to) the membrane-water interface. As a consequence of the close proximity of the membrane, λ_{max} at position 45 (505 nm in DOPE/DOPG and 500 nm in DOPC/DOPG) does not reach the wavelength of 520 nm obtained in water (*30*). The conclusion is further supported by the fact that the C-terminus is not accessible to proteases K in topology experiments with Pf3 major coat protein (*6*).

The local environment at a specific position gives rise to a fine-structure in the pattern of both the polarity and quenching plot. The presence of e.g. a charged residue near the monitored position increases the local polarity, which is reflected in a slightly higher λ_{max}. The opposite is true for a flanking hydrophobic residue. Efficient fluorescence quenching can be blocked by steric hindrance of neighboring amino acids (or local tertiary structure) resulting in an unexpected value of K_{sv}. Furthermore, K_{sv} is not only dependent on the accessibility of the probe to the quencher acrylamide but also on the fluorescence lifetime. The lifetime of the probe is longer in an apolar solvent than in a polar solvent (*30*). Therefore, the differences are smaller in the actual accessibility of the fluorescence probe as a function of the position. This also explains the variations in fine-structure that occur between the polarity and quenching plot.

The variation between K_{sv} and λ_{max}, giving rise to the fine structure, appear to be stronger in DOPE/DOPG. A possible explanation for this effect could be the thinner interfacial region in DOPE/DOPG as compared to DOPC/DOPG. This leads to a much steeper polarity gradient in the DOPE/DOPG interface. Small shifts in position of the probe in the interface can subsequently give rise to stronger variations in K_{sv} and λ_{max} as a function of the position in the protein.

Spruijt et al. (1996) (*26*) measured the relative depth of amino acids of the M13 major coat protein in a membrane using an identical approach as was used in this study for the Pf3 major coat protein. Information about the local polarity of the environment was obtained of positions in the transmembrane helix and the C-terminus. Due to a different instrumental set-up in the measurements of that study, the wavelength of maximum emission was about 10 nm too low for all the positions (the scanning approach was repeated for these positions). At this moment, information about the polarity of the environment is also available of the N-terminal positions of the reconstituted M13 major coat protein in DOPC/DOPG (80/20 mol/mol) (see, chapter 2 of this thesis).

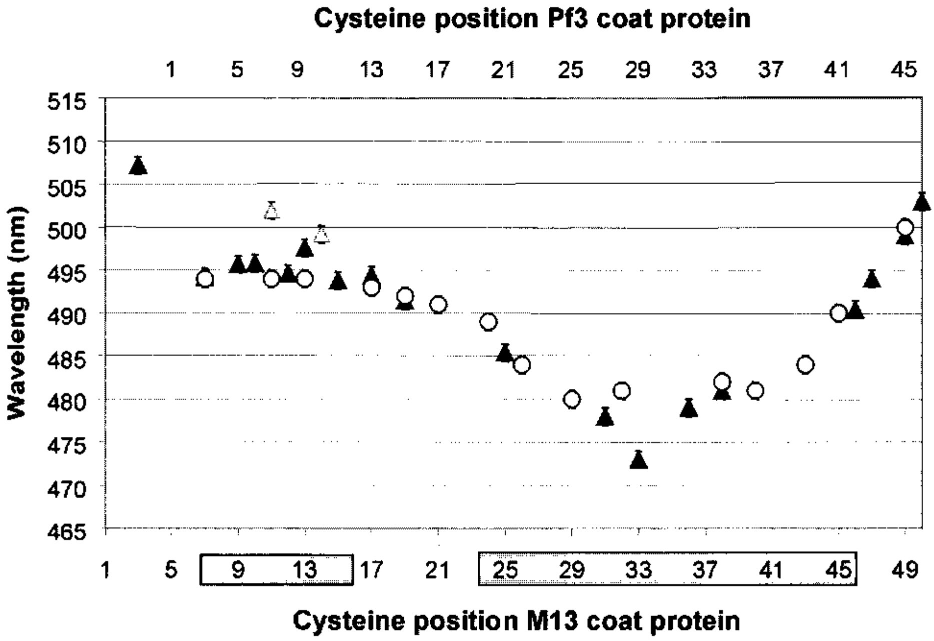

Figure 4: Overlay of the polarity plots of the labeled M13 and Pf3 major coat protein reconstituted in DOPC/DOPG (80/20 mol/mol). The top horizontal axis represents the primary structure of the Pf3 coat protein with: in circles, the Pf3 data points. The bottom horizontal axis represents the primary structure of the M13 coat protein (*10*) indicated is the amphipathic helix from residue 7 to 16, and the transmembrane helix from residue 25 to 45 (*12*) with: in triangles, the M13 data points. For further details about the strongly deviating M13 positions 11 and 14 (gray triangles) see, chapter 2 of this thesis.

A striking similarity can be seen in the shape of the polarity plots of both the Pf3 and M13 membrane-bound coat proteins (Figure 4). We aligned the positions in the primary structure of both proteins such that the environments of the different positions match in polarity. The above-mentioned alignment of the polarity plot clearly indicates a strong similarity in depth of the amino acid positions of the M13 and Pf3 coat protein. Even the replacement of the charged residue at position 7 of the Pf3 coat protein did not result in a strong deviation between the results of both proteins. The N-terminal positions 3, 11 and 14 of the M13 coat protein deviate from the other positions. Position 3 is part of the unstructured N-terminal end of the M13 protein, and is probably in the aqueous phase. The substitution of the membrane anchoring amino acids phenylalanine 11 and leucine 14, result in a rearrangement of the N-terminal arm with respect to the surface of the membrane. Further details about these amino acids are described in chapter 2 of this thesis. The similarity, observed in Figure 4, is a strong indication for a structural resemblance between both proteins. This is remarkable taking into account the lack of primary sequence homology.

Much structural information is available about the membrane-bound M13 coat protein. A model, proposed for the membrane-bound M13 coat proteins, shows an L-shaped membrane-bound assembly. A transmembrane helix, which is perpendicular to the membrane surface, is connected by a flexible linker or loop to an amphipathic α-helix that is parallel to the membrane surface (*14, 15, 42*). Much less information is available about the membrane-bound Pf3 coat protein. It is known that it predominantly contains an α-helical structure (*9*). Like the M13 coat protein an amphipathic α-helix can be constructed of the N-terminus (*43*). The striking similarity between the polarity plots (Figure 4) of both proteins strongly suggests the presence of an L-shape in the membrane-bound Pf3 coat protein. The asymmetrical shape of both the polarity and quenching plot (Figure 2 and 3a) is a direct result of this protein topology. The presence of the loop-structure or flexible linker can explain the result of a more gradual increase in K_{sv} and λ_{max} at the N-terminal side of the protein from position 25 to 13.

It is tentative to extract more information out of the above-mentioned alignment between M13 and Pf3 coat protein (Figure 4 also shows the assignment of the structural domains of the M13 coat protein). The limited structural information about the Pf3 coat protein makes it difficult to assign the amino acids to structural domains. Based on the alignment, we could speculate that the amphipathic helix of the membrane-bound Pf3 coat is approximately between amino acid 3 and 12 followed by a loop or linker between 14 and 20 that is subsequently connected to the transmembrane helix.

Relative depths of C-terminal amino acids residues in the membrane

The primary structure of the Pf3 coat protein contains an arginine at position 37 and a lysine at position 40. Two phenylalanines (position 43 and 44) are at the C-terminal end of the protein (Figure 1). One would expect to find both charged residues at the polar interface, and the two phenylalanines in the hydrophobic region of the membrane. This would form a tight anchor of the C-terminus to the membrane.

A closer examination of the polarity and quenching plot (Figure 2 and 3a,b) is required to determine the location of those amino acids in the membrane. In our experimental approach, it is not possible to measure the absolute depth with respect to the membrane surface. There is no reference value for λ_{max} and K_{sv} of probes (attached to the protein) in the water-phase that can be used as a starting point from which we can deduce the depth of the amino acids. Nevertheless, on a relative scale the probed positions 36 and 39 can be used to give information about the relative location of arginine 37 and lysine 40. Position 45 can be used to monitor the location of both phenylalanines.

The positions 36 and 39 exhibit a small K_{sv} and λ_{max} as compared to position 45. This result suggests a deeper penetration of the charged residues in the membrane than both phenylalanines. Probably, the Cα-backbone of the amino acid side-chains (at least arginine 37) are in the hydrophobic part of the membrane with the charged group sticking out in the polar interface (the 'snorkeling effect' (*18, 20*)). A similar result was found for the lysine residues at the positions 40, 43 and 44 of the M13 coat protein with ESR and fluorescence studies (*19, 26*).

Contrary to the suggestion following from the results (a high value of K_{sv} and λ_{max} at position 45), it is still possible that the phenylalanines bend back to the hydrophobic part of the membrane. This can be explained as follows. The AEDANS probe at the outer C-terminus encounters only one neighboring amino acid. This reduces the amount of steric hindrance, and might give the probe enough freedom to reach for the outside of the membrane. If both residues are indeed located in the interface, additional (unknown) interactions of the phenylalanines with the interfacial region are to be expected. Perhaps both phenylalanines have the ability to form a π-stack, or cation-π interactions (*44*) play a role in stabilizing the phenylalanines in the interface.

Conclusions

The location of amino acids of Pf3 mutants in the membrane, as was studied by site-specific fluorescence probing, shows a single membrane spanning protein with both the C- and N-terminus remaining close to the surface of, or are in the membrane. Unfortunately, it was only possible to obtain relative locations of the amino acids in the membrane. A comparison with a similar study performed on the M13 coat protein reveals striking similarities. The structural coherence that follows from this comparison suggest an L-shaped tertiary structure of the membrane-bound Pf3 coat protein. A similar model was also proposed for the membrane-bound Pf1 coat protein. It appears that not only the mechanisms in viral reproduction are comparable but also the structure of the involved major coat proteins. A higher polarity was detected in the interface of PE/PG than PC/PG. Furthermore, the PE/PG interface appears to have a steeper polarity gradient than the PC/PG head-group region, upon going from the outside to the inside of the membrane. This follows direct from a smaller interfacial region, and a more polar head-group region of DOPE/DOPG as compared to DOPC/DOPG.

References

1. Stanisich, V. A. (1974) *J. Gen. Microbiol. 84*, 332-342.
2. Russel, M. (1991) *Mol. Microbiol. 5*, 1607-13.
3. Marvin, D. A. (1998) *Curr. Opin. Struct. Biol. 8*, 150-158.
4. Welsh, L. C., Symmons, M. F., Sturtevant, J. M., Marvin, D. A., and Perham, R. N. (1998) *J. Mol. Biol. 283*, 155-177.
5. Kuhn, A., Rohrer, J., and Gallusser, A. (1990) *J. Struct. Biol. 104*, 38-43.
6. Kiefer, D., Hu, X., Dalbey, R., and Kuhn, A. (1997) *EMBO J. 16*, 2197-2204.
7. Luiten, R. G. M., Schoenmakers, J. G. G., and Konings, R. N. H. (1983) *Nucleic. Acids. Res. 11*, 8073-85.
8. Putterman, D. G., Casadevall, A., Boyle, P. D., Yang, H. L., Frangione, B., and Day, L. A. (1984) *Proc. Natl. Acad. Sci. U.S.A. 81*, 699-703.
9. Thiaudiere, E., Soekarjo, M., Kuchinka, E., Kuhn, A., and Vogel, H. (1993) *Biochemistry 32*, 12186-12196.
10. Van Wezenbeek, P. M. G. F., Hulsebos, T. J. M., and Schoenmakers, J. G. G. (1980) *Gene 11*, 129-48.
11. Nakashima, Y., Wiseman, R. L., Konigsberg, W., and Marvin, D. A. (1975) *Nature 253*, 68-71.
12. Papavoine, C. H. M., Christiaans, B. E. C., Folmer, R. H. A., Konings, R. N. H., and Hilbers, C. W. (1998) *J. Mol. Biol. 282*, 401-419.
13. Shon, K. J., Kim, Y. G., Colnago, L. A., and Opella, S. J. (1991) *Science 252*, 1303-1304.
14. McDonnell, P. A., Shon, K., Kim, Y., and Opella, S. J. (1993) *J. Mol. Biol. 233*, 447-463.
15. Marassi, F. M., Ramamoorthy, A., and Opella, S. J. (1997) *Proc. Natl. Acad. Sci. U.S.A. 94*, 8551-8556.
16. Killian, J. A. (1998) *Biochim. Biophys. Acta.*, 401-416.
17. von Heijne, G., and Gavel, Y. (1988) *Eur. J. Biochem. 174*, 671-8.
18. Tanford, C., and Reynolds, J. A. (1976) *Biochim. Biophys. Acta 457*, 133-70.
19. Stopar, D., Jansen, K. A. J., Pali, T., Marsh, D., and Hemminga, M. A. (1997) *Biochemistry 36*, 8261-8268.
20. Mishra, V. K., Palgunachari, M. N., Segrest, J. P., and Anantharamaiah, G. M. (1994) *J. Biol. Chem. 269*, 7185-91.
21. Killian, J. A., Salemink, I., Deplanque, M. R. R., Lindblom, G., Koeppe, R. E., and Greathouse, D. V. (1996) *Biochemistry 35*, 1037-1045.
22. Doyle, D. A., Cabral, J. M., Pfuetzner, R. A., Kuo, A., Gulbis, J. M., Cohen, S. L., Chait, B. T., and MacKinnon, R. (1998) *Science 280*, 69-77.
23. Ostermeier, C., Iwata, S., and Michel, H. (1996) *Curr. Opin. Struct. Biol. 6*, 460-6.
24. Reithmeier, R. A. (1995) *Curr. Opin. Struct. Biol. 5*, 491-500.
25. von Heijne, G. (1994) *Ann. Rev. Biophys. Biomol. Struct.. 23*, 167-92.
26. Spruijt, R. B., Wolfs, C. J. A. M., Verver, J. W. G., and Hemminga, M. A. (1996) *Biochemistry 35*, 10383-10391.
27. Flitsch, S. L., and Khorana, H. G. (1989) *Biochemistry 28*, 7800-7805.

28. Altenbach, C., Flitsch, S. L., Khorana, H. G., and Hubbell, W. L. (1989) *Biochemistry 28*, 7806-7812.
29. Lakey, J. H., Baty, D., and Pattus, F. (1991) *J. Mol. Biol. 218*, 639-53.
30. Hudson, E. N., and Weber, G. (1973) *Biochemistry 12*, 4154-61.
31. Studier, F. W., Rosenberg, A. H., Dunn, J. J., and Dubendorf, J. W. (1990) *Methods Enzymol. 185*, 60-89.
32. Schägger, H., and Von Jagow, G. (1987) *Anal. Biochem. 166*, 368-79.
33. Rüegg, U. T., and Rudinger, J. (1977) *Methods Enzymol. 47*, 111-114.
34. Spruijt, R. B., Wolfs, C. J. A. M., and Hemminga, M. A. (1989) *Biochemistry 28*, 9158-65.
35. Lehrer, S., S. (1971) *Biochemistry 10*, 3254-63.
36. Lehrer, S. S., and Leavis, P. C. (1978) *Methods Enzymol. 49*, 222-236.
37. Spruijt, R. B., and Hemminga, M. A. (1991) *Biochemistry 30*, 11147-11154.
38. Moro, F., Goni, F. M., and Urbaneja, M. A. (1993) *FEBS. Lett. 330*, 129-32.
39. Wiener, M. C., and White, S. H. (1992) *Biophys. J. 61*, 437-47.
40. White, S. H., Wimley, W. C., Ladokhin, A. S., and Hristova, K. (1998) *Energ. Biol. Macromol. B 295*, 62-87.
41. Tieleman, D. P., Marrink, S. J., and Berendsen, H. J. C. (1997) *Biochem. Biophys. Acta 1331*, 235-270.
42. Papavoine, C. H. M., Remerowski, M. L., Horstink, L. M., Konings, R. N. H., Hilbers, C. W., and van de Ven, F. J. M. (1997) *Biochemistry 36*, 4015-4026.
43. Kishchenko, G., and Makowski, L. (1997) *Prot. Struct. Funct. Gen. 27*, 405-409.
44. Dougherty, D. A. (1996) *Science 271*, 163-168.

Chapter 5

Membrane-anchoring interactions of M13 major coat protein

Alexander B. Meijer, Ruud B. Spruijt, Cor J.A.M. Wolfs,
and Marcus A. Hemminga

Abstract

The response of the membrane-bound M13 major coat protein to hydrophobic mismatch is measured by site-directed fluorescence and ESR spectroscopy. For this purpose, we investigated the anchoring interactions of different domains of the M13 major coat in membrane model systems consisting of phosphatidylcholine lipids of varying thickness. Mutant coat proteins were prepared with an AEDANS or proxyl labeled single cysteine residue in the hinge region of the protein or at the C-terminal side of the transmembrane helix. In addition, the fluorescence of the tryptophan residue in wild type proteins was used as a monitor for the N-terminal side of the transmembrane helix. The fluorescence results show that the hinge region and C-terminal side of the transmembrane helix hardly respond to hydrophobic mismatch. In contrast, the N-terminal side of the helical transmembrane domain shifts to a more apolar environment, when the hydrophobic thickness is increased. The apparent strong anchoring interactions of the C-terminus are confirmed using a mutant that contained a longer transmembrane domain. As a result of this mutation, the tryptophan residue at the N-terminal side of the helical domain clearly shifted to a more polar environment, whereas the labeled position 46 at the C-terminal side is not affected. The anchoring interactions of the C-terminal part are found to arise from the lysine and phenylalanine amino acid residues in the C-terminus. This is

demonstrated with fluorescence experiments in combination with site-directed ESR spin probe measurements on a mutant in which both phenylalanines are replaced by alanine residues. The lysine and phenylalanine residues in the C-terminus affect the location of the entire helical transmembrane domain of the protein in the membrane.

Introduction

The membrane-bound major coat protein of M13 bacteriophage is an excellent model system to study fundamental aspects of protein-lipid interactions. These interactions are important for the formation of the correct membrane assembly of not only the M13 major coat protein but also membrane-proteins in general. A main determinant in the formation of the correct membrane assembly will be the anchoring interactions of the protein with the membrane. Anchoring can be accomplished by several factors. Important are the hydrophobic interactions, which will be mainly determined by the length and hydrophobicity of the transmembrane helix. Then there are the aromatic amino acid residues, which are often found at the membrane-water interface, and are thought to play a role in the interactions of a protein with the polar head-group region of the membrane. A comparable function can be ascribed to the presence of charged amino acid residues in the interface (reviewed in Killian and von Heijne (*1*)).

In recent years, several chemosynthetic peptide analogues were produced to gain insight in the function of specific amino acids for membrane anchoring interactions with model membranes, which varied in thickness. Studies on lysine-flanked peptides revealed that a too short α-helix under strong mismatch conditions move to a non-transmembrane orientation (*2-4*). On the contrary, a too long α-helix has the tendency to form oligomers (*2, 3*). Mismatch did not result in significant adaptations of the peptide backbone conformation in the fluid phase (*5*). However, changes in phase-transition temperature in response to mismatch have been reported indicating that the acyl chain order is affected to some extend (*6*).

De Planque et al. showed that synthetic peptides, flanked with tryptophan or lysine residues, can induce non-bilayer phases under mismatch conditions at high peptide to phospholipid ratio. The main response on increasing mismatch at low peptide to phospholipid ratio is occlusion of the peptide material from the membrane. Especially, in case of negative mismatch, in which the peptide is too short to accommodate the membrane, occlusion is an dominant response (*7, 8*). The phenomenon of hydrophobic mismatch has been studied in biological membranes as well. With a "glycosylation mapping" technique (*9*), it is shown that tryptophan pulls a poly-Leucine segment towards the membrane-water interface. An affinity for the hydrophobic core was demonstrated for phenylalanine (*10*).

With respect to anchoring interactions of a protein to the membrane, M13 major coat protein possesses interesting characteristics. The M13 coat protein can be roughly divided into three structural domains (Figure 1). First there is the helical transmembrane domain. The second part is the amphipathic N-terminal arm, which is thought to be mainly parallel to the surface of the membrane (*11, 12*). Finally, there is a hinge region connecting both the helical transmembrane domain and the amphipathic N-terminal arm. The helical transmembrane domain at the C-terminal side contains four lysine amino acid residues at the positions 40, 42, 43 and 48. Furthermore, this side contains two phenylalanine residues at the positions 42 and 45. A tryptophan residue at position 26 is present at the N-terminal side of the helical transmembrane domain. The hinge region contains two tyrosine residues at the positions 21 and 24 (Figure 1). These aromatic and positively charged residues could provide the anchoring interactions, which influence the position of the protein within the membrane (*1, 13*). M13 coat protein possesses an additional anchoring interaction via the N-terminal segment of the protein. The arm is in equilibrium between a membrane-bound and water-phase configuration. The ratio between both configurations can be altered by a mutation of Leu14 and/or Phe11 (see, chapter 2 and 3 in this thesis (*14, 15*).

By studying the M13 major coat protein under mismatch conditions in this paper, additional information is acquired about role of specific amino acids at the membrane-water interface. The relative depth of Trp26 under mismatch conditions is followed by fluorescence spectroscopy. Furthermore, site-specific information about the relative depth of desired positions in the protein is acquired by attaching an ESR spin label or fluorescence probe to a cysteine residue of a single cysteine mutant of the protein.

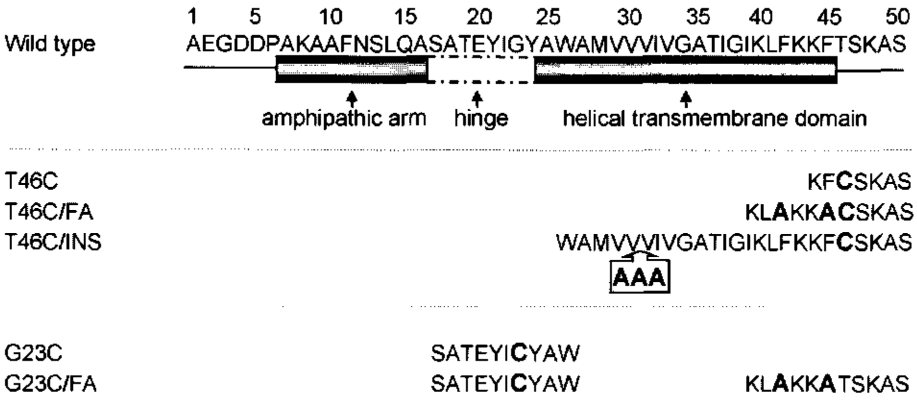
1 5 10 15 20 25 30 35 40 45 50
Wild type
AEGDDPAKAAFNSLQASATEYIGYAWAMVVVIVGATIGIKLFKKFTSKAS
amphipathic arm
hinge
helical transmembrane domain
T46C
KFCSKAS
T46C/FA
KLAKKACSKAS
T46C/INS
WAMVVVIVGATIGIKLFKKFCSKAS
AAA
G23C
SATEYICYAW
G23C/FA
SATEYICYAW
KLAKKATSKAS

Figure 1: Primary structure of wild type (*36*) and mutant coat proteins. The amino acid residues that differ from the wild type protein are printed in bold. The structural domains are indicated below the primary structure of the wild type protein.

Materials and methods

Materials

Dimyristoleoylphosphatidylcholine (DMoPC), dioleoylphosphatidylcholine (DOPC), dieicosenoylphophatidylcholine (DEiPC), dierucoylphosphatidylcholine (DEuPC) were purchased from Avanti Polar Lipids. Fine chemicals were purchased from Merck.

Preparation and purification of labeled single cysteine mutants

Site-specific cysteine mutants were prepared with the QuikChange™ Site-Directed Mutagenisis Kit from Stratagene. PT7-7, with geneVIII as insert was, used as the template for this procedure (*14*). The oligo-nucleotides were purchased from Amersham

Pharmacia Biotech. The sequence of the mutant DNA was verified using automated DNA sequencing. Correctly mutated plasmid DNA was transformed into competent *E. coli* BL21(DE3) cells (*16*).

Mutant M13 coat protein was purified, and labeled with IAEDANS as is described in detail in chapter 2 of this thesis (*14*). Firstly, mutant protein was overexpressed in *E. coli,* and the membrane fraction was collected. Secondly, the membrane proteins were extracted from the membrane, and separated on hydrophobicity using reversed phase chromatography. After this step, the about 85% pure mutant coat protein was in a mixture of isopropanol/water and 0.1% triethylamine (v/v). The mutant coat protein was subsequently labeled with IAEDANS. Slight modifications were introduced in the procedure for the attachment of maleimido-proxyl spin label to the single cysteine mutants. An excess of spin label was added to the protein fraction after reversed phase chromatography. The label was allowed to react with the SH-groups of the mutants for 20 min at room temperature at pH 7. In the final step, free label and remaining impurities were removed from the labeled mutant coat proteins using size exclusion chromatography. The about 95% pure protein, labeled with AEDANS or proxyl, was now in a buffer containing 50 mM cholate, 10 mM Tris-HCl (pH 8), 1 mM EDTA, and 150 mM NaCl.

Reconstitution of labeled M13 coat protein

Labeled M13 major coat protein was reconstituted into PC phospholipids using the cholate-dialysis method (*17*). The amount of protein was chosen such that the lipid-to-protein molar ratio (L/P) exceeded 200. Typically, samples contained about 4 mg phospholipids for ESR spectroscopy and about 1 mg for fluorescence spectroscopy. Chloroform was evaporated from the desired amount of phospholipid solution and the residual traces of chloroform were removed by drying under vacuum for at least two hours. The lipids were subsequently solubilized in 400 mM cholate, 1 mM EDTA, 150 mM NaCl, 10 mM Tris-HCl, pH 8, and mixed with labeled protein. In the following step, the lipid-protein mixture was dialyzed for 60 hours against a 100-fold excess buffer containing 1 mM EDTA, 150 mM NaCl, 10 mM Tris-HCl, and pH 8. The buffer was replaced every 12 hours.

Steady-state fluorescence spectroscopy

Fluorescence spectra of the labeled mutants were collected at 20±0.5°C using a excitation wavelength of 340 nm for AEDANS and 290 nm for tryptophan on a SPEX Fluorolog 3-22 fluorometer equipped with a 450 W Xenon lamp as an excitation source. The background samples contained DOPC with and without wild-type protein. Excitation and emission bandwidths were set to 1 and 2 nm, and spectra were recorded between 400 and 600 nm for AEDANS and between 300 and 400 for tryptophan with an integration time of 0.5 s. 1 ml samples were in 1 cm light-path fused silica cuvettes (Hellma model 114F-QS), and the optical density at 340 nm or 280 nm never exceeded 0.1. The spectra were corrected for background signal and sensitivity of the photomultiplier.

ESR spectroscopy

A comparable experimental set up was used as is described in Stopar et al. (*18*). 1 ml samples of reconstituted mutant coat protein was freeze-dried overnight, and dissolved in 10 mM Tris-HCl, 1 mM EDTA, 150 mM NaCl, pH 8, yielding multilamellar vesicles. The vesicles were concentrated by centrifugation at 30,000 rpm in a Beckman Ti75 rotor at 20°C. 50 µl glass capillaries were filled up to 5 mm with vesicles containing labeled mutant coat protein. These capillaries were inserted into standard 4 mm diameter quarts tubes. ESR spectra were recorded on a Bruker ESP 300E ESR spectrometer equipped with a 108TMH/9103-microwave cavity. The temperature was regulated with a nitrogen gas-flow temperature system. The ESR settings for all recorded spectra were: 6.38 mW microwave power, 0.1 mT modulation amplitude, 40 ms time constant, 160 s scan time, 10 mT scan width, and a 342.0 mT center field. Up to 20 recorded spectra were accumulated.

Results

The primary structure of the mutants, which were constructed for this study, are shown in Figure 1. These mutants were prepared to reach the following goals. (a) A cysteine residue, which is labeled with AEDANS, is introduced at position 46 to monitor the changes in relative position at the C-terminal side of the transmembrane helical domain. (b) The changes in position of the hinge region are followed via a labeled cysteine residue at position 23. (c) The effect of a longer transmembrane domain is studied using the T46C/INS mutant, in which three alanines are introduced, between positions 30 and 31. (d) The mutants G23C/FA and T46C/FA are prepared to determine the importance of the Phe42 and Phe45 for the position of the protein in the membrane. The changes in wavelength of maximum emission (λ_{max}) of Trp26 are monitored to measure the response on the N-terminal side of the helical transmembrane domain of the wild type and mutant proteins.

The λ_{max} of tryptophan and AEDANS was recorded of (mutant) coat proteins that were reconstituted into bilayers of varying thickness (Figure 2, 3). The hydrophobic thickness of the three-phosphatidylcholine bilayers, used in this study, is defined as the distance between the acyl chain C-2 atoms of two opposing lipids. This results in a hydrophobic thickness of 20 Å for DMoPC, 27 Å for DOPC, and 30,5 Å for DEiPC (*7, 19*). The tryptophan emission maximum of the wild type coat protein is equal to that of the tryptophan residue in the (AEDANS labeled) T46C mutant within the model membranes (Figure 2). Apparently, the presence of the AEDANS probe at position 46 has no influence on the wavelength of maximum emission of the tryptophan residue for this mutant. The tryptophan fluorescence intensity of the G23C and G23C/FA mutants was low. The close proximity of the AEDANS labeled cysteine at position 23 probably causes a quenching of the tryptophan fluorescence via energy transfer and/or quenching by the sulfur group. Because of this effect, the tryptophan wavelength of maximum emission could not reliably be determined.

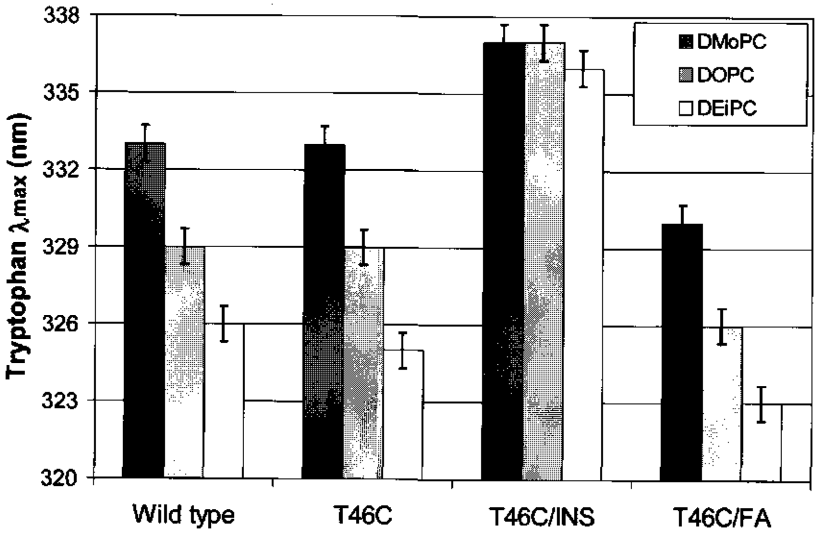

Figure 2: The tryptophan emission maximum of wild type and mutant protein, reconstituted in PC bilayers with varying thickness. The three bars per mutants represent in black DMoPC, in gray DOPC, and in white DEiPC. The vesicles were in 150 mM NaCl, 10 mM Tris-HCl and 1 mM EDTA, pH 8 at 20°C.

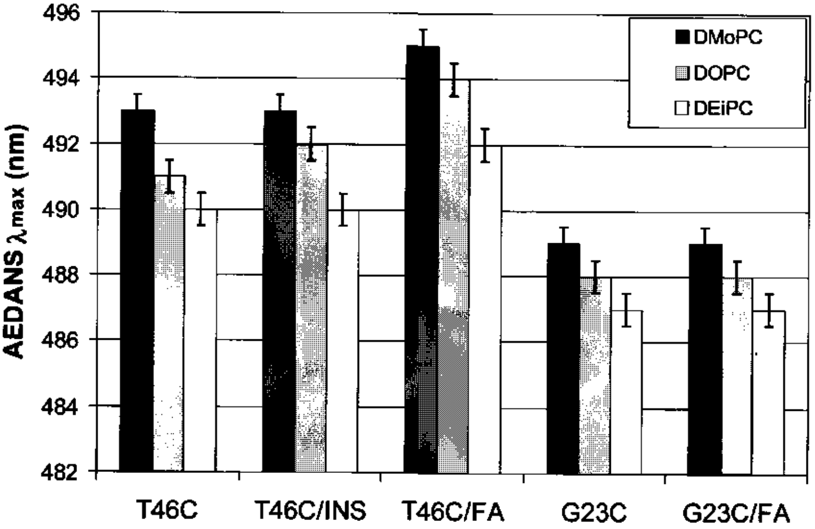

Figure 3: The AEDANS emission maximum of labeled mutant protein, reconstituted in PC bilayers with varying thickness. The three bars per mutants represent in black DMoPC, in gray DOPC, and in white DEiPC. The vesicles are in 150 mM NaCl, 10 mM Tris-HCl and 1 mM EDTA, pH 8 at 20°C.

For additional information about the location of position 46, ESR spectra were acquired of spin labeled T46C and T46C/FA reconstituted in DOPC (Figure 4). The ESR spectrum of the T46C mutant displays a superposition of two components, which was also found by Stopar et al. (*20*). The spectrum consists of a sharp three-line spectrum representing mobile probes on the ESR time-scale (10^{-11} s $\leq \tau_c \leq 3\times10^{-9}$ s), and a broad spectral component indicative for motion in the slow regime ($\tau_c \geq 2\times10^{-9}$ s) (*21*).

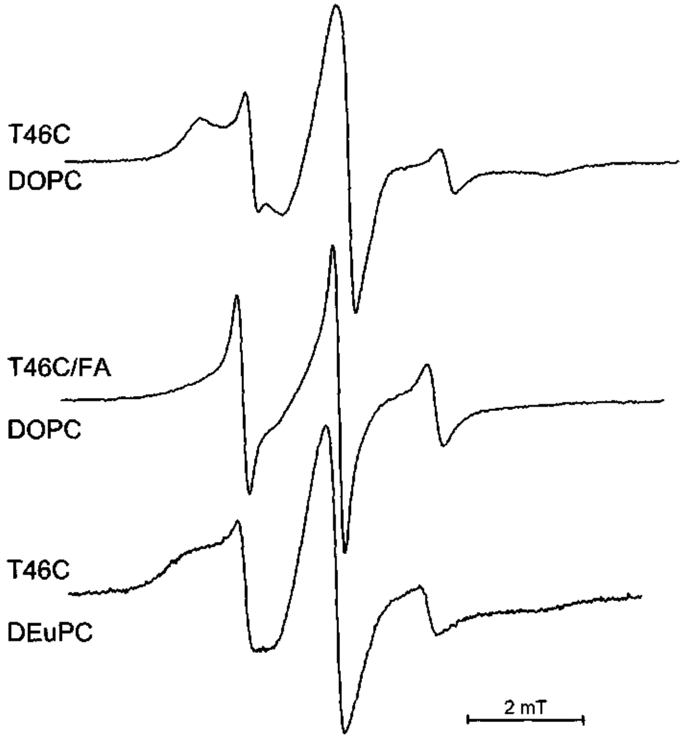

Figure 4: ESR spectra of proxyl labeled position 46 of the T46C and T46C/FA mutants, reconstituted into DOPC, and the T46C mutant, reconstituted into DEuPC. The vesicles are in 150 mM NaCl, 10 mM Tris-HCl and 1 mM EDTA, pH 8 at 20°C.

The replacement of the both phenylalanines by alanines in the T46C/FA mutant produces a spectrum in which the broad component has almost completely disappeared. Figure 4 also shows the spin labeled T46C mutant reconstituted into DEuPC membranes. ESR experiments on the mutants reconstituted in DEuPC show abnormal broad spectra indicating a large variety of spectral components, and perhaps spin-spin interactions as a result of protein aggregation. Probably, the protein exists in several orientations and/or configurations in this model membrane as was also found for Lys-flanked polypeptides under strong mismatch conditions (*2-4*). For this reason, the results in this lipid system are excluded from this paper.

Under unfavorable conditions, M13 major coat protein has the ability to irreversibly aggregate, which shows up as a β-sheet conformation in CD spectra. This phenomenon is not found *in vivo*, and is therefore regarded as an artifact (*22*). Since the hydrophobic mismatch experiments and the use of mutants could induce this β-sheet formation, the conformation of the proteins was checked with CD spectroscopy. For all mutants in all model bilayer systems the results showed similar spectra typical for α-helices (data not shown), which indicates the absence of irreversible protein aggregation.

Discussion

To record possible adaptations of the protein to mismatch conditions and/or specific mutations, changes at both sides of the transmembrane helical domain (residues 25 to 46) were monitored in our work (Figure 1). As a monitor for the N-terminal side of the helical transmembrane domain, we selected the intrinsic fluorescence probe tryptophan at position 26, which wavelength of maximum emission is sensitive to the polarity of the environment. This is reflected in a red-shifted emission maximum in the aqueous phase as compared to the value of λ_{max} in a hydrophobic phase. This property provides a tool to measure the relative depth of Trp26 in the membrane. A similar approach was used for chemosynthetic peptides described by Ren et al. (*2, 3*).

To monitor the hinge region and the C-terminal side of the transmembrane helical domain, key positions were labeled with the fluorescence probe AEDANS. This probe is designed to be sensitive to the polarity of the environment (*23*). Moreover, it was shown that λ_{max} of AEDANS is highly sensitive to small changes in the depth of labeled positions in the membrane, when attached to single cysteine mutants of the M13 major coat protein (*14, 24*). As a monitor for the C-terminal side of the helical domain, a cysteine residue is introduced at position 46 by site-specific mutagenisis. The cysteine residue is subsequently labeled with AEDANS. Earlier studies with the cysteine scanning approach indicated that position 46 is located near the edge of the transmembrane domain (Figure 1) (*24, 25*). To monitor the hinge region of the protein, a mutant is selected with a cysteine at position 23. NMR experiments on the protein dissolved in SDS showed that the hinge is composed of the amino acid residues 17 to 24, which show a relatively high flexibility (*26, 27*). Not much is known about the structure of the hinge region in phospholipid bilayers. The hinge is not located in the water phase, but is buried within the membrane, close to the polar head group region of the bilayer (see, chapter 2 (*14*)).

In DOPC, the tryptophan residue of the wild type protein exhibits a λ_{max} of 329 nm (Figure 2). This value is at the blue side of what would be expected for a tryptophan at the interface of a DOPC bilayer. De Planque et al. reported values of 337 nm for WALP peptides of which it was suggested that the tryptophan residues are in the interface (*28*). In our model systems, a value of 333 nm is obtained in DMoPC bilayer, and 326 nm in DEiPC. Apparently, the tryptophan residue is located deeper in the membrane as compared to the WALP peptides, and moves to a more apolar environment, when the hydrophobic thickness is increased. A comparable result is obtained for the AEDANS labeled T46C and G23C mutants (Figure 3). The λ_{max} of AEDANS, attached to position 46, changes from 493 to 490 nm going from DMoPC to DEiPC. The λ_{max} of AEDANS at position 23 shows a blue shift of 2 nm in these bilayers. These results show that the general response to an increased hydrophobic thickness appears to be a deeper penetration of the monitored key positions of the protein in the membrane.

At first sight, it is difficult to deduce from these experiments which side of the protein exhibits stronger anchoring interactions with the membrane-water interface. However, both the positions 23 and 46 are located at the membrane-water interface (*14, 24, 25*). This region of the membrane exhibits a steep polarity gradient on going from the outside to the inside of the membrane (*29*). A change in position of AEDANS in this region will result in a large change in λ_{max}. Nevertheless, both the labeled positions 46 and 23 show only a change in λ_{max} of 3 and 2 nm, respectively. These experiments suggest that the position 46 and 23 show a small change in relative depth under mismatch conditions. The finding that the C-terminal side (position 46) of the protein is less liable to move to a deeper position in the membrane under mismatch conditions is further supported by results obtained from the T46C/INS mutant. The insertion of 3 amino acids shows hardly any effect on the λ_{max} of AEDANS at position 46 in the PC bilayers as compared to λ_{max} of AEDANS attached to the T46C mutant (Figure 3). However, a strong response can be seen N-terminal side of the helical transmembrane domain as monitored by the tryptophan residue. The comparison between the λ_{max} of tryptophan of the wild type protein and the T46C/INS mutant reconstituted in DMoPC shows an increase from 333 nm in the wild type protein to 337 nm in the T46C/INS mutant (Figure 2). No change is measured in the tryptophan's λ_{max} of the T46C/INS mutant between DMoPC and DOPC, and a small shift is visible in DEiPC. Such an unchanged λ_{max} of the tryptophan residue as a function of hydrophobic thickness was also found by De Planque et al. for WALP peptides, which varied in hydrophobic length (*28*). Apparently, the tryptophan residue is now located in the interface of the membrane, where it has strong anchoring interactions with the polar head-group region of the bilayer.

From the above-mentioned experiment, it can be concluded that the C-terminal side of the helix (position 46) exhibits stronger anchoring interactions than the N-terminal side (position 26). The C-terminal side contains two phenylalanines and four lysine amino acid residues. In an earlier study it was shown that especially Lys40 is buried within the membrane hydrocarbon core. It was suggested earlier that the charged NH_2 group could just reach the polar head-group region of the membrane by the so called the "snorkeling" effect (*30, 31*). On the contrary, phenylalanine residue 42, but especially 45 are suggested to be located in the more polar head-group region, and probably bend back towards the hydrophobic core of the membrane (*20, 24, 25*). This arrangement of the amino acids would explain the strong anchoring interactions of the C-terminal part of the protein.

To study the role of the lysine and phenylalanine residues in these interactions, a mutant was prepared in which both phenylalanines are replaced by alanine residues. Interestingly, position 46 clearly moves to the water phase in this mutant, as can be concluded from the red shift of the AEDANS emission maximum (Figure 3). The relocation of position 46 as a result of the mutation is confirmed by ESR spectroscopy (Figure 4). The spectrum of the proxyl-labeled position 46 exhibits a broad component in agreement with Stopar et al. (*20*). The consequence of the mutation of both phenylalanines is an almost complete disappearance of the immobile component, which in turn suggests a movement of this position towards the water phase. The result of the mutation of the phenylalanines is a blue shift of the tryptophan residue as compared to the wild type protein in all PC bilayers (Figure 2). This suggests a deeper burial of the tryptophan residue into the membrane. Combining these movements of position 46 and tryptophan 26 suggest a shift of the entire helical transmembrane domain when both phenylalanines are replaced by alanines. Apparently, the phenylalanine residues provide an inside directed force on the helical domain, which compensate the outward directed force exercised by the lysine residues.

The AEDANS probe at position 23 in the hinge region does not reflect the effect of the phenylalanine mutations. This confirms the strong anchoring interactions of the hinge region with the membrane. There are several possibilities that can explain these interactions. The amino acids composition in the hinge can be important with, for instance, the two tyrosine residues at the positions 21 and 24. It is suggested that tyrosine residues similar as tryptophan prefer to be localized in the interface region of the membrane (*32, 33*). Another possibility can be that the amphipathic N-terminal arm on the one side and the helical transmembrane domain on the other side are responsible for the apparent fixed location of the hinge region.

It is not straightforward to construct a model of the membrane-bound M13 major coat protein that agrees with the behavior of the wild type protein under mismatch conditions. A number of possible adaptations can be suggested when the hydrophobic thickness of the bilayer is increased. For instance: the elastic lipid bilayers can adapt, the local conformation of the protein can change (undetectable with CD spectroscopy), and the tilt angle of the helical transmembrane domain can vary with the hydrophobic thickness (*13*). Probably, all these effects will play a role when the M13 protein is studied under mismatch conditions. However, there are two arguments that suggest the presence of a tilt angle of the helical transmembrane domain of M13 major coat protein. Firstly, a tilt angle of 20°±10° has been deduced from ^{13}C-MAS NMR spectroscopy on the protein, reconstituted into dimyristoyl phosphatidylcholine (*34*). This tilt angle could increase when the thickness of the bilayer decreases as was suggested for lysine-anchored peptides by Harzer et al. (*35*). As a result of this, positions in the interface will not show large shifts in position as is indeed found for the 23 and 46 position in the protein in our work. Secondly, a tilt angle is more energetically favorable for the lysine and phenylalanine rich C-terminus. In a helical conformation, the lysines are opposite to both Phe42 and Phe45. The presence of a helical tilt brings the amide group of Lys40 closer to the polar head-group region. On the other hand, both phenylalanines (especially Phe45) on the opposite face of the helix can more easily reach the hydrophobic core of the membrane. Furthermore, Trp26 is at the same face of the helix as the lysine residues. As a result of a tilted arrangement, the tryptophan residue is directed towards the hydrophobic core of the membrane, which could explain the relatively deep burial of this residue.

Conclusion

The C-terminal side of the transmembrane helix and the hinge region of M13 protein show hardly any response to hydrophobic mismatch. Apparently, these protein regions have strong anchoring interactions with the membrane-water interface. The existence of strong anchoring interactions of the C-terminus is confirmed using the T46C/INS mutant. The anchoring interactions of the C-terminal part are found to arise from the lysine and phenylalanine amino acid residues. The lysine residues apply a force on the hydrophobic transmembrane domain in the direction of the C-terminus of the protein, and the phenylalanines apply a force in the opposite direction. These forces are important for the location of this domain in a membrane. The hinge region is not affected in the 23C/FA mutant, which shows strong anchoring interactions of this region of the protein to the interface. In conclusion, the protein is kept in position in the membrane not only by the hydrophobic domain itself, but also by a combination of forces brought about by specific amino acid residues which reside in the membrane-water interface.

References

1. Killian, J. A., and von Heijne, G. (2000) *Trends Biochem Sci 25*, 429-434.
2. Ren, J., Lew, S., Wang, Z., and London, E. (1997) *Biochemistry 36*, 10213-20.
3. Ren, J. H., Lew, S., Wang, J. Y., and London, E. (1999) *Biochemistry* 38, 5905-5912.
4. Webb, R. J., East, J. M., Sharma, R. P., and Lee, A. G. (1998) *Biochemistry* 37, 673-679.
5. Zhang, Y. P., Lewis, R. N., Hodges, R. S., and McElhaney, R. N. (1995) *Biochemistry 34*, 2362-71.
6. Zhang, Y. P., Lewis, R. N., Hodges, R. S., and McElhaney, R. N. (1992) *Biochemistry 31*, 11579-88.
7. De Planque, M. R. R., Greathouse, D. V., Koeppe, R. E., Schafer, H., Marsh, D., and Killian, J. A. (1998) *Biochemistry 37*, 9333-9345.
8. de Planque, M. R. R., Kruijtzer, J. A. W., Liskamp, R. M. J., Marsh, D., Greathouse, D. V., Koeppe, R. E., de Kruijff, B., and Killian, J. A. (1999) *J. Biol. Chem. 274*, 20839-20846.
9. Nilsson, I., Saaf, A., Whitley, P., Gafvelin, G., Waller, C., and von Heijne, G. (1998) *J. Mol. Biol. 284*, 1165-1175.
10. Braun, P., and von Heijne, G. (1999) *Biochemistry 38*, 9778-9782.
11. Marassi, F. M., Ramamoorthy, A., and Opella, S. J. (1997) *Proc. Natl Acad. Sci. USA 94*, 8551-8556.
12. McDonnell, P. A., Shon, K., Kim, Y., and Opella, S. J. (1993) *J. Mol. Biol. 233*, 447-463.
13. Killian, J. A. (1998) *Biochim. Biophys. Acta.*, 401-416.
14. Spruijt, R. B., Meijer, A. B., Wolfs, C. J. A. M., and Hemminga, M. A. (2000) *Biochim. Biophys. Acta 1509, 311-323*
15. Meijer, A. B., Spruijt, R. B., Wolfs, C. J. A. M., and Hemminga, M. A. (2000) *Biochemistry in press.*
16. Studier, F. W., Rosenberg, A. H., Dunn, J. J., and Dubendorf, J. W. (1990) *Methods Enzymol. 185*, 60-89.
17. Spruijt, R. B., Wolfs, C. J. A. M., and Hemminga, M. A. (1989) *Biochemistry 28*, 9158-65.

18. Stopar, D., Spruijt, R. B., Wolfs, C. J. A. M., and Hemminga, M. A. (1998) *Biochemistry 37*, 10181-10187.
19. Lewis, B. A., and Engelman, D. M. (1983) *J. Mol. Biol. 166*, 211-7.
20. Stopar, D., Spruijt, R. B., Wolfs, C. J. A. M., and Hemminga, M. A. (1996) *Biochemistry 35*, 15467-15473.
21. Marsh, D. (1981) in *Membrane Spectroscopy* (Grell, E., Ed.) pp 51-142, Springer-Verlag, Berlin Heidelberg New York.
22. Hemminga, M. A., Sanders, J. C., Wolfs, C. J. A. M., and Spruijt, R. B. (1993) *New Comprehensive Biochemistry 25*, 191-212.
23. Hudson, E. N., and Weber, G. (1973) *Biochemistry 12*, 4154-61.
24. Spruijt, R. B., Wolfs, C. J. A. M., Verver, J. W. G., and Hemminga, M. A. (1996) *Biochemistry 35*, 10383-10391.
25. Stopar, D., Jansen, K. A. J., Pali, T., Marsh, D., and Hemminga, M. A. (1997) *Biochemistry 36*, 8261-8268.
26. Papavoine, C. H. M., Remerowski, M. L., Horstink, L. M., Konings, R. N. H., Hilbers, C. W., and van de Ven, F. J. M. (1997) *Biochemistry 36*, 4015-4026.
27. Papavoine, C. H. M., Konings, R. N. H., Hilbers, C. W., and Vandeven, F. J. M. (1994) *Biochemistry 33*, 12990-12997.
28. De Planque, M. R. R. (2000) *Hydrophobic Matching and Interfacial Anchoring of Transmembrane Peptides,* Thesis Utrecht University.
29. Wiener, M. C., and White, S. H. (1992) *Biophys. J. 61*, 437-47.
30. Tanford, C., and Reynolds, J. A. (1976) *Biochim. Biophys. Acta 457*, 133-70.
31. Mishra, V. K., Palgunachari, M. N., Segrest, J. P., and Anantharamaiah, G. M. (1994) *J Biol Chem 269*, 7185-91.
32. White, S. H., and Wimley, W. C. (1999) *Anu .Rev. Biophys. Biomol. Struc. 28*, 319-365.
33. White, S. H., Wimley, W. C., Ladokhin, A. S., and Hristova, K. (1998) *Ener. Biol. Macromol. PT B 295*, 62-87.
34. Glaubitz, C., Grobner, G., and Watts, A. (2000) *Biochem. Biophys. Acta*, 151-161.
35. Harzer, U., and Bechinger, B. (2000) *Biochemistry 39*, 13106-13114.
36. Van Wezenbeek, P. M. G. F., Hulsebos, T. J. M., and Schoenmakers, J. G. G. (1980) *Gene 11*, 129-48.

Chapter 6

Summarizing discussion

The M13 and Pf3 major coat proteins are stored in the inner membrane of a cell during infection of M13 and Pf3 bacteriophages. Protein-lipid anchoring interactions determine the formation of the correct structure and position of these proteins in the membrane, enabling fast and efficient phage assembly. From an energetics point of view, anchoring interactions can be defined as the preference of individual amino acids, or domains, for a specific position in the membrane (*1*). In general, these interactions with the membrane can be accomplished by several factors, for instance (a) hydrophobic interactions, which will be mainly determined by the length and degree of hydrophobicity of the hydrophobic domains in the protein, (b) electrostatic interactions between the protein and phospholipid head groups, and (c) the presence of the aromatic amino acids residues tyrosine and tryptophan near the interface region (*1-3*).

In earlier studies, these interactions were mainly investigated using artificial chemosynthetic proteins in a membrane (*4-7*). In this thesis the role of these interactions is studied for the determination of the correct membrane-bound position of the Pf3 and M13 major coat protein. M13 and Pf3 coat proteins are useful model systems for studying these fundamental aspects of the protein-lipid interactions. Firstly, both proteins have a continuous stretch of about 18-19 hydrophobic amino acids. Secondly, the C-termini of both proteins are rich in positively charged amino acid residues. Thirdly, the aromatic amino acids tyrosine and tryptophan are found at the N-terminal end of the hydrophobic stretch in the M13 coat protein. These amino acids are, however, not present in this region of the primary structure of the Pf3 coat protein (*9-11*) (Figure 2, Chapter 1).

To study the overall position of the M13 major coat protein in the membrane, this protein is systematically scanned with a site-specific labeling approach. For this purpose, a number of single cysteine mutants are prepared of the M13 coat protein. By attaching a fluorescence or ESR probe to these specific sites, information about the relative depth and local dynamics is acquired from this protein. In an earlier study, the C-terminal half of the protein was scanned with the cysteine scanning approach (*12-14*). In this thesis, the approach is extended towards the N-terminal half of the protein. The results of these studies are described in chapters 2 and 3.

The amphipathic N-terminal section of the protein reveals interesting aspects. In previous structural views of the membrane-bound state of the M13 coat protein, the protein is thought to be an L-shape, in which the N-terminal arm is embedded along the membrane surface perpendicular to the transmembrane segment (*15, 16*). Chapter 3 describes the presence of at least two configuration of the entire amphipathic N-terminal arm. ESR experiments show that a fraction of the N-termini is bound to the membrane. Another fraction is in a more extended configuration closer to the water phase. The N-terminal arm of the membrane-associated coat protein is not just firmly fixed to the membrane, and can move off the membrane surface into solution. Apparently, there is no tight association of the N-terminal arm to the membrane surface.

Replacement of either Phe11 or Leu14 (residues of the N-terminal helix which face the membrane) for a labeled cysteine results in the relocation of the N-terminal arm to the more extended configuration (Chapter 2). This result is clearly observed with double mutants in which Leu14 or Phe11 are replaced with an alanine residue, and the response is monitored at position 7. It turns out that the N-terminus is again relocated towards the water phase. The opposite effect is found when Ala10 is replaced by an isoleucine. The introduction of the more hydrophobic amino acid leads to a deeper burial of the N-terminal arm in the membrane. By ESR spectroscopy (Chapter 3), it is shown that these mutations affect the ratio between the membrane-bound and extended configuration of the N-terminal section of the protein. In this respect, the hydrophobic amino acids facing the membrane side of the N-terminal arm clearly play an important role in the topology of the helix at the membrane surface.

The apparent loose association of the N-terminal arm of the M13 protein to the surface of the membrane may have consequences for the protein in its role in the assembly process of the phage. During assembly the proteins must come together in the membrane (*17*). This requires a close approach of the transmembrane domains of the coat protein, which may be hindered by steric effects of the protein in the L-shape. However, as the N-terminal arm of the membrane-bound protein is loosely associated to the membrane, it can easily adapt to a more extended I-shape. In this state, the protein also has the proper configuration to form the viral coat, enabling fast and efficient phage assembly.

The cysteine-scanning approach on the relatively unknown Pf3 major coat protein is addressed in chapter 4. The location of amino acids of Pf3 mutants in the membrane, as was studied by site-specific fluorescence probing, clearly shows a single membrane spanning protein with both the C- and N-terminus remaining close to the surface of the membrane. The comparison with the results obtained from the M13 coat protein reveals striking similarities between the overall shape of the polarity plots of the positions of the proteins. There clearly is a structural coherence between both proteins in spite of the poor sequence homology (Figure 2, Chapter 1). Therefore, it is concluded that the tertiary structure of the Pf3 major coat protein closely resembles the membrane-bound structure of the M13 coat protein. This suggests that domains of amino acids, which are comparable in chemical-physical characteristics but lack sequence homology, can integrate in the membrane in similar way.

Another similarity between both proteins is the location of the positively charged amino acid residues in the membrane. Arginine at position 37 and lysine at position 40 in the Pf3 coat protein are buried within the hydrophobic core of the membrane similar as is found for the lysine residue of the M13 major coat protein. It is suggested that the ε-amine side group of lysine at position 40 in the M13 coat protein can just reach the polar head-group region via the so-called snorkeling effect (*12, 14, 18*). Apparently, the arginine residue in the Pf3 coat protein can interact with the interface in a similar manner.

The anchoring interactions of the hinge region, and the hydrophobic transmembrane α-helix of the M13 major coat protein are addressed in chapter 5. For this purpose, mutants and wild-type proteins are reconstituted into phosphatidylcholine membranes that vary in thickness. The C-terminal side of the transmembrane helix and the hinge region of M13 protein show hardly any response to hydrophobic mismatch. In contrast, the N-terminal side of the helical transmembrane domain, which is monitored via the tryptophan residue at position 26, clearly shifts to a more apolar environment, when the hydrophobic thickness is increased. The apparent strong anchoring interactions of the C-terminus are confirmed using a mutant that contains a longer transmembrane domain. As a result of this mutation, the tryptophan residue at the N-terminal side of the helical domain clearly shifts to a more polar environment, whereas the C-terminal side is hardly affected. No evidence is found for a preferred location in the interface of the tryptophan residue in the wild-type protein. The reason for this may be that the tryptophan residue is too deeply buried in the membrane to exhibit interactions with the interface.

The anchoring interactions of the C-terminal part of the transmembrane segment are arising from a combined effect of both the lysine and phenylalanine amino acid residues as is shown with a mutant, in which both Phe42 and Phe45 are replaced by alanines. These amino acids prove to be important for the location of the entire helical transmembrane domain. In the M13 coat protein, the Phe45 and Lys40 are at the opposite face of the α-helix. Therefore, a tilt angle of the helical transmembrane domain may be invoked to place both the Phe45 and Lys40 in their preferred location in the membrane. Moreover, a tilt angle of 20 ±10° has been deduced from ^{13}C-MAS NMR spectroscopy on the protein, reconstituted into dimyristoyl-phosphatidylcholine (*19*). Interestingly, such a tilt angle directs the tryptophan residue away from the interface towards the hydrophobic core of the membrane.

The location of the hinge region is not affected upon the removal of the phenylalanine residues, and appears to be strongly anchored with the interface. There are several possibilities that can explain these interactions. For instance, the amino acids composition in the hinge can be important with the isoleucine and two tyrosine residues. It is suggested that tyrosine residues, similar as tryptophan, prefer to be localized in the interface region of the membrane (*2*). Another possibility can be that the amphipathic N-terminal arm on the one side and the helical transmembrane domain on the other side are responsible for an apparent fixed location of the hinge. These results can be summarized in a tentative model of the protein in the membrane, which is presented in Figure 1.

To our knowledge this is the first time that the importance of specific amino acids for the position in the membrane is demonstrated of a natural protein. From our work, it follows that the relatively simple phage proteins are positioned in the membrane via a complicated set of protein-lipid interactions provided by individual amino acids as well as domains of amino acids; (a) Individual hydrophobic amino acids in the N-terminal arm of the M13 coat protein are important in determining the topology of the amphipathic helix on the surface of the membrane via hydrophobic interactions, (b) The C-terminal domain provides membrane-anchoring interactions via electrostatic interactions of the lysine residues and hydrophobic interactions via the phenylalanine residues, (c) The aromatic tyrosine residues are probably involved in the determination of the position of the hinge region of the M13 major coat protein, (d) The comparison between the data of the Pf3 and M13 coat protein shows that domains of amino acids, which are comparable in physical and chemical characteristics but lack sequence homology, can integrate in the membrane in a similar way. These findings illustrate the importance for these proteins of hydrophobic interactions of individual amino acids, and domains of amino acids for the topology and membrane assembly of membrane proteins.

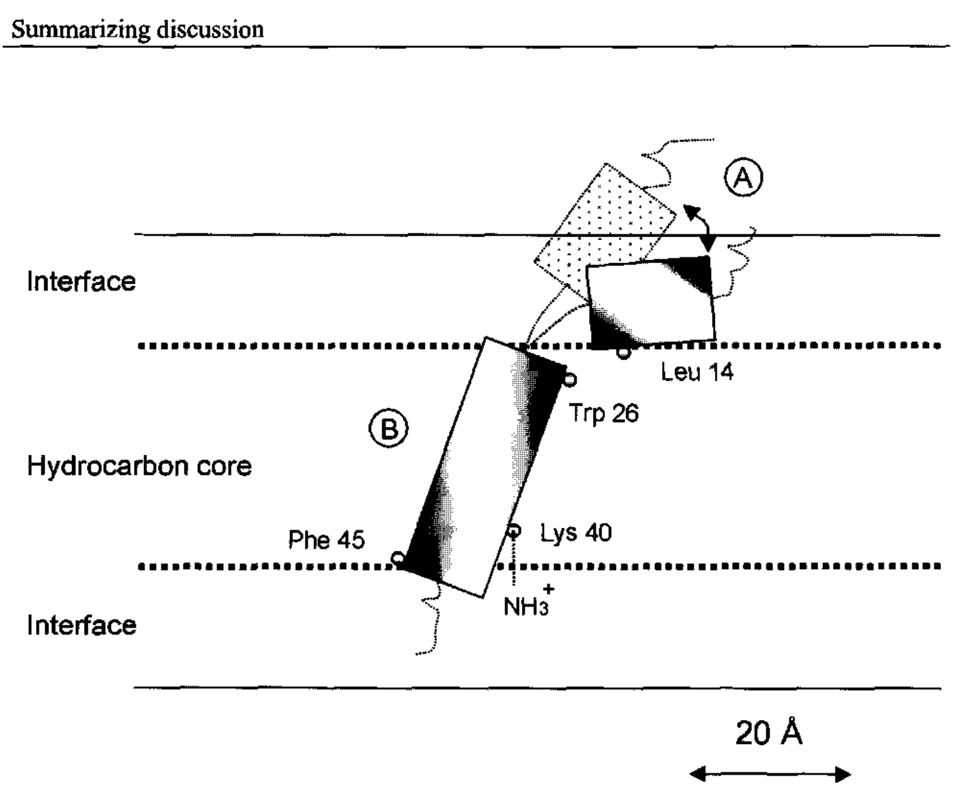

Figure 1: Schematic model of the position of the M13 major coat protein in the membrane. The 1,2-dioleoyl-*sn*-glycero-3-phosphocholine bilayer structure by Wiener and White is taken as a model membrane (*20*).

(A) The N-terminal section of the protein is in equilibrium between a more extended state of unknown topology and structure, and a membrane-bound state. The ratio between both configurations can be changed via site specific mutation of leucine 14.

(B) Representation of the transmembrane domain constructed by the residues 25 to 45, under a tilt angle of 20° with respect to the membrane normal (*19*). As a result of this tilt, the tryptophan residue at position 26 is directed towards the hydrophobic core of the membrane. The lysine residue at position 40 is able to reach the polar head-group region of the membrane, and the phenylalanine 45 at the opposite face of the helix can interact with hydrophobic core of the membrane.

References

1. White, S. H., Wimley, W. C., Ladokhin, A. S., and Hristova, K. (1998) *Ener. Biol. Macromol. PT B 295*, 62-87.
2. Killian, J. A., and von Heijne, G. (2000) *Trends Biochem.Sci.25*, 429-434.
3. Killian, J. A. (1998) *Biochim. Biophys. Acta.*, 401-416.
4. Ren, J. H., Lew, S., Wang, J. Y., and London, E. (1999) *Biochemistry 38*, 5905-5912.
5. Zhang, Y. P., Lewis, R. N., Hodges, R. S., and McElhaney, R. N. (1995) *Biochemistry 34*, 2362-71.
6. de Planque, M. R. R., Kruijtzer, J. A. W., Liskamp, R. M. J., Marsh, D., Greathouse, D. V., Koeppe, R. E., de Kruijff, B., and Killian, J. A. (1999) *J. Biol. Chem. 274*, 20839-20846.
7. Webb, R. J., East, J. M., Sharma, R. P., and Lee, A. G. (1998) *Biochemistry 37*, 673-679.
8. Arkin, I. T., and Brunger, A. T. (1998) *Biochim. Biophys. Acta* 113-128.
9. Van Wezenbeek, P. M. G. F., Hulsebos, T. J. M., and Schoenmakers, J. G. G. (1980) *Gene 11*, 129-48.
10. Luiten, R. G. M., Schoenmakers, J. G. G., and Konings, R. N. H. (1983) *Nucleic. Acids. Res. 11*, 8073-85.
11. Putterman, D. G., Casadevall, A., Boyle, P. D., Yang, H. L., Frangione, B., and Day, L. A. (1984) *Proc. Natl. Acad. Sci. USA 81*, 699-703.
12. Stopar, D., Jansen, K. A. J., Pali, T., Marsh, D., and Hemminga, M. A. (1997) *Biochemistry 36*, 8261-8268.
13. Stopar, D., Spruijt, R. B., Wolfs, C. J. A. M., and Hemminga, M. A. (1996) *Biochemistry 35*, 15467-15473.
14. Spruijt, R. B., Wolfs, C. J. A. M., Verver, J. W. G., and Hemminga, M. A. (1996) *Biochemistry 35*, 10383-10391.
15. Marassi, F. M., Ramamoorthy, A., and Opella, S. J. (1997) *Proc. Natl. Acad. Sci. USA 94*, 8551-8556.
16. McDonnell, P. A., Shon, K., Kim, Y., and Opella, S. J. (1993) *J. Mol. Biol. 233*, 447-463.
17. Marvin, D. A. (1998) *Curr. Opin. Struct. Biol. 8*, 150-158.
18. Tanford, C., and Reynolds, J. A. (1976) *Biochim. Biophys. Acta 457*, 133-70.
19. Glaubitz, C., Grobner, G., and Watts, A. (2000) *Biochem. Biophys. Acta*, 151-161.
20. Wiener, M. C., and White, S. H. (1992) *Biophys. J. 61*, 428-33.

Summary

The major coat proteins of the filamentous bacteriophages Pf3 and M13 are stored in the inner membrane of the cell during the reproductive cycle. In this process, protein-lipid anchoring interactions are important for the formation of the correct structure of these proteins in the membrane, enabling fast and efficient phage assembly. The focus of this thesis is on the role of domains and specific amino acids on the position of these proteins in the membrane. Both proteins are studied using site-specific probing using fluorescence and ESR spectroscopy. This biophysical approach provides information about the relative depth and dynamics of specific sites of the protein in the membrane. In previous structural views of the membrane-bound state of the M13 coat protein, the protein is thought to be in an L-shape, in which the N-terminal arm of the protein is positioned along the membrane surface. The spectroscopic studies described in this thesis show that the amphipathic N-terminus of the protein is not firmly associated with the membrane surface, but is also present in a more extended configuration. It is demonstrated that the hydrophobic amino acids in the N-terminal arm play an important role in the topology of the helix at the membrane surface. Furthermore, it is found that at the C-terminal side of the helical transmembrane domain, the charged lysines and hydrophobic phenylalanines are involved in strong anchoring interactions with the membrane interface region. These amino acids affect the location of the entire helical transmembrane domain. The results of a site-specific probing study on the Pf3 major coat protein reveals striking similarities with those obtained from the M13 major coat protein. Both proteins exhibit a strong structural coherence, in spite of the low primary sequence homology. Therefore, the tertiary structure of the Pf3 major coat protein should closely resemble the membrane-bound structure of the M13 coat protein. Apparently, domains of amino acids, which are comparable in physico-chemical characteristics, but lack sequence homology, are able to assemble in a structural coherent manner. In conclusion, the relatively simple coat proteins are positioned in the membrane via a complicated set of protein-lipid interactions provided by individual amino acids as well as domains of amino acids.

Samenvatting

De manteleiwitten van de bacteriofagen Pf3 en M13 worden opgeslagen in het binnenmembraan van de cel tijdens de reproductiecyclus. Een juiste structuur en positie van de eiwitten in het membraan zijn essentieel voor een efficiënte bacteriofaagreproductie. De focus van dit proefschrift ligt op de rol van specifieke aminozuren en domeinen van aminozuren op de positie van de eiwitten in het membraan. Met behulp van plaatsgerichte mutagenese zijn cysteïnemutanten gemaakt voor de toepassing van ESR-spinlabeling en fluorescentiespectroscopie. Deze technieken zijn bijzonder geschikt voor het bepalen van de diepte en dynamica van eiwitposities in modelmembranen. In voorgaande opvattingen over de membraangebonden structuur van het M13 manteleiwit lag de N-terminale arm van het eiwit parallel aan het oppervlak van het membraan. De spectroscopische studies in dit proefschrift tonen aan dat deze arm niet stevig aan het membraanoppervlak is gebonden. De positie en oriëntatie van de arm worden mede bepaald door hydrofobe aminozuren in de N-terminale arm. De lysine- en phenylalaninerijke C-terminus van de transmembraanhelix heeft sterk verankerende interacties met het membraan. Deze aminozuren beïnvloeden de positie van de gehele transmembraanhelix. De resultaten van de spectroscopische studie aan het Pf3 manteleiwit laten een sterke overeenkomst zien met de resultaten die verkregen zijn met het M13 manteleiwit. Dit wijst op een vergelijkbare tertiaire structuur van beide membraangebonden eiwitten, terwijl de primaire structuurhomologie zeer laag is. Hieruit volgt dat domeinen van aminozuren met overeenkomende fysisch-chemische eigenschappen een vergelijkbare structuur kunnen aannemen in het membraan. Concluderend, de relatief eenvoudige manteleiwitten worden in het membraan gepositioneerd met behulp van gecompliceerde lipide-eiwitinteracties die afkomstig zijn van individuele aminozuren en domeinen van aminozuren.

Curriculum vitae

Alexander Benjamin Meijer werd geboren op 14 april 1971 in Maassluis. Na het behalen van zijn atheneum-B diploma aan de Rijksscholengemeenschap te Den Briel, begon hij in 1990 met de studie Moleculaire Wetenschappen aan de Wageningen Universiteit. Deze studie werd afgerond met afstudeervakken bij de vakgroepen Biochemie en Moleculaire Fysica. Vanaf 1996 was hij werkzaam als Onderzoeker in Opleiding (NWO) bij het Laboratorium voor Biofysica aan de Wageningen Universiteit en verrichtte hij onderzoek dat leidde tot dit proefschrift.